REACTOR
AND FUEL-PROCESSING
TECHNOLOGY

A Quarterly Technical Progress Review

Summer 1968

- VOLUME 11

- NUMBER 3

TECHNICAL PROGRESS REVIEWS

The United States Atomic Energy Commission publishes the Technical Progress Reviews to meet the needs of industry and government for concise summaries of current nuclear developments. Each journal digests and evaluates the latest findings in a specific area of nuclear technology and science. *Nuclear Safety* is a bimonthly journal; the other three are quarterly journals.

Isotopes and Radiation Technology
P. S. Baker, A. F. Rupp, and Associates
Isotopes Information Center, Oak Ridge National Laboratory

Nuclear Safety
Wm. B. Cottrell, W. H. Jordan, J. P. Blakely, and Associates
Nuclear Safety Information Center, Oak Ridge National Laboratory

Reactor and Fuel-Processing Technology
Argonne National Laboratory

Reactor Materials
E. M. Simons and Associates
Battelle Memorial Institute, Columbus Laboratories

All are available from the U. S. Government Printing Office. See the back cover for ordering instructions.

Availability of Reports Cited in This Review

United States Atomic Energy Commission (USAEC) reports are available at USAEC depository libraries and are sold by the Clearinghouse for Federal Scientific and Technical Information (CFSTI), National Bureau of Standards, U. S. Department of Commerce, 5285 Port Royal Road, Springfield, Va. 22151. All reports sold by CFSTI are $3.00 for printed copy and $0.65 for microfiche. Each separately bound part of a report is priced as a separate report. Some reports may not be available because of their preliminary nature; however, the information contained in them will generally be found in later progress or topical reports on the subject.

Other U. S. Government agency reports identified in this journal generally are available from CFSTI.

Private-organization reports should be requested from the originator.

United Kingdom Atomic Energy Authority (UKAEA) and Atomic Energy of Canada Limited (AECL) reports are available at USAEC depository libraries. UKAEA reports are sold by Her Majesty's Stationery Office, London; AECL reports are sold by the Scientific Document Distribution Office, Atomic Energy of Canada Limited, Chalk River, Ontario, Canada. UKAEA and AECL reports issued after March 1, 1967, are sold by CFSTI to purchasers in the United States and its territories.

Contents

Reactor and Fuel-Processing Technology

is a quarterly review of developments in reactor and reactor fuel technology. As such, this journal reports and interprets progress in the reactor field in terms of its significance to the reactor designer, operator, and fuel-cycle specialist. Articles either summarize and critically evaluate recently reported developments or review the "state of the art" of a particular topic. Both types of articles reference reports and publications that merit study; readers are urged to consult the references for additional information and the judgments of the original authors. If a reader has information that causes his evaluation to reinforce, modify, or contradict the opinions of our reviewers, he is encouraged to write to the Editor.

The scope of the journal encompasses:

CONCEPTS and APPLICATIONS: Progress in evaluating the applicability and economics of various reactor types and systems (including unconventional approaches), as well as of fuel resources and cycles, for utility central-station generation of electricity, auxiliary power, process radiation and heat, desalting, and propulsion—and for terrestrial, undersea, aerospace, and other advanced uses.

ANALYSIS and EXPERIMENTATION: Advancements in the techniques of reactor physics, fluid and thermal technology, energy conversion, fuel elements, materials, mechanics, control and dynamics, and reactor safety.

SYSTEMS and COMPONENTS: Experience as reflected in design and construction practice, components, systems technology, and operating performance of various specific types of reactors—including pressurized- and boiling-water reactors, molten-salt, organic-, gas-, and liquid-metal-cooled reactors, as well as generally applicable aspects of research and test reactors.

FUEL PROCESSING: Recent research and development on fuel aqueous processing, nonaqueous processing, waste disposal, and processing safety.

This journal is prepared by Argonne National Laboratory at the request of the Division of Technical Information of the U. S. Atomic Energy Commission. At Argonne, the Reactor Engineering Division (L. J. Koch, Director) and the Chemical Engineering Division (R. C. Vogel, Director) have the principal responsibility for the preparation of *Reactor and Fuel-Processing Technology,* with the regular assistance of the Reactor Physics Division (R. A. Avery, Director) and the Idaho Division (M. Novick, Director) and the occasional assistance of other divisions (Metallurgy, Chemistry, and Reactor Operations). Thus, unless noted otherwise, the reviewers and authors of articles are Laboratory staff members. The editors welcome interpretive review articles contributed by authors outside the Laboratory.

A Review of the Experimental and Analytical Results of the High-Conversion Critical Experiment

By Karl E. Plumlee and Edwin M. Pennington

Critical experiments[1,2] and calculations[3] have been reported for a sequence of 3 and 5% enriched UO$_2$-fueled H$_2$O-moderated cores assembled at Argonne National Laboratory to investigate the advantages of densely loaded power-reactor cores, including high conversion ratios and high power densities. High conversion ratios retard the depletion of fissile isotopes during core cycles, thereby conserving reactivity and extending core life. Fuel costs are reduced by lowering the net cost for fissile material and also by lengthening the core life, which postpones the expenditure for a replacement core.

Loading additional fuel elements into a given core volume increases the heat-transfer surface and the permissible power density up to a point where coolant flow is limiting. A significant advantage of a densely loaded core is this capability for increased power without use of a larger reactor vessel.

The experiment involved a range of fuel loading densities, from the tightest packed lattice achievable to a loose lattice that could be compared with the results of other experiments.[4]

Fuel and Core Description

The experiments were performed using 3 and 5% enriched UO$_2$ fuel clad with 304 stainless steel and 3% enriched UO$_2$ fuel clad with 6061T-6 aluminum. The 5% enriched (BORAX-5 boiling zone) fuel elements averaged 374 g of UO$_2$ pellets having a density of 10.2 g/cm^3, including 16.27 g of ^{235}U (Ref. 2). These pellets were 0.87 cm in diameter and were loaded as 61-cm-long columns into 0.96-cm-OD stainless-steel tubing having a 0.04-cm-thick wall. The 3% enriched fuel elements averaged 853 g of UO$_2$ pellets having a density of 10.2 g/cm^3, including 22.89 g of ^{235}U. The 3% pellets were 0.94 cm in diameter and were loaded as 122-cm-long columns into 1.06-

cm-OD aluminum or stainless-steel tubing having a 0.05-cm-thick wall.

Lattice pitch and fuel selection were chosen to obtain a range from 0.16 to 1.5 in volume ratio of H$_2$O/UO$_2$, or 0.5 to 4.7 in atom ratio of H/^{238}U. Two-zone cores were necessary for criticality with the two tightest triangular lattices. Table 1 describes several of the cores and lists measured and calculated values of critical buckling, reflector savings, fission ratio ^{238}U/^{235}U, modified conversion ratio (MCR), and initial conversion ratio (ICR).

Measured vs. Calculated Results

Excellent agreement between measured and calculated initial conversion ratio was indicated for the 4.65 H/^{238}U atom-ratio core fueled by 3% enriched UO$_2$; but with higher H/^{238}U ratios and also with 5% enrichment, the measured results were a few percent lower than the calculated conversion ratios, as shown in Fig. 1 and Table 2.

The modified conversion ratios (MCR's) are the ratios of ^{238}U captures to ^{235}U fissions in each core. The initial conversion ratios (ICR's) are obtained by dividing the MCR's by $(1 + \alpha^{25})$, where α^{25} is the capture-to-fission ratio of ^{235}U in each core. The values of α^{25} were obtained from GAM-I (Ref. 5) and THERMOS[6] computed flux-energy distributions. One measurement of α^{25} was made by sample oscillation,[7] with standardization by a ^{252}Cf spontaneous fission source and by manganese absorber solutions. This was in the 1.24-cm-square lattice; the measured and calculated values agreed within experimental error.

The measured critical masses were plotted vs. H/^{238}U ratios, as shown in Fig. 2. More fuel was required for criticality with uniform or fully loaded lattices than with nonuniform loadings. The nonuniform loadings were obtained by removing every 16th,

Table 1 DESCRIPTION OF TYPICAL CORES

Core code*	Critical mass, kg ^{235}U	Atom ratio, H/^{238}U	Critical buckling, 10^4 cm^{-2}		Radial reflector savings, cm		Fission ratio, ^{238}U/^{235}U		MCR†		ICR‡
			Exper.	Calc.	Exper.	Calc.	Exper.	Calc.	Exper.	Calc.	Calc.
B1.27□S	10.45	4.65	107.6 ± 1.9	108.7	7.35 ± 0.27	7.21	0.065		0.344	0.421	0.342
H1.349□S	Zoned	4.16	Zoned	66.4			0.074	0.066	0.542	0.547	0.448
H1.349□A	13.48	4.15	91.8 ± 0.8	89.9	7.38 ± 0.12	7.73		0.064		0.514	0.422
B1.27△S	15.63	3.53	91.5 ± 0.7	93.0	7.55 ± 0.10	7.57	0.119		0.397	0.494	0.396
H1.24□S	40.42	2.92	47.5 ± 0.3	49.7	7.69 ± 0.08	7.76	0.101	0.084	0.594	0.668	0.540
H1.24□A	21.75	2.91	70.8 ± 0.7	71.7	8.13 ± 0.16	8.45		0.082		0.622	0.505
H1.27△S	Zoned	2.29	Zoned	37.6			0.116	0.097	0.702	0.763	0.610
H1.27△A	32.44	2.29	55.4 ± 0.2	57.8	8.77 ± 0.17	9.02		0.097		0.707	0.568
H1.166△S	Zoned	1.33	Zoned	7.5			0.154	0.134	1.033	1.078	0.836
H1.166△A	115.69	1.32	24.4 ± 0.1	26.5	10.73 ± 0.14	10.86		0.135		0.979	0.765
H1.127△S	Zoned	0.98	Zoned	-4.8			0.188	0.154		1.265	0.964
H1.127△A	Zoned	0.98	Zoned	13.8				0.157	1.155	1.137	0.873
H1.069△S	Zoned	0.50	Zoned	-27.7			0.262	0.198	1.705	1.834	1.339

*Core code: B or H indicates 5% or 3% enrichment; the number is lattice spacing in cm; the symbol □ or △ indicates square or triangular lattice; S or A indicates stainless-steel or aluminum cladding on the fuel.

†MCR = Modified conversion ratio = ratio of ^{238}U captures to ^{235}U fissions in each core. Standard deviation is estimated to be ±0.02.

‡ICR = Initial conversion ratio = MCR/$(1 + \alpha^{25})$, where α^{25} is the capture-to-fission ratio of ^{235}U in each core.
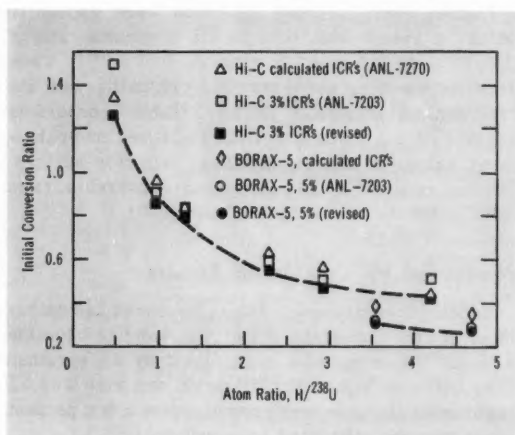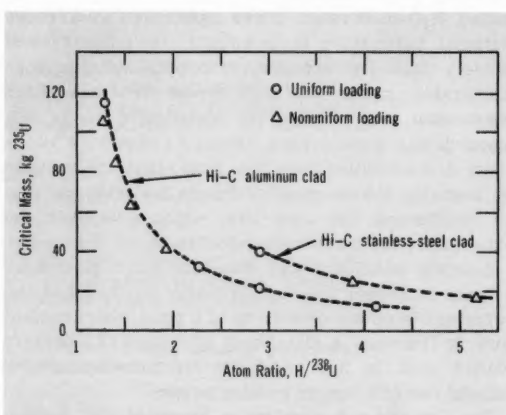

Fig. 1   *Conversion ratios for 3% enriched UO$_2$–H$_2$O cores.*

Fig. 2   *Measured critical masses of Hi-C 3% enriched cores.*

Table 2   REVISED CONVERSION RATIOS IN Hi-C AND BORAX-5 CORES

Lattice	Core No.	Atom ratio, H/^{238}U	Modified conversion ratio (MCR)	α^{25}	Initial conversion ratio (ICR)
1.27-cm-square BORAX-5	1	4.65	0.344	0.236	0.278 ± 0.02 (2)*
1.27-cm-triangular BORAX-5	2	3.53	0.397	0.252	0.317 ± 0.02 (1)
1.349-cm-square Hi-C	4	4.16	0.542	0.225	0.442 ± 0.01 (6)
1.24-cm-square Hi-C	8 and 9	2.92	0.594	0.244	0.478 ± 0.01 (16)
1.27-cm-triangular Hi-C	12	2.29	0.702	0.257	0.558 ± 0.02 (4)
1.166-cm-triangular Hi-C	14	1.33	1.033	0.296	0.797 ± 0.01 (6)
1.127-cm-triangular Hi-C	19	0.98	1.155	0.317	0.877 ± 0.02 (9)
1.069-cm-triangular Hi-C	21	0.50	1.705	0.362	1.252 ± 0.04 (9)

*Numbers in parentheses denote the number of independent determinations.

12th, 9th, 8th, 6th, or 4th fuel element from a uniform loading, to provide intermediate $H/{}^{238}U$ ratios, rather than reload the cores with several additional lattice spacings. These nonuniformities reduced the critical masses by as much as 12% below the curve through the uniformly loaded data points.

Critical bucklings were compared as shown in Fig. 3. The measured values were obtained by least-squares iterative fit of cosine (axial shape) and Bessel J_0 (radial shape) functions to foil-activation traverse data. A computer program provided re-
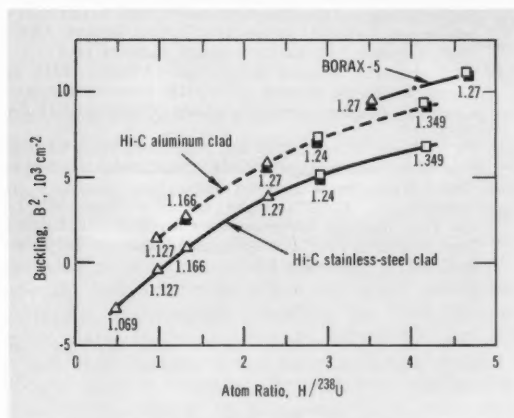

Fig. 3 Experimental (solid symbols) and calculated (open symbols) bucklings. Lattice shapes are indicated by squares and triangles.

petitive fits of progressively shortened traverses to permit selection of extrapolated dimensions that were not affected by flux perturbations near reflector regions. Good agreement was found between measured and calculated values after revision of the cross-section set used for calculation as discussed in the following section.

Calculational Methods

Calculations were mostly with four-group constants using GAM-I (P-1 option) to obtain cross sections for three fast groups having lower energy boundaries at 1.35 Mev, 1.23 kev, and 0.414 ev; THERMOS was used for thermal-group cross sections. Bucklings were badly overestimated until the ^{235}U and ^{238}U cross sections recommended by Liikala[8] were used to replace corresponding values in the GAM-I library tape. The resulting good agreement with measured values is indicated in Table 1 and in Fig. 3. Use of GAM-I (B-1 option) changed the diffusion constants significantly but made little difference in calculated bucklings or in reflector savings. The two options should give identical results for zero buckling.

Thermal lattice parameters were calculated using THERMOS, which accommodates 27 energy groups below 0.415 ev (these were edited to determine the thermal cross sections), and three more groups between 0.415 and 0.785 ev. At still higher energies, a $1/E$ flux distribution is assumed by THERMOS. Free-gas kernels are used except for hydrogen scattering, for which the Nelkin, the Brown–St. John, or the free-gas kernel may be selected as options. The Nelkin option gave the hardest spectrum, and the free-gas option gave the lowest scattering cross sections of the three. The Nelkin kernel was used for most calculations. These options affected calculated average velocities and absorption or fission cross sections by as much as 4%, but buckling calculations were not significantly affected.

Calculated thermal disadvantage factors based on THERMOS were consistently about 8% higher than measured values, except for $H/{}^{238}U$ atom ratios of ~1 or less. The data are shown in Fig. 4. Monte Carlo calculations carried out at Bettis Atomic Power Laboratory indicate that perturbations resulting from the presence of a foil may account for part of this discrepancy between calculated and measured disadvantage factors.[9]

Calculations of ^{238}U and ^{235}U cadmium ratios and reaction rates appear to agree with the experiment (within the stated error limits) except for fast fissions in ^{238}U. Changing from a homogeneous model to a heterogeneous model made little difference in the calculated $^{238}U/{}^{235}U$ fission ratios, as might be expected in such tight lattices. MUFT-4 cross sections[10] resulted in slightly higher values for ^{238}U fission than GAM-I cross sections, but both were lower than the measured values. The cause of this discrepancy was not discovered. Although ^{238}U fissions are significant, the calculational error, if it exists, appears tolerable. The error may originate in the fast cross sections that were used. The prominence of ^{238}U fissions in these cores may have made it possible to detect a problem that has escaped notice in looser lattices.
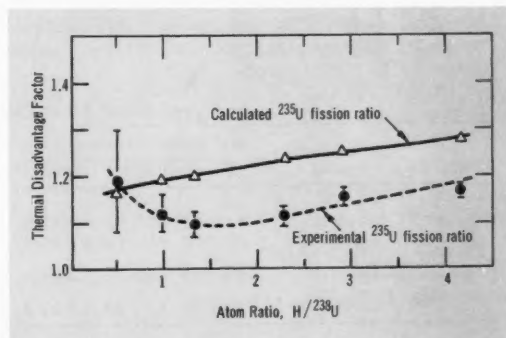

Fig. 4 Measured and calculated disadvantage factors.

Conclusions

Calculations and measurements are in good agreement with respect to critical mass and buckling of tight latticed UO_2–H_2O cores. Reaction rates are not in very close agreement, with differences of a few percent being found in conversion ratios, $^{238}U/^{235}U$ fission ratios, and disadvantage factors. Difficulty in calculating and in measuring such quantities leaves room for debate whether the discrepancies are primarily attributable to theoretical limitations or to experimental-error limits. However, these discrepancies are not very significant in comparison to the mechanical limitations encountered in nuclear reactor design.

References

1. K. E. Plumlee, Addendum to the Report on the High Conversion Critical Experiment, USAEC Report ANL-7203 Addendum, Argonne National Laboratory, to be published.
2. A. R. Boynton et al., High Conversion Critical Experiments, USAEC Report ANL-7203, Argonne National Laboratory, January 1967.
3. E. M. Pennington, Analysis of High Conversion Critical Experiments, USAEC Report ANL-7270, Argonne National Laboratory, March 1967.
4. G. A. Price, Uranium–Water Lattice Compilation, Part I, BNL Exponential Assemblies, USAEC Report BNL-50035, Brookhaven National Laboratory, Dec. 30, 1966, and Part II (in preparation).
5. G. D. Joanou and J. S. Dudek, GAM-I, A Consistent P-1 Multigroup Code for Calculation of Fast Neutron Spectra and Multigroup Constants, USAEC Report GA-1850, General Atomic Division, General Dynamics Corp., June 28, 1961.
6. H. C. Honeck, THERMOS, A Thermalization Transport Code for Reactor Lattice Calculations, USAEC Report BNL-5826, Brookhaven National Laboratory, September 1961.
7. W. C. Redman and M. M. Bretscher, Reactor Oscillator Determination of Capture-to-Fission Ratio in an Undermoderated Critical Assembly, USAEC Report ANL-7143, Argonne National Laboratory, January 1966.
8. R. C. Liikala, Updated R.B.U. Basic Library, Vols. 1, 2, and 3, USAEC Report HW-75716, General Electric Company, Hanford Atomic Products Operation, May 20, 1963.
9. F. E. Dunn, Flux Dipping and Peaking in Foils Used in Thermal Disadvantage Factor Measurements, *Trans. Amer. Nucl. Soc.*, 9(1): 189 (1966).
10. H. Bohl, Jr., E. M. Gelbard, and G. H. Ryan, MUFT-4—Fast Neutron Spectrum Code for IBM-704, USAEC Report WAPD-TM-72, Westinghouse Electric Corporation, Bettis Plant, July 1957.

Review of Results of the DIMPLE Critical Experiment

By Karl E. Plumlee

The DIMPLE critical experiment,[1] which was conducted by the UKAEA Reactor Group at Winfrith, provided additional information and confirmation of the results discussed in the previous article (see page 117) for 3% enriched UO_2 cores with H_2O moderator and reflector. The additional information includes measurements of temperature effects, void worths, and activation ratios for some additional materials. Calculations preceding the DIMPLE program, using the computer codes METHUSELAH[2] and WIMS,[3] had underestimated the reactivities of tightly packed lattices. This underestimation was typical also of the results of few-group calculations that had preceded the Hi-C experiment. Three cores were assembled, including one very loose lattice, and one of these was modified by installation of void pins to obtain a fourth H_2O/UO_2 volume ratio.

Fuel and Core Description

The fuel used in the DIMPLE cores consisted of 1.01-cm-diameter (0.4 in.) UO_2 pellets. The nominal column length in a fuel element was 69.2 cm; the 68 pellets in each fuel element were rolled into aluminum wrappers, resulting in "pencils" of 8 and 9 pellet lengths. These were contained in 1.0925-cm-OD (0.43 in.) stainless-steel tubing of 0.0267-cm wall thickness and 71.83-cm length. The ends of the tubes were plugged by 1-cm-long aluminum bungs. The average weight of a fuel element included 580.65 g of UO_2, 48.3 g of stainless steel, and 3.6 g of aluminum foil, plus approximately 1.8 g of stainless steel and about 4.5 g of aluminum in the portions extending above and below the UO_2.

Volume ratios of H_2O/UO_2 of 0.779, 1.001, and 3.164 were obtained by loading fuel elements into 1.25-, 1.32-, or 1.87-cm square lattices. An H_2O/UO_2 volume ratio of 0.857 was obtained by loading aluminum void pins into the 1.32-cm lattice. The 0.384-cm-diameter aluminum pins weighed 0.314 g per centimeter of length.

Experimental Results

Tabulated data for the DIMPLE cores are listed in Table 1. The critical masses fall intermediately between the aluminum-clad and stainless-steel-clad Hi-C loadings, which can be attributed to the thinner stainless-steel cladding (half that of the Hi-C fuel) and to the slightly larger fuel-pellet diameter of the DIMPLE fuel.

The relative conversion ratios (RCR's) reported for the DIMPLE experiment are the ratios of conversion ratios in these cores to that in a thermal reference. These have been multiplied by the factor 0.155 to obtain the modified conversion ratios (MCR's) as discussed in the Hi-C report.[4] The factor 0.155 is the calculated flux-averaged conversion ratio in a thermal flux, using $\sigma_c^{28} = 2.73$ barns, $\sigma_{fiss}^{25} = 577.1$ barns, and the relative flux-averaging (Westcott g)

Table 1   DESCRIPTION OF DIMPLE CORES

Lattice, cm	Atom ratio, H/^{238}U	No. of fuel rods	Equivalent radius, cm	Critical H_2O height, cm	Extrapolation distance, cm			Critical buckling, 10^4 cm^2	MCR*
					Radial	Top	Bottom		
1.25, square	2.34	2820	37.47	48.40 ± 0.14	8.6 ± 0.2	8.9 ± 0.4	7.3 ± 0.4	51.0 ± 0.3	0.742
1.32†	2.57	2252	35.34	53.95 ± 0.13	8.2 ± 0.2	8.4 ± 0.4	7.4 ± 0.4	50.8 ± 0.3	0.699
1.32, square	3.00	1565	29.44	48.83 ± 0.03	7.9 ± 0.1	7.7 ± 0.5	6.9 ± 0.5	66.0 ± 0.2	0.643
1.87, square	9.49	665	27.15	34.01 ± 0.03	6.2 ± 0.1	6.3 ± 0.5	4.7 ± 0.5	100.4 ± 0.6	

*Modified conversion ratio = ratio of ^{238}U captures to ^{235}U fissions in each core.
†Voided by aluminum void pins.

factor of 1.03. One adjustment which was made for the Hi-C data, but which might not have been made for the RCR's, was to remove the epithermal reaction rates from the foils activated for normalization purposes in a thermal column. Without that adjustment, which reduced the Hi-C MCR's by ~4%, the two sets of MCR's would be in very close agreement.

^{176}Lu/^{55}Mn Activation Ratios

Significant changes were measured in the activation ratio of ^{176}Lu/^{55}Mn as a result of changing the lattice spacing, the H_2O/UO_2 volume fraction, or the core temperature. The change from 1.32 to 1.25 cm lattice spacing at room temperature decreased the ratio by about 4%, reportedly because the ^{55}Mn resonance activation increased more than the ^{176}Lu activation. Increasing the core temperature from 20 to 80°C increased the ^{176}Lu/^{55}Mn ratio by ~7%. Both changes should have increased the ^{176}Lu 0.14-ev resonance activation and decreased the *thermal* activation of ^{55}Mn. These results are given in Table 2.

Table 2   ACTIVATION RATIO MEASUREMENTS

Lattice, cm	Atom ratio, H/^{238}U	^{176}Lu/^{55}Mn ratio	^{239}Pu/^{235}U fission ratio
1.25	2.34	1.112	1.661
1.32*	2.57	1.121	1.646
1.32†	2.92†	1.241†	1.637†
1.32	3.00	1.160	1.589

*Voided by aluminum void pins.
†Measurements made at 80°C; all others were at 20°C.

^{239}Pu/^{235}U Fission Ratios

The fission ratio of ^{239}Pu/^{235}U is also sensitive to the thermal-neutron temperature because of fissions by the 0.3-ev ^{239}Pu resonance; this might be particularly useful as a spectral index at higher temperatures. Also of interest is the buildup of ^{239}Pu during a core cycle and its rate of destruction by fissioning.

The ^{239}Pu/^{235}U fission ratio increased by about 4.5% as a result of changing the lattice spacing from 1.32 to 1.25 cm, ~3.6% from insertion of void pins in the 1.32-cm lattice, and ~3.0% on raising the temperature of the 1.32-cm lattice from 20 to 80°C, as shown in Table 2. These results seem much less complicated than the Lu/Mn activation ratios, but not enough points were provided to determine whether there might be a linear relation similar to those for cadmium ratios of various materials reported for the Hi-C cores.[4]

Differences in Bucklings of Fast and Thermal Fluxes

The DIMPLE program included measurements of axial flux shapes with ^{235}U and ^{238}U fission chambers

in an effort to find any difference between the thermal flux shape and that above the ~1.1-Mev fission threshold of ^{238}U. A "barely significant" difference was reported (i.e., 0.43 ± 0.47 cm, for an extrapolated height of 44 to 45 cm in the 1.87-cm lattice).

Similar efforts had been reported[5] at least as early as 1958, and interest in this topic has persisted since then. For the Hi-C cores,[4] only the bare and cadmium-covered traverses had been examined, with no indication of any significant differences between thermal and epicadmium flux shapes.

A recent thesis indicates "qualitative" experimental confirmation of theoretical predictions of such differences.[6] Using a ^{232}Th fission cap with a silicon-barrier semiconductor detector, the fast flux (i.e., above ~1.35 Mev) was reported to yield a 5 to 10% (± 5%) different buckling than the thermal flux. This measurement was made in the Cornell University Zero Power Reactor, using 2% enriched UO_2 fuel of 1.52-cm diameter in 122-cm-long fuel rods. The core composition was 1.5/1 volume ratio of H_2O/UO_2, and the radius was about 21 cm.

The Cornell measurements were in a core for which the difference was expected to be relatively large; the fast flux detection by ^{232}Th fissions may have been more accurate than the ^{238}U fission measurement of the DIMPLE experiment. (It was not stated whether any ^{235}U was present in the ^{238}U fission counter.)

These results justify some tentative conclusions. First, the fast leakage at or above energies where differences in flux shape become detectable is not very large in a thermal reactor. Second, the difficulty in measuring these differences in flux shape implies that the differences are small. Finally, all measurements seem consistent, in sign and magnitude, with the expected differences.

References

1. W. A. Brown et al., Measurements of Material Buckling and Detailed Reaction Rates in a Series of Low Enrichment UO$_2$ Fuelled Cores Moderated by Light Water, British Report AEEW-R-502, September 1967.

2. D. Hicks, Few Group Nuclear Design Methods for Heavy Water Reactors, British Report AEEW-R-249, January 1963.

3. J. R. Askew, F. J. Fayers, and P. B. Kemshell, A General Description of the Lattice Code WIMS, *J. Brit. Nucl. Energy Soc.*, 5: 564-585 (October 1966).

4. A. R. Boynton et al., High Conversion Critical Experiments, USAEC Report ANL-7203, Argonne National Laboratory, January 1967.

5. J. R. Brown et al., Kinetic and Buckling Measurements on Lattices of Slightly Enriched Uranium or UO$_2$ Rods, USAEC Report WAPD-176, Westinghouse Electric Corporation, January 1958.

6. R. A. Shaw, An Experimental Comparison of the Fast and Thermal Neutron Bucklings in a Uranium Dioxide Light-Water Moderated Critical Assembly, Ph. D. Thesis, Cornell University, February 1967.

How To Use Quasi-Linear Programming for Calculating Optimum Reactor Control

By H. J. Price* and R. R. Mohler, University of New Mexico

Linear programming sometimes can be used effectively to compute optimal-control trajectories for systems of high dimension with numerous physical constraints — such as nuclear reactors. A recursive algorithm is developed from a sequence of linear-programming problems to handle nonlinear reactor problems. Then a coolant–optimal-control process is computed for a nonlinear nuclear rocket reactor. Availability of canned linear-programming routines makes such computations most feasible.

This article illustrates how linear programming can be applied to solve complicated optimal-control problems in reactor design. Reactor designers and operators who are concerned with optimal configurations and fuel management will find that the same technique can be used to solve their problems. Available routines make linear programming feasible with digital computers. (The reader who is unfamiliar with linear programming will find Ref. 1 useful.)

COMPLICATIONS IN PRACTICAL PROBLEMS

Practical optimization problems usually are complicated by high dimensionality, physical state, and control limitations to ensure system safety and mechanical integrity. For example, one model for a nuclear rocket engine involves 40 state variables (such as temperatures, powers, coolant flow rates, and pressures) and numerous constraints on temperatures, reactor power, reactivity, and coolant flow rate. Of course, similar complications enter into the design of any high-performance nuclear power system.

Unfortunately, analytical techniques such as the maximum principle and the calculus of variations are not very practical for obtaining solutions to problems of high dimension and numerous state constraints. Reference 2, which uses these analytical techniques,

presents the solution for the minimal-coolant control of a seventh-order model of a nuclear rocket reactor with magnitude constraints on reactivity, coolant flow rate, and reactor power. Although such calculations were necessary to solve some practical problems, they also indicate the type of control process that is generally optimal. However, they are of limited use when applied to more complicated problems. (For a review of past work on optimal reactor control, see Ref. 3.)

The digital computer is an obvious tool that can be used most effectively with a quasi-linear-programming algorithm for solving more difficult problems. On the other hand, classical dynamic programming is unable to cope with high dimensionality. Gradient techniques also are ineffective because of divergent optimal modes for reactor problems. Divergent modes can cause the dynamic range of the digital computer to be exceeded during steepest gradient search techniques.

Numerical Algorithm

The algorithm used here is based on an iterative sequence of linear-programming problems. Each iterate of the sequence is formed from a linearization of (in general) nonlinear system equations about the previous iterate. Inequality magnitude and rate constraints on both state and control variables fit naturally into a linear-programming formulation. In addition, the linear approximation at each iterate can easily be forced to lie within a closed bounded region of state–control–time space, so that some problems of system instability are absent. Because of the Newtonian character of the algorithm, convergence (if it occurs) will be quadratic. For example, a convergence proof for a limited class of control problems is presented in Ref. 4. Even earlier, linear programming was suggested for the solution of optimal-control problems.[5]

*Present address: Kaman Nuclear, Garden of the Gods Road, Colorado Springs, Colo. 80907.

124

Assume that the optimal-control problem is to determine a vector function $\vec{u}$, within an admissible class of functions Ω that minimizes the integral criterion

$$J = \min_{\vec{u} \in \Omega} \int_{t_0}^{t_1} f_0(\vec{x}, \vec{u}, t) \, dt \qquad (1)$$

The vector functions $\vec{x}$ and $\vec{u}$ are constrained by the differential equation

$$\dot{\vec{x}} = \vec{f}(\vec{x}, \vec{u}, t) \qquad (2)$$

with $\vec{x}(t_0) = \vec{x}_0$. Furthermore, the components of the vector functions $\vec{x}$ and $\vec{u}$ (and possibly their rates of change) are required to satisfy the constraints

$$\alpha_i \leq z_i \leq \beta_i \qquad (3)$$

where z_i can be a component of either state or control (or, more generally, a linear combination of state and control).

The standard linear-programming problem is to determine a vector function $\vec{y}$ that minimizes (or maximizes) the linear-objective function

$$\Phi(\vec{y}) = \vec{c}'\vec{y} \qquad (4)$$

where $\vec{c}'$ is a constant row vector. Also, the vector function $\vec{y}$ must satisfy the constraints

$$A\vec{y} \leq \text{or} = \text{or} \geq \vec{b} \qquad (5)$$

where A is a matrix of constants and $\vec{b}$ is a constant vector. Finally, the individual components of $\vec{y}$ must be nonnegative.

To transform the nonlinear optimal-control problem into a form suitable for linear programming, we must obtain a set of discrete algebraic approximations to the continuous system of Eqs. 1 and 2, which can be done by standard numerical integration. For example, the calculations here use the second-order difference relations

$$\vec{x}_{i+1} - \vec{x}_i = \frac{\Delta t}{2} \left[\vec{f}(\vec{x}_i, \vec{u}_i, t_i) + \vec{f}(\vec{x}_i, \vec{u}_{i+1}, t_{i+1}) \right] \qquad (6)$$

The control function, $\vec{u}$, is assumed to be piecewise constant with $\vec{u}_i$ the control over $t_i < t < t_{i+1}$. Also, the integral criterion of Eq. 1 is approximated by the sum

$$J = \Delta t \sum_i f_0(\vec{x}_i, \vec{u}_i, t_i) \qquad (7)$$

The formulation of the linear-programming problem is completed by linearizing Eqs. 6 and 7 by retaining the first two terms (constant and linear terms) in the Taylor-series expansions (in "iteration space") of these equations. For example, the linearized representation of Eq. 6 used here is

$$\vec{x}_{i+1} - \vec{x}_i = \frac{\Delta t^*}{2} \left\{ \left[\vec{f}(\vec{x}_i, \vec{u}_i^*) + \vec{f}(\vec{x}_{i+1}, \vec{u}_{i+1}^*) \right] \right.$$
$$+ \left[\frac{\partial \vec{f}}{\partial \vec{x}_i} \bigg|_* (\vec{x}_i - \vec{x}_i^*) + \frac{\partial \vec{f}}{\partial \vec{x}_{i+1}} \bigg|_* (\vec{x}_{i+1} - \vec{x}_{i+1}^*) \right]$$
$$+ \left. \left[\frac{\partial \vec{f}}{\partial \vec{u}_i} \bigg|_* (\vec{u}_i - \vec{u}_i^*) + \frac{\partial \vec{f}}{\partial \vec{u}_{i+1}} \bigg|_* (\vec{u}_{i+1} - \vec{u}_{i+1}^*) \right] \right\}$$
$$+ \frac{1}{2} \left[\vec{f}(\vec{x}_i^*, \vec{u}_i^*) + \vec{f}(x_{i+1}^*) + \vec{f}(x_{i+1}^*, \vec{u}_{i+1}^*) \right] (\Delta t - \Delta t^*)$$

where the asterisk indicates evaluation at the previous linear-programming solution (similarly, the previous numerical-integration solution might be used).

Rate constraints can be incorporated by inequality constraints of the form

$$\vec{x}_{i+1} - \vec{x}_i \leq \Delta t \, \dot{\vec{x}}_{i \text{ max}}. \qquad (8)$$

The Computation

The linear-programming algorithm then is used to obtain an approximation to the optimal solution for startup of a nuclear rocket reactor. Briefly, the rocket engine (described in Ref. 2) operates by heating liquid hydrogen with a nuclear reactor. The rocket thrust is obtained most efficiently from the reaction force of hot hydrogen gas as it exhausts through a suitable nozzle. The optimality criterion is minimum hydrogen consumption, which can permit smaller on-board storage tanks and, therefore, greater payload.

The computational scheme can be illustrated in a simple manner by using the following differential equations to approximate the system:

$$\dot{Q} = \frac{u_1 - \beta}{l} Q + \lambda C \qquad (9)$$

$$\dot{C} = \frac{\beta}{l} Q - \lambda C \qquad (10)$$

$$\dot{T} = \frac{Q}{M_c} - a u_2 T \qquad (11)$$

where Q = heat generated by the reactor core
C = neutron-precursor level
$C(t_1)$ = free
T = average core temperature
u_1 = reactivity
u_2 = hydrogen flow rate
β = delayed-neutron fraction
l = mean neutron-generation time
λ = precursor decay constant
M_c = effective mass heat capacity of the core
a = convective heat-transfer coefficient

The optimality criterion is

$$J = \min_{\vec{u}} \int_0^{t_1} u_2(t) \, dt \qquad (12)$$

For safety, mechanical, and other physical considerations, the following inequality magnitude constraints are imposed on the variables:

$$0 \le Q \le Q_m, \quad 0 \le C, \quad 0 \le T \le T_m, \quad \dot{T} \le \dot{T}_m,$$

$$|u_1| \le \alpha, \quad |\dot{u}_1| \le \eta, \quad \text{and} \quad w_1 \le u_2 \le w_2$$

Optimal-control trajectories for the nuclear rocket reactor are evaluated numerically by using the quasi-linear-programming algorithm discussed in the previous section. The linear-program calculations were performed on an IBM-360/40 digital computer. The Mathematical Programming System 360 (MPS/360) was used, the input data for which were generated by a FORTRAN program (for details of these programs and their use for optimization, see Refs. 6 to 8).

Results

Figure 1 shows the results of a typical numerical calculation. An interesting feature of these trajectories is the apparent oscillatory behavior of reactor power when the temperature is increasing at maximal rate. This phenomenon is caused by the form of the system dynamics and the fact that the difference equa-

tions only approximate the continuous differential equations. By using the difference equation for temperature, we see that, along portions of the trajectory where temperature is increasing at maximal rate,

$$Q_{i+2} - Q_i = -(Q_{i+1} - Q_i) + 2au_{2i}M_c\dot{T}_{max}.\Delta t \quad (13)$$

If the flow rate, u_2, is on its lower bound, Eq. 13 indicates that Q consists of an alternating term superimposed on a linear term. Numerical evaluation of the linear term shows that the slope is very small.

Figure 2, which shows the behavior of the trajectories when the time increment, Δt, is approximately halved, illustrates the behavior of Eq. 13 in more detail. The linear part of Eq. 13 is shown as a dashed curve.

COMPUTING TIME

The IBM-360/40 computing time to obtain the trajectories of Figs. 1 and 2 is approximately 80 min each. Obtaining the starting iteration required that the differential equations be integrated using maximum reactivity and minimum flow rate, for 1.5 min as suggested by the analysis in Ref. 2. Seven itera-
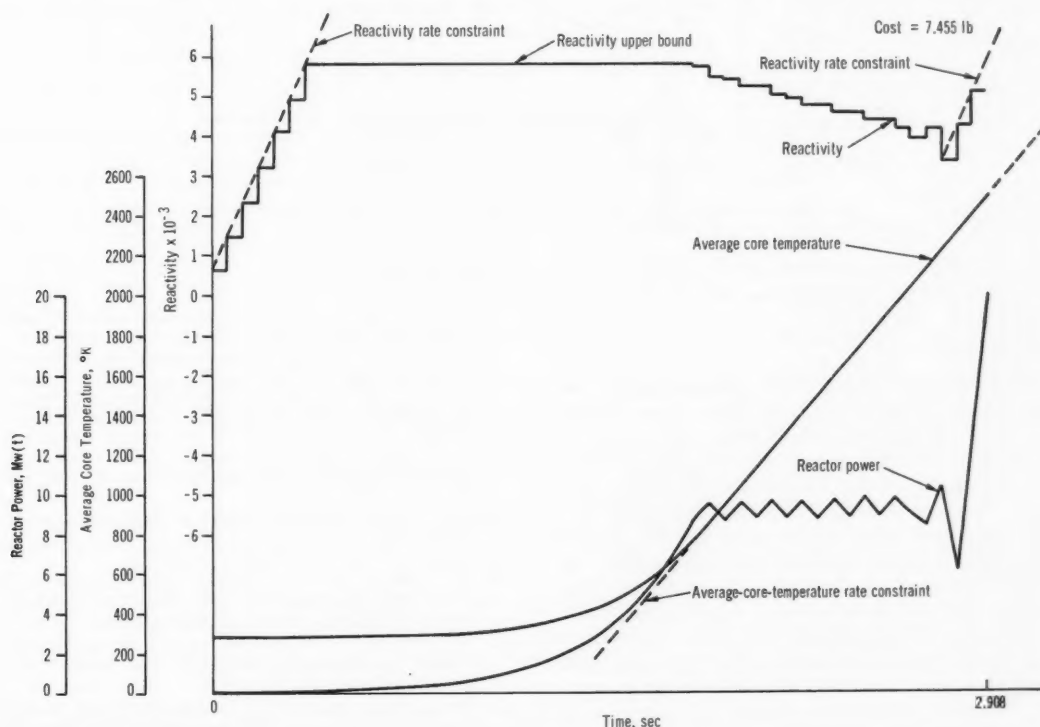

Fig. 1 Nuclear rocket reactor trajectories with temperature rate constraint of 1600°K/sec and control rate constraint of 0.015/sec. The hydrogen flow rate was on its lower bound (2 lb/sec), except that it was 30.17 lb/sec in the last interval.
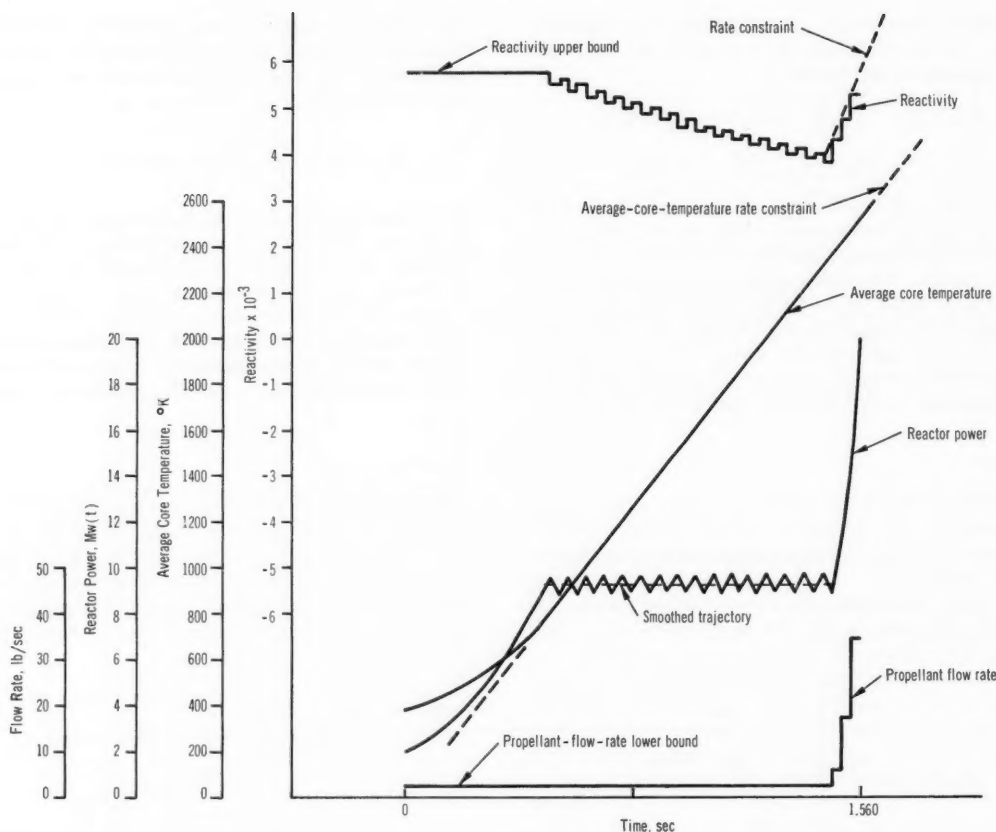
Fig. 2   Nuclear rocket reactor trajectories with increased definition.

tions with 50 time increments were required to ob-
tain convergence to approximately one part in 10^6.

Conclusions

Linear programming can be effective in solving
many optimal-control problems with a large number
of inequality constraints in both state and control. As
an example, the fuel-optimal startup of a nonlinear
nuclear rocket reactor is computed by means of a
digital computer. Although the quasi-linear-program-
ming algorithm yields only a local optimum, Ref. 6
shows that singular solutions do not exist for the
problem analyzed here, and physical reasoning along
with the analysis made in Ref. 2 makes optimality of
the computed trajectories almost certain. On the other
hand, the control synthesized in practice would most
likely be a suboptimal approximation to the numeri-
cally computed trajectories unless the reactor sys-
tem used an on-line digital computer.

References

1. George F. Hadley, *Linear Programming,* Addison-Wesley
   Publishing Company, Inc., Reading, Mass., 1962.
2. R. R. Mohler, Optimal Nuclear Rocket Engine Control,
   in *Neutron Dynamics and Control,* pp. 137-163, Tucson,
   Ariz. Apr. 5-7, 1965, D. L. Hetrick and L. E. Weaver
   (Coordinators), AEC Symposium Series, No. 7 (CONF-
   650413), May 1966.
3. R. R. Mohler, Let's Apply Optimal Control Theory and
   Nonlinear Analysis, *Power Reactor Technol.,* 9(4): 169-
   173 (Fall 1966).
4. J. B. Rosen, Iterative Solution of Nonlinear Optimal-
   Control Problems, *SIAM (Soc. Ind. Appl. Math.) J.
   Contr.,* 4(1): 223-244 (February 1966).
5. L. A. Zadeh and B. H. Whalen, On Optimal Control and
   Linear Programming, *IEEE (Inst. Elec. Electron. Eng.)
   Trans. Automat. Contr.,* 7: 45-46 (July 1962).
6. R. R. Mohler and H. J. Price, Optimal Nuclear Reactor
   Control, USAEC Report SC-CR-67-2746, Sandia Corp.,
   August 1967.
7. *Mathematical Programming System 360 (360A-CO-14X)
   Control Language User's Manual,* International Business
   Machines, Armonk, N. Y. 10504, 1966.
8. *Mathematical Programming System 360 (360A-CO-14X)
   Linear Programming User's Manual,* International Busi-
   ness Machines, Armonk, N. Y. 10504, 1966.

Large Valves for Liquid-Metal-Cooled Reactors

By O. S. Seim

Valve deficiencies and the lack of operating experience have shaped the general design practice pertaining to the use of valves in liquid-metal-cooled reactors. This practice for large sodium-cooled plants has been to avoid the incorporation of valves, if possible.

Valves are needed in liquid-metal coolant systems for the same reasons that they are needed in conventional systems—to isolate loops from the system, to regulate and direct coolant flow, and to protect the system and particularly the pumps against flow reversal (see Fig. 1).

Valve design requirements have been summarized[1] on the basis of fast reactor conceptual designs by Allis-Chalmers,[2] Atomics International,[3] Combustion Engineering,[4] General Electric,[5] and Westinghouse.[6] Service conditions include normal operating temperatures to 1140°F, transients to 1200°F, and pressures to 150 psig. Future liquid-metal-cooled fast breeder reactors (LMFBR) will almost certainly include:

• Check valves ~30 in. in diameter, designed for a 20-year life in primary-loop service, a radiation environment of ~10^5 r/hr.

• Flow-control valves 12 to 20 in. in diameter for 20-year life in secondary loops. Some of these flow-control valves must have good control in the 20 to 50% range; others must be capable of throttling the secondary system to 10% of rated flow within 2 sec.

If such valves are available, future LMFBR's will probably use:

• Blocking valves ~30 in. in diameter for isolation service in secondary loops.

• Slow-response control valves to throttle the discharge from constant-speed pumps and thus eliminate the need for variable-speed pumps.

The technical problems—leakage and sticking—in the development of valves for high-temperature-sodium service, and the high cost, have prohibited valve manufacturers from testing in liquid-metal loops. But these tests are required if we are to acquire the operating experience needed to ensure reliability. One way to obtain this experience is to
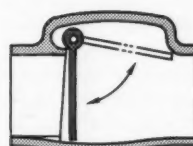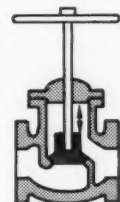

Disk hinged at one edge permits flow in only one direction.

Check Valve

Disk pivots around a central axis to block or regulate flow.

Butterfly Valve

Gate is lowered to block flow and thus to isolate a loop. It is not used to regulate flow.

Gate Valve

Cone with a throughport is rotated 90° to block or open flow.

Plug Valve

Disk is moved toward or away from seat to regulate or block flow.

Globe Valve

Ball within cage is moved axially to block or regulate flow.

Ball Valve

Fig. 1   Valve forms and functions.

establish a jointly financed test facility to be used by all concerned. The advantages of such a facility — less expensive testing and uniformity of test procedures — would result in more accurate evaluations.

Future Applications

Performance and maintenance expectations will largely determine valve application in LMFBR's. In the past, valves from 2 to 16 in. in diameter have been used in liquid-metal coolant systems with varying — but limited — success. Generally, these systems have been associated with programs designed to advance the development of coolant·technology — not valve technology. As a result, the usual approach has been to tolerate valve deficiencies or to eliminate the valves. Design studies[2-6] of liquid-metal-cooled 1000-Mw(e) plants have used existing valves and then only where absolutely necessary; in one design[6] the need for valves was eliminated altogether.

Multiple parallel reactor cooling circuits will be required. It seems desirable to design for operation with some of the circuits inoperative. To accomplish this, the system must include numerous large-diameter valves with (effectively) no seat leakage. Valves can, of course, be installed in series, and

seals can also be made by freezing the liquid metal, but these techniques increase both the cost and complexity of the system.

PROPOSED PLANT CONCEPTS

Two concepts of liquid-sodium coolant systems are presented in Ref. 1. Each of these concepts includes six primary loops; these were necessary to keep the component size within the limits of current technology. Each concept uses a minimum number of valves; no provisions have been made to apply valves to shut off the coolant from any of the circuits and to continue operation with some of the cooling circuits inoperative. One concept uses six 30-in. check valves and six 12-in. shutoff flow-control valves. The other concept uses six 30- and 28-in. check valves, plus two 20-in. and six 12-in. shutoff flow-control valves. The check valves are used at the discharge of each of the variable-speed pumps. The 12-in. valves are proposed for the steam-generator bypass lines. The 20-in. valves are proposed for reheater sodium-outlet lines.

Flexibility. Figure 2 shows a plant concept with greater flexibility. This design includes 24 large-diameter valves in the main coolant-circulating system — 12 check valves (24 in.) and 12 shutoff flow-
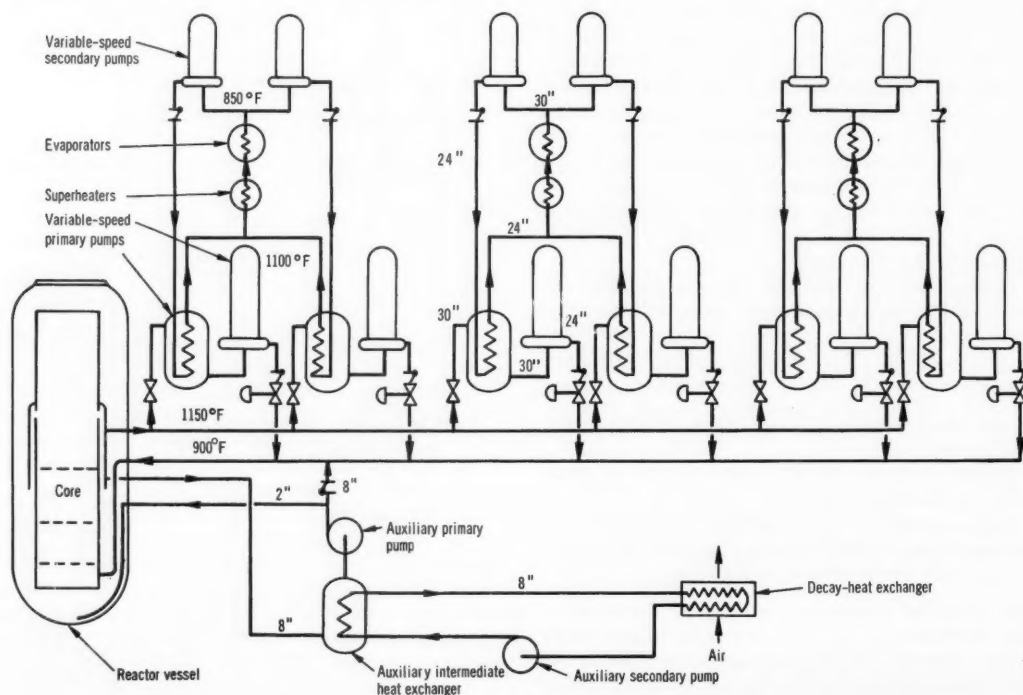

Fig. 2 Schematic of a large LMFBR. This design uses six primary loops and incorporates 24 large valves — enough to permit simultaneous reactor operation and loop repair.

control valves (six 24 in. and six 30 in.). These three concepts show that a larger number of valves can increase operational flexibility and permit continuous operation during loop repair.

AVAILABILITY

These concepts propose the use of valves up to 30 in. in diameter for sodium flow rates of 19×10^6 lb/hr. However, there are no tested sodium valves available over 16 in. in diameter; further, the valve study program[1] indicates that, although some of the smaller valves have been successful, they have design features that are not suitable for extrapolation to these larger sizes. Experience obtained with smaller valves has identified some of the major problem areas associated with valves for sodium service.

Valve-Development Problems

The application of valves in sodium-cooled systems has introduced many problems not encountered (or not so serious) in the more conventional water- or gas-cooled systems. These problems include radioactive coolant, leakage of sodium at valve seats and stems, reaction of sodium with the atmosphere, self-welding and galling, excessive space requirements, sodium hammer, and — probably the most important — cost.

COOLANT

Pure sodium is not corrosive, but trace leakage to an air atmosphere forms a concentrated hydroxide solution which, at high temperatures, is very corrosive to stainless steels. Larger leaks (to air) cause fires. In addition, sodium in the primary coolant circuits of liquid-metal systems becomes very radioactive (^{24}Na; half-life, 15 hr). As a consequence, these loops must be shielded to prevent excessive radiation exposure.

Components are usually installed in steel-lined cells with concrete shielding walls up to ~6 ft thick. The cells contain an inert gas to exclude oxygen and prevent corrosion.

Maintenance work on the valves or loops contained within the shielding must be delayed for several days after reactor shutdown to allow radiation decay before opening the cells. Moreover, if the insulation must be removed from a valve area for maintenance, the trace heating system that is wrapped around the components (to melt or maintain the liquid sodium above its melting point of 208°F) must be unwound and later replaced — another delay.

LEAKAGE

The potential for corrosion and fire makes zero leakage at valve seats and stem seals a necessary goal of valve design.

Seat Leakage. Only with confidence that a valve will have zero seat leakage is it practicable to shunt the liquid metal to one of the parallel cooling circuits and isolate a primary-circuit loop for maintenance. Seat leakage usually results from distortion of nonuniform metal thicknesses caused by high temperatures and steep temperature transients. Rapid temperature changes in the liquid metal are transferred to the valve materials without attenuation because of the very high heat-transfer capabilities of liquid metals. As a result, designers must compensate for steep temperature transients. Reference 7 discusses possible design approaches such as freestanding valve-seat configurations.

Stem Leakage. Zero stem leakage is also necessary for valves in liquid-metal service. To prevent leakage, three types of stem seals can be used, either individually or in combination:

(1) Bellows seals — The bellows seal consists of metal bellows welded at both ends to the valve components to contain the liquid sodium. Bellows may be arranged in tandem so that both must fail if the liquid sodium is to leak to atmosphere. Another alternate is to use bellows of multiple-ply construction.

(2) Freeze seals — An area around the stem is cooled enough to freeze the metal coolant. Cooling coils, if used for this seal with water or certain organic coolants, may be a problem. It is preferable to use convection cooling with ambient gas over fins attached to this area.

(3) Stem packings — Packing is usually employed as a secondary stem seal; seldom is it used alone. Graphitized asbestos reinforced with Inconel wire or nickel braid is preferred because of its high-temperature properties.

MECHANICAL FACTORS

Other factors that should influence the design of valves for sodium service include a tendency for self-welding, the problem of sodium hammer, and the space requirements when designs are scaled up.

Self-Welding. Self-welding between two metal surfaces submerged in liquid sodium does occur.[1] The degree of self-welding appears to depend on the contact materials, temperature, and time rather than contact pressure. Below 1200°F, self-welding is generally considered to be no problem. However, the self-welding tendency may lead to galling at considerably lower temperatures.

Hammer. Sudden flow stoppage — always the cause of hammer in pipelines — can produce excessive forces and damage components. Sodium hammer is easily brought about by the buildup of sodium oxide between the pin and sleeve of a check valve; the oxides may bind and prevent the flapper from closing gently as flow reverses. Until sufficient reverse-flow pressure is built up to break the resistance

from these oxides, the flapper remains open. Then it slams shut and stresses the system.

Excessive Space Requirements. The necessity for removable shielding, which is expensive, puts a premium on small components for liquid-metal systems. As a result, some designs should not be considered. For example, although the gate valve has a very promising record in small sizes, it is unsuitable for extrapolation. The stem length for bellows travel required (as much as 28 ft for a 30-in. valve) as well as the length for the stem seal would be beyond practical dimensional limits.

COST

Because there are no large sodium valves, there is no adequate history on which to base maintenance predictions. In addition, because maintenance of liquid-metal valves is difficult, costly, and time-consuming, conventional valve reliability is insufficient. The high cost of the valves and their maintenance may logically influence nuclear plant designers to minimize the number of valves required.

Suppliers of 30-in. valves cannot test them in a liquid-metal environment, so the cost of these specially designed valves is not easily evaluated or even available from any valve manufacturer. Estimates for 30-in. valves range from $40,000 for a balanced swing-cycle check valve to $125,000 for an in-line flow-control valve including the internal operator portion of its control system.[1] A bellows-sealed flow-control valve would cost $8500 more than the freeze-sealed-stem version of the same valve ($87,000).[1] Because of the high cost of quality bellows, this seems to be a realistic difference.

Valve Experience

In addition to the limited experience with valves in liquid-metal-cooled reactors (Table 1), some experience has accumulated through the operation of test loops by Atomics International, Argonne National Laboratory (ANL), Atomic Power Development Associates, General Electric, Pratt & Whitney, and Mine Safety Appliances Co.[8] Valves in service include check valves and various bellows-sealed and freeze-sealed units designed for throttling and isolation service.

CHECK VALVES

Figures 3 and 4 show check valves that have been employed in sodium service. At the Fermi plant it was found desirable to add a dashpot to avoid valve hammer.[9] The check valves at the Hallam Nuclear Power Facility had a tilted seat similar to Fig. 4 to cause the valve disk to hang open and permit unobstructed flow rates of less than 10% flow.

Examination of a 304 stainless-steel swing check valve that had locked in the open position in the Sodium Reactor Experiment (SRE) facility disclosed that the disk-supporting bushings were not aligned and carbonaceous material had deposited between the shaft surface and the supporting bushings.[10] The shaft could not pivot freely in the bushings, but the disk turned on the shaft. The check valve was located in the cold leg of the system, and the valve bushings provided a low turbulence area which trapped oxides and carbon.

The Experimental Breeder Reactor II (EBR-II) uses single primary and secondary sodium coolant loops but does not require check valves because the primary loop contains two pumps in parallel; the use of check valves is avoided by permitting (on reactor scram) a reverse flow through the nonoperating or failed pump. Because of the one operating pump, flow in the forward direction remains at $\sim \frac{1}{3}$ normal, which is more than adequate under reactor scram conditions.

BELLOWS-SEALED VALVES

Globe, gate, ball, and plug valves with bellows stem seals have been used successfully at various loca-

Table 1 LARGE VALVES IN LIQUID-METAL-COOLED REACTORS

| Reactor	Valve function	Total valves in loops		Valve specifications			Service conditions				Remarks
		Primary	Secondary	Size, in.	Body material (stainless-steel type)	Stem seal	Liquid metal	Approx. temp., °F	Approx. pressure, psi	Approx. flow, gal/min	
EBR-I[19]	Block	8	7	4, 6	347	Double bellows	NaK	600	20	291	Monitored between bellows
EBR-II[20]	Throttle	2	0	4	304	Close clearance	Na	700	56	630	Outer blanket flow control
Fermi[20]	Throttle	3	0	6	304	Double bellows	Na	600	118	1,000	Blanket flow control
	Check	3	0	16	304	None	Na	600	118	10,000	
Hallam[8]	Block	6	3	14, 16	304	Freeze seal	Na	950	57	6,750	Throttle on decay flow
	Check	3	0	16	304	None	Na	610	57	6,750	
SRE[21]	Block	2	7	6	304	Bellows and freeze seal	Na	850			
SRE-PEP[22]	Block	0	4	4, 6	304	Bellows and freeze seal	Na	1160	47	1,540	
	Throttle	1	0	8	304	Torque tube	Na	650	19	1,420	Cone-type electromagnetic brake backup
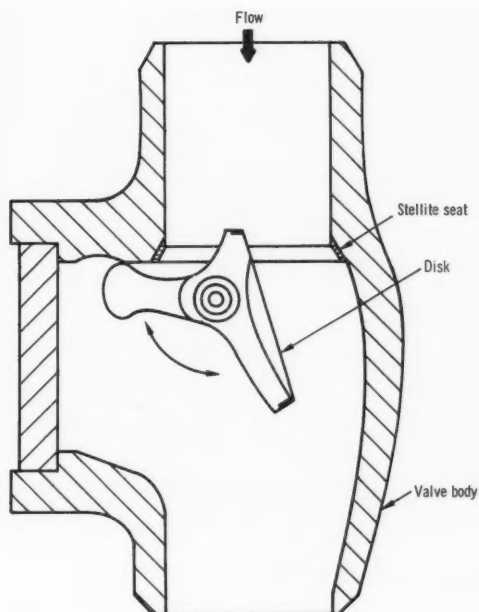
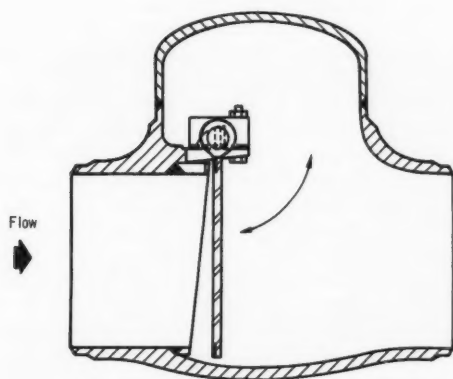Fig. 3 *Check valve of the type used in the Fermi reactor.*[9]

Fig. 4 *Check valve used at Hallam included a tilted seat to reduce low-flow resistance.*[18]

tions and in numerous test loops. Generally, all with extended high-temperature service have exhibited some seat leakage, which is attributed mainly to accumulated thermal distortion.

Stem Seal Problems. Occasionally a bellows seal fails because of vibration in the loop. One of these failures occurred in an ANL test loop because a long horizontal bellows sagged, rubbed on the valve stem, and wore away. In all the bellows-seal failures of recall, the secondary stem packing (usually braided

nickel) restrained the leakage to an amount small enough to preclude ignition.

The only major valve problem in the SRE reactor heat-transfer system was caused by the bellows seals.[10] Valve bellows were ruptured during attempts to operate a valve while a portion of the sodium in the bellows was frozen. Valve bellows also ruptured during preheating of a pipe system because thawing was not initiated at a free surface—there was no room for expansion.

Of the bellows-sealed valves used in auxiliary portions of the Hallam sodium heat-transfer systems, approximately 12% suffered bellows failures that were generally associated with throttling over a period of several years.[11] Under these conditions the bellows vibrated to the extent that it could be detected audibly when the pressure drop across the valve was high. These oscillations eventually led to fatigue failure of the bellows. In some instances a system revision reduced the pressure drop required of the valve.

Globe and Gate Valves. Globe, wye-pattern globe, and gate valves with bellows seals have been used in small systems (≤ 3 in.) for throttling with small pressure drops. Operation for many hours at high valve pressure drops has resulted in bellows failure. Twelve-inch wye-pattern gate valves[12] used in test loops at ANL had excessive vibration (0.1-in. maximum piping displacement) at pressure drops above 40 psi. This vibration was alleviated by installing an orifice in series with the valve to reduce the pressure drop in the valve to 10-psi maximum. No valve-stem sealing-bellows failures occurred in the 16,000 hr of operation of this configuration.

Special 3-in. globe valves of 316 stainless steel were designed and tested[13] in NaK at temperatures to 1500°F and in lithium at 1000°F for the CANEL project. With improved seat-lapping methods, the seat leakage at 15-psi pressure differential was about 30 cm^3/day; no stem leakage was observed. Stem seals in these valves were formed double-ply primary and edge-welded secondary bellows. Five bellows assemblies were mechanically cycled 1000 times (each) and did not fail.

Plug Valves. An advantage of the plug valve is its low pressure drop. Chief disadvantage is that seat leakage may be expected to be relatively high for a high-temperature plug-type valve. There are two reasons: (1) because it is difficult to have quite massive castings completely free of distortion at elevated temperatures, some minute deformations will occur and will create seat-leakage paths; (2) liquid-metal oxide particles may lodge between valve seating surfaces and hold them apart to produce leakage paths.

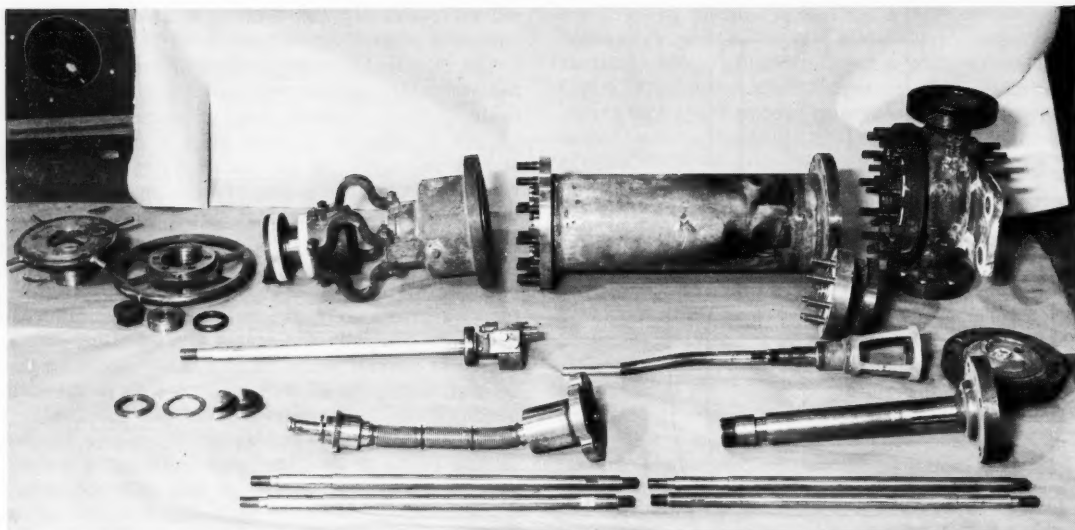A rotating plug concept (Fig. 5) developed at ANL uses a bellows closure over a crank-type drive with

Fig. 5   Components for a rotating plug valve with a flexible bellows seal.

associated gearing to eliminate torsion on the bellows. Only a bending motion is required of the bellows. The required 90° rotation of the valve plug is accomplished with a bellows-sealed crank attachment on the plug. The crank is rotated by a planetary gear drive. A jack (driven by a handwheel) is used to raise and lower the valve plug a slight distance to unseat the plug for rotation. A slight change in bellows length accommodates the vertical movement of the plug.

A plug valve of this design was tested statically in the facility shown in Figs. 6 and 7. Electrical level probes located in pipe legs pressurized with argon were used to measure leakage rates at various temperatures and with pressure differentials of 5 to 30 psi.

Almost all bearing surfaces in the stainless-steel portions of the valve as well as the sliding surfaces of the valve plug and valve body wetted by the sodium were provided with hardened surfaces (Stellite 6 or Colmonoy 6), or were of Inconel X. The plug-lifting mechanism always performed perfectly, but the drag on the rotation mechanism slowly increased and rotation became difficult.

Final disassembly and inspection of the valve showed no significant wear on the valve seating surfaces. Because there was no oxide-removal system in this test facility, the oxide content approached saturation at the operating temperature and increased the severity of the test. Figure 8 shows the valve plug and the valve body after sodium test. Figure 9 shows the typical scatter obtained during the leakage tests of this valve.

Ball Valves. Bellows-sealed ball valves can be built with the desirable feature of in-line flow in the full open position. The linear seating surface where the ball seats against its seat ring is made as short as possible so as to minimize leakage. (A short seating contact and a spherical closing ball minimize thermal distortions.)

A valve of this type was tested at ANL in the installation shown in Fig. 10. The valve seat, valve ball, and wearing surfaces on the ball support cage were surfaced with a hard Stellite facing material. During the entire 11,600 hr that the valve was in sodium test service, the operating mechanism performed smoothly. Figure 11 shows the spread of test data for the five temperature levels (400 to 1050°F) employed. The greater seat leakage at 450°F was repeated in most of the tests and probably resulted from an increase of oxide precipitated as the sodium temperature was reduced below the saturation temperature for the amount of sodium oxide present.

FREEZE-SEALED VALVES

There is sodium test-loop experience with freeze-sealed ball, globe, gate, and butterfly valves. In addition, freeze-sealed ball valves were used in the Hallam Nuclear Power Facility with modest success (see Table 1).

Seal Performance. Operating experience with valve freeze seals in various test loops, such as the Large Component Test Loop (LCTL) at Atomics International,[14] shows that repetitive strokes and natural cold trapping on longitudinal-motion valves lead to
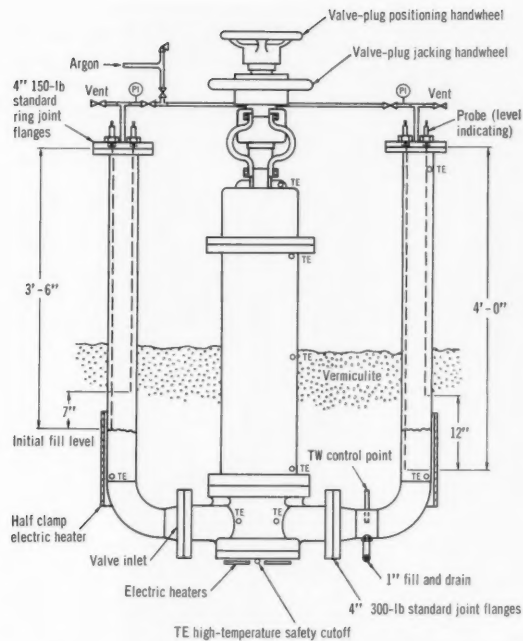
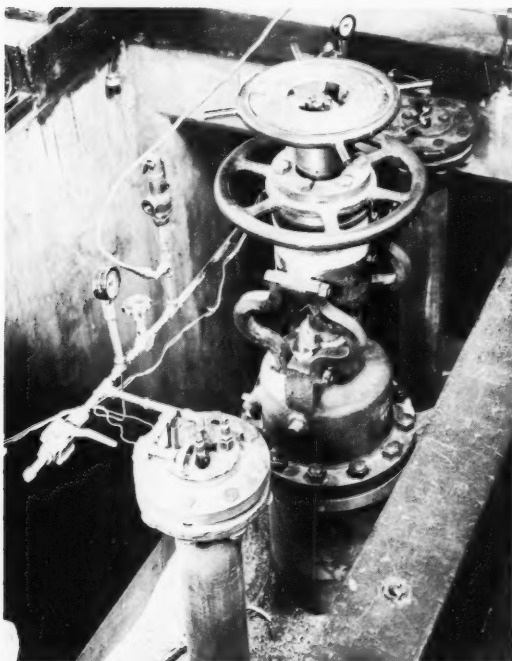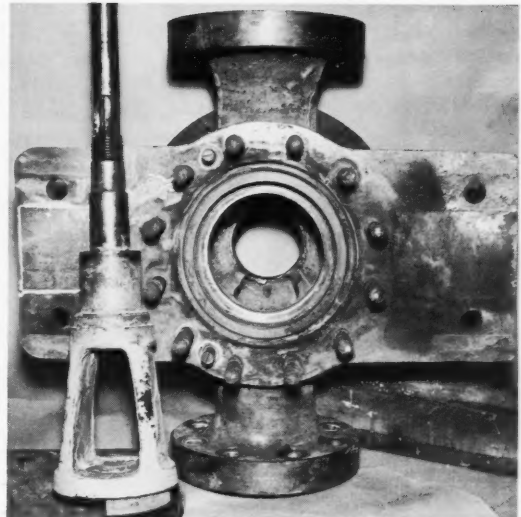Fig. 6 Static test facility used to test 4-in. plug valves.

Fig. 8 Condition of valve plug and body after 6075 hr of test operation at temperatures from 500 to 900°F.

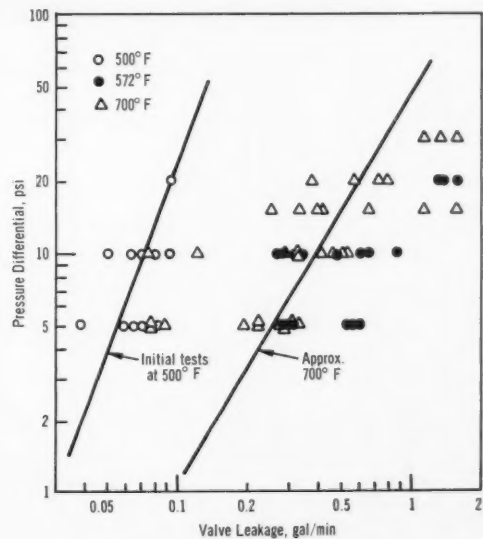Fig. 7 Sodium test facility of Fig. 6 with rotating plug valve under test.

Fig. 9 Typical scatter obtained in leakage measurements with a 4-in. plug valve.

oxide deposition along the valve stems. In as little as 6 months of operation, valve stems may become bound. The sodium-wetted valve stem gathers oxygen when fully open, and oxide precipitates lodge in the area of low solubility adjacent to the frozen sodium.

Bound valves have been restored by pressurizing with inert gas between the frozen shaft and the ex-
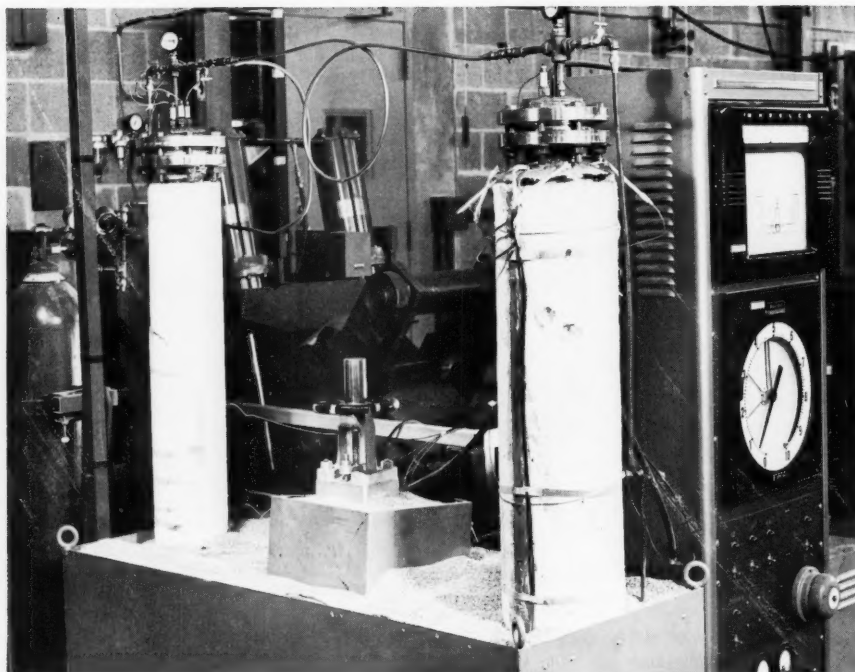
COMPONENTS

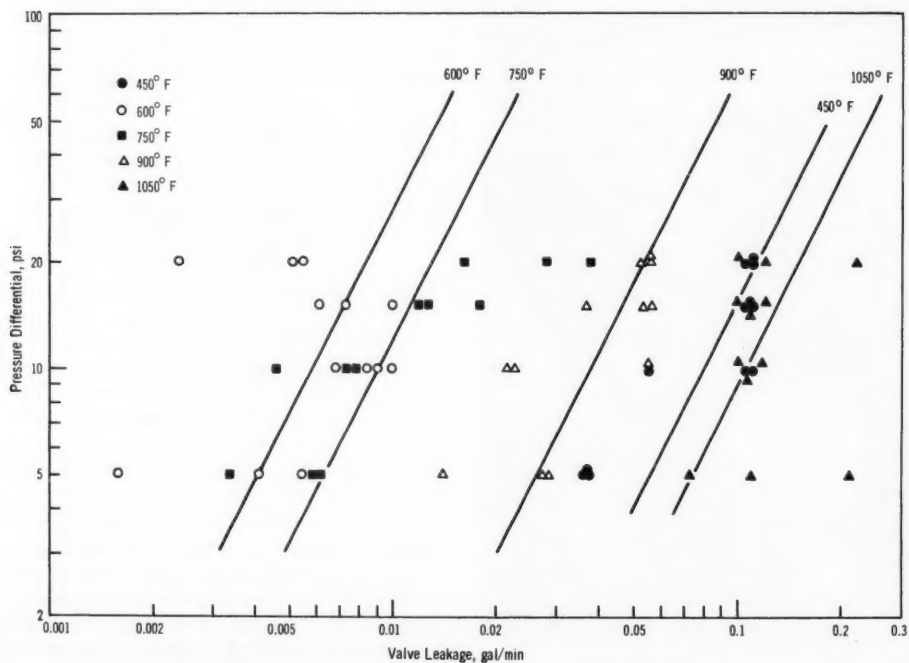Fig. 10 Facility used for testing bellows-sealed ball valves at ANL.

Fig. 11 Test data for five temperature levels obtained during evaluation of a ball valve in the facility in Fig. 10.

ternal packing. This allows the valve to heat up and forces the impurities into the sodium system. (But this restoration procedure is not acceptable for a reactor system because the fuel coolant passages are small and plugging there must be avoided.) Valve freeze seals have operated well on constant-position throttling service, but poorly on modulating service.

Ball Valves. Atomics International tested two 12-in. ball valves that were provided with water-cooled freeze-sealed stems.[15] Each valve incorporated a secondary high-temperature packing as the usual safety measure. The valve seals were subjected to a differential pressure of 50 psi and did not leak at any time. These two valves were thermally cycled at the rate of 3°/min between 680 and 1060°F; seat leakage from the better valve increased to 0.5 gal/min at 900°F after 236 cycles.

A refinement of these ball valves (Fig. 12) was evaluated[15] and used at the Hallam Nuclear Power Facility (see Table 1). The refinement was the installation of an extended valve-seat support that reduced the disto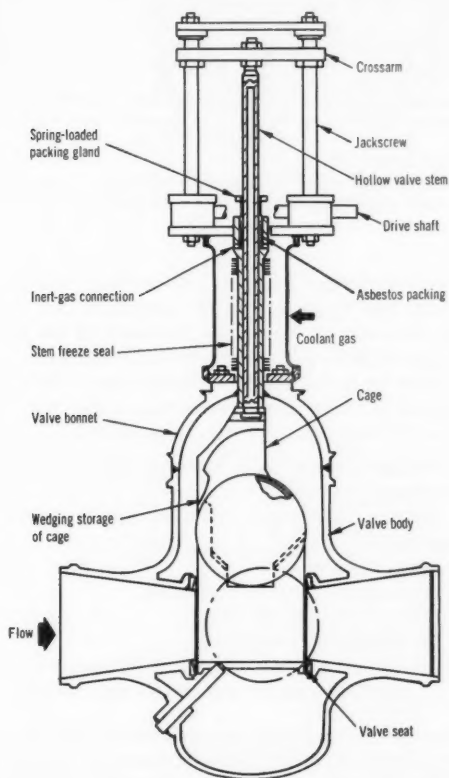rtion of the seat area. These valves were equipped with forced-convection gas-cooled stem freeze seals designed by Atomics International. They were installed as primary- and secondary-system throttle valves to close quickly on reactor scram and reopen to throttle convective flows as required for reactor decay-heat removal. Valve actuation difficulties were experienced as a result of starting friction, which was increased by the accumulation of sodium oxide in the stem seal.[11]

Globe and Gate Valves. Several designs have used freeze seals to prevent leakage around the stems of globe and gate valves. Figure 13 shows one of these
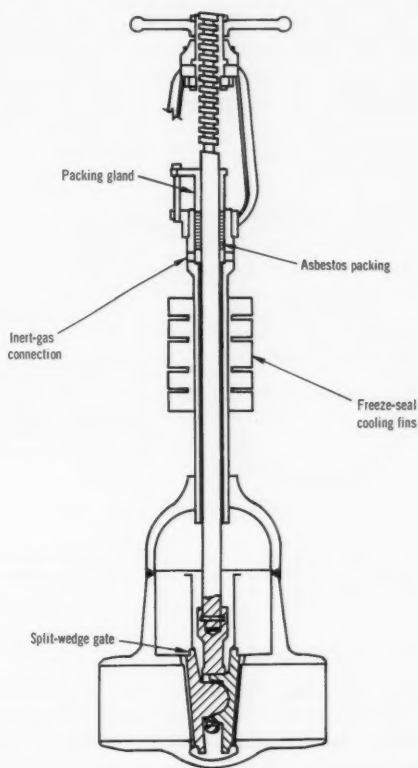

Fig. 13 Gate valve with a gas-cooled freeze seal in the stem.[7] The split wedge provides two seat seals and improves effectiveness.

designs that is provided with forced-convection gas cooling.[16]

Two 12-in. gate valves of a similar design, but water cooled, were fabricated by Crane Co. and Cooper Alloy Co.; these valves had secondary stem seals of high-temperature packing.[15] In tests, no stem leakage occurred while the valves were at 50 psi and 900°F. Seat leakage was also reported to be zero for both valves under thermal-cycling con-

Fig. 12 Design of a ball valve in which the stem seal is effected by freezing sodium with a coolant gas.[7] A secondary high-temperature asbestos packing is also provided.

COMPONENTS

ditions (160 cycles with temperature changes at 3°/min between 680 and 960° F and 200 cycles at 6°/min between 960 and 1090° F).

The good results are attributed to the wedge design (Fig. 13), which provides two seat seals—one on each face of the wedge. The pressure between the seat seals was not measured; however, it may have been low, which would improve the effectiveness of the stem seal. Regardless, a high-temperature packing was used as a backup for the stem seal.

Butterfly Valves. Figure 14 shows the general nature of a butterfly valve with a freeze-sealed stem. Six of these butterfly valves[14] have been built by Fisher-Continental for the Sodium Component Test Installation (SCTI) operated by Atomics International. Because the stem merely rotates, this type of valve appears promising for modulating service where seat leaktightness is not mandatory.
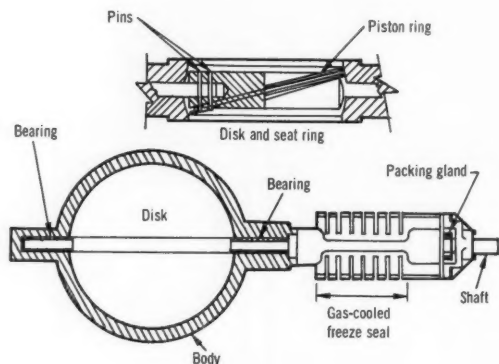

Fig. 14 A butterfly valve with a freeze-sealed stem now being tested[14] seems promising for service where zero seat leakage is not required.

TORQUE-TUBE-SEALED PLUG VALVE

Figure 15 shows a plug-valve design in which the stem is sealed with a welded multiple-torque-tube assembly. The operator rotates the plug by twisting the tube assembly. A 60° rotation valve of this type was built by the Ohio Injector Co.[17] for flow throttling, not tight closure. In tests at the SCTI, perfect shaft sealing was maintained. The tests included −30° F/sec thermal shocks from 1000 to 850° F and extended operation at 1200° F. After thermal distortion in the valve body (0.010 in.) and in the leading edge of the closing gate (0.002 in.) reduced the original clearance (0.012 in.) to zero, the binding was alleviated by machining.

Conclusions and Recommendations

Generally, the design and study programs (Refs. 1, 7, 13, and 18) agree that the principal valve problems
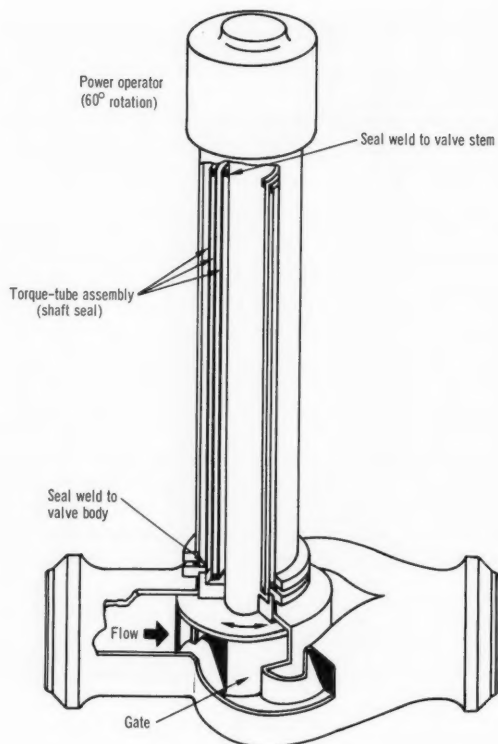
Fig. 15 Welded-seal torque-tube plug valve operates on principle of twisting the long tube assembly to rotate the plug.

are seat and stem leakage, self-welding, and valve sticking; that check valves are essential; that fast-acting flow-control valves are not essential but would add significantly; and that conventional valves cannot be scaled up successfully. Although each of the study programs contains some recommendations, they are essentially summed up in Ref. 1, as follows:

1. Design the new 30-in. valves so that they can be extrapolated to 42 in.

2. Develop five valve concepts for final design evaluation:
  (a) A check valve.
  (b) An angle flow-control valve.
  (c) An angle shutoff valve.
  (d) A butterfly valve.
  (e) An in-line flow-control valve for combination flow-control and shutoff application.

The interest in larger liquid-metal-cooled reactor power plants normally would be incentive enough for the valve manufacturer to develop and test the larger valves required. But the high cost of valves and of testing facilities makes it impossible for each manufacturer to set up liquid-metal test loops. Yet the

burden of the test program could easily be shared among all concerned; a joint test facility where any manufacturer or buyer could test valves would be economically justified. Uniformity of test results and more accurate evaluations are added incentives for the establishment of such a facility.

References

1. L. E. Phillips and J. M. Horn, Conceptual Design of Large Sodium Valves, USAEC Report ACNP-65579, Allis-Chalmers Mfg. Co., March 1966.
2. Allis-Chalmers Mfg. Co., Large Fast Reactor Design Study, USAEC Report ACNP-64503, January 1964.
3. Atomics International, 1000-MWE SGR and Prototype Evaluation Study, USAEC Report NAA-SR-9213, December 1963.
4. Combustion Engineering, Inc., Liquid Metal Fast Breeder Reactor Design Study, USAEC Report CEND-200, January 1964.
5. General Electric Company, Atomic Power Equipment Department, Liquid Metal Fast Breeder Reactor Design Study, USAEC Report GEAP-4418, January 1963.
6. R. B. Steck (Comp.), Liquid Metal Fast Breeder Reactor Design Study, USAEC Report WCAP-3251-1, Westinghouse Electric Corp., January 1964.
7. O. J. Foust (Ed.), *Liquid Metals Handbook*, Chap. 13 — Valves, Liquid Metal Engineering Center, Atomics International, to be published.
8. Atomics International, Liquid Metal Engineering Center Quarterly Technical Progress Report, July-September 1967, USAEC Report NAA-SR-12585, Nov. 15, 1967.
9. J. J. Morabito, Sodium Components in Nuclear Reactor Systems, Proceedings of the American Power Conference, XXVI, Chicago, Ill., April 1964.
10. A. I. Hansen, The Effects of Long-Term Operation on SRE Sodium System Components, USAEC Report NAA-SR-11396, Atomics International, Aug. 31, 1965.

11. J. E. Price (Comp. and Ed.), Final Evaluation Report — Hallam Nuclear Power Facility, Vol. I, USAEC Report NAA-SR-9777, Atomics International, Sept. 29, 1964.
12. F. D. Cotterman and W. S. Black, Valves and Throttling Devices Used for Molten Sodium, Technical Report No. 1, USAEC Report AECU-4709, Corwith Co., Apr. 24, 1959.
13. D. E. Smith, LCRE Valve Development. Final Report. USAEC Report PWAC-401(Pt. II), Pratt & Whitney Aircraft Division, United Aircraft Corp., May 4, 1964.
14. R. Cygan and W. Hallett, Atomics International, personal communication, Apr. 29, 1964.
15. C. J. Baroczy, Thermal Cycling and Leakage Tests of 12-Inch Valves for Sodium Service, USAEC Report NAA-SR-4947, Atomics International, May 1, 1960.
16. B. Brooks, R. Galantine, and F. Bergonzoli, The Selection, Design Modification, and Analysis of Sodium Valves for Hallam Nuclear Power Facility, USAEC Report NAA-SR-5463, Atomics International, Dec. 1, 1960.
17. Atomics International — Sodium Components Test Installation, Sodium Control Device, Technical Report, USAEC Contract No. AT-(11-1)-680, Feb. 23, 1960.
18. Atomics International, Final Summary Safeguards Report for the Hallam Nuclear Power Facility, USAEC Report NAA-SR-5700, Apr. 15, 1961.
19. R. O. Haroldsen et al., Safety Analysis Report, EBR-I, Mark IV, USAEC Report ANL-6411, Argonne National Laboratory, February 1963.
20. Atomic Power Development Associates, Inc., Enrico Fermi Atomic Power Plant, USAEC Report APDA-124, January 1959.
21. J. O. Nicholson, SRE Heat Transfer System Demolition, USAEC Report NAA-SR-11414, Atomics International, Aug. 31, 1965.
22. W. J. Freede and J. K. Roberts (Eds.), Sodium Reactor Experiment Power Expansion Program, Heat Transfer Systems Modifications, USAEC Report NAA-SR-10379, Atomics International, October 1964.

Toward Automatic and Continuous Plugging Meters

By Stanley B. Skladzien

The purity of the sodium coolant in engineering systems must be maintained so as to limit corrosion and minimize the possibility of plugging narrow coolant or instrument channels. Various purification systems are used to remove impurities, but sodium purity must be monitored on a continuous or periodic basis to ensure the effectiveness of these systems. Improvements in plugging meters continue to make such instruments attractive for monitoring the purity of sodium in reactor coolant systems.

A number of techniques and devices — in addition to plugging meters — are being developed to monitor impurity levels in sodium. These developments, which include electrolytic oxygen cells, rhometers (resistivity meters), vacuum-distillation sodium sampling, and other sampling and chemical analysis techniques, were discussed at a symposium on alkali-metal coolants.[1]

Nevertheless, at this stage it is worthwhile to note two central facts: (1) our knowledge of the chemistry of sodium and its impurities is far from complete, and (2) there is not yet a truly satisfactory device for monitoring impurities in sodium. However, in my opinion, until other in-line purity-measuring methods match the simplicity, reliability, and accuracy of plugging meters, plugging meters will continue to be used to monitor the purity of liquid metals.

Early Plugging Meters

During the early research and development stages of liquid-sodium systems, sodium oxide was pinpointed as a main impurity of concern. There was a definite need for a rapid, easy method to measure sodium oxide concentrations. The problem of measuring oxide concentration in large dynamic systems was once thought to have been solved by the use of plugging meters called oxygen or oxide meters; however, it is now recognized that the presence of other impurities influences plugging-meter response. None-theless, although such meters cannot differentiate between oxides and other insoluble precipitates, they have been used for years[2,3] to estimate the oxygen content in liquid metals.

BASIC PRINCIPLES

Plugging meters are in common use for monitoring the purity of sodium in engineering systems. By determining the temperature at which impurities precipitate and block fine orifices within the sodium stream, such meters provide at least comparative measurement of impurity concentration in the sodium. As purity or temperature decreases, the possibility of precipitation and plugging increases. Of the impurities found in operating sodium systems (e.g., O, H, C, and N), oxygen is the most likely to cause difficulties, and its concentration must be kept low — a few parts per million. For convenience, oxide usually is assumed to be the impurity that plugs the orifice in the meter, and its concentration is read from solubility–temperature correlations such as Fig. 1.

Application. The plugging meter provides an engineered constriction in the coolant system at which oxides are made to precipitate under controlled flow and temperature conditions. The constriction may be in the form of an orifice plate or a specially modified valve with either a fluted stem or seat. Schematic diagrams of some restrictions are shown in Fig. 2. In each case the assembly is cooled at (or just upstream from) the constriction or intended collection site. When the oxide saturation temperature is reached, the oxide precipitate tends to build up at the collection site. When the precipitate accumulation is sufficient to cause a measurable flow reduction, as seen on the flowmeter, the temperature measured at the collection site is defined as the plugging temperature.

Tests with the earlier plugging meters revealed five objectionable features:

• Each plugging run required an hour or more.

• Unplugging often required considerable time and special effort that was incompatible with practical operation of the coolant system.

• Data were not reproducible.

• Oxide precipitated prematurely upstream of the collection site.

• The instrument cannot differentiate between oxygen and other impurities that might be precipitating.
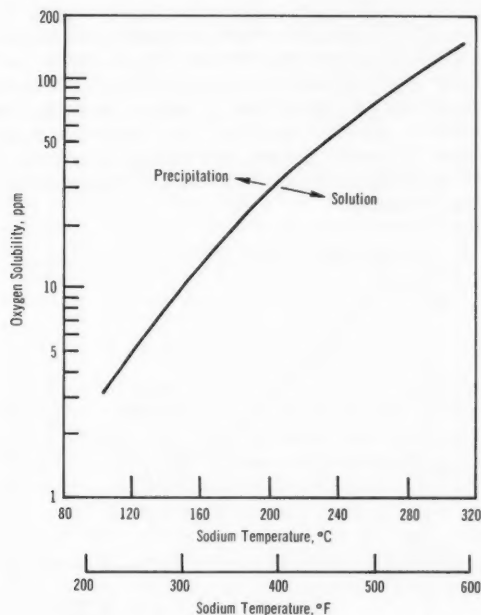

Fig. 1 Typical curve showing variation of sodium oxide solubility with temperature.[6]

Faster Operation

Atomics International developed[4] an improved plugging meter (Fig. 3) by substituting a solenoid-operated rod for the manually operated threaded-stem rod, by adding a blower, and by directing the cooling air around the orifice region. In tests in an experimental system, the results of ~200 plugging runs showed good repeatability and a fast operating time of 5 min. Threefold variation of cooling rate and sodium flow rate did not affect the plugging temperature significantly.

During operation of the plugging meter, process-stream sodium enters the central tube and flows toward the collection site, or plugging orifice. Because cooling air is directed onto the plugging-orifice end of the central tube, oxide precipitation is greatest in this vicinity. When the center rod is in its normal down position, sodium passes through the four small orifice holes. When the sodium tempera-
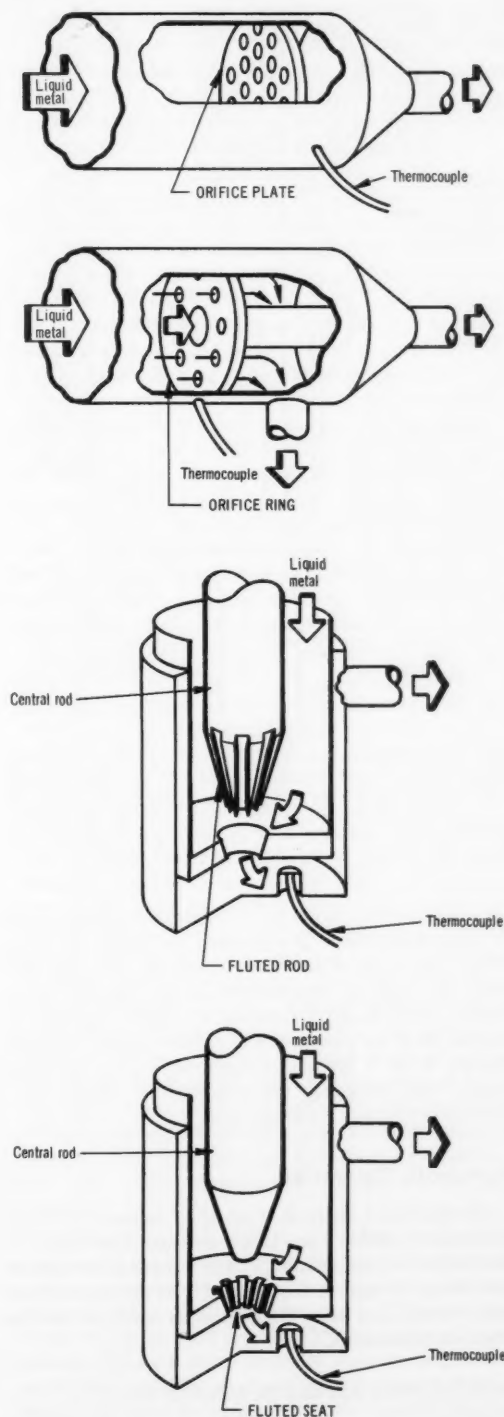

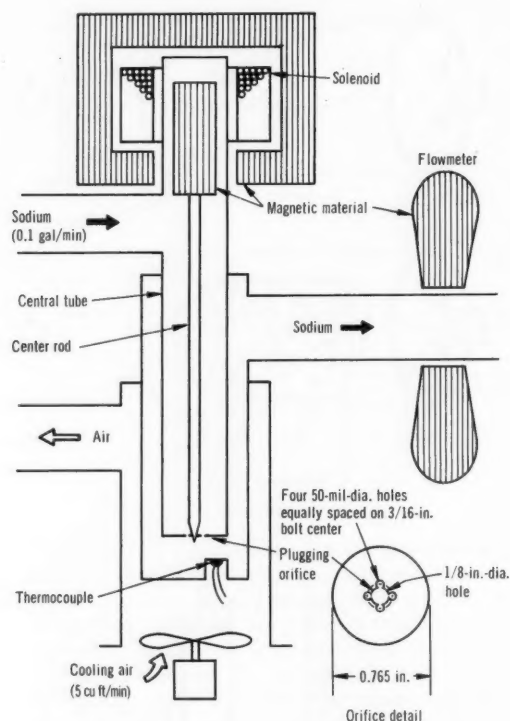Fig. 2 Four types of plugging-meter constrictions.

Fig. 3 Process-stream sodium enters central tube of plugging meter and flows down through the four orifice holes. After flowmeter shows that plugging occurred, the operator restores flow by activating solenoid that raises pointed center rod, by turning blower off, and by energizing heater (not shown) to dissolve oxide plug.[4]

ture is lowered below the temperature corresponding to saturation, oxide precipitates and plugs the small holes, which stops the flow of sodium. The operator notes the sodium temperature at the time the flowmeter shows that flow begins to cease; then he restores flow to prepare for another measurement. Figure 4 is a typical temperature–flow recorder trace. The plugging temperature is shown by a marked decrease in sodium flow.

Automatic Operation

Automatically controlled plugging meters have been developed in France and Great Britain. They differ in the degree of automation of the temperature control and in the design of the orifice. Two processes have been tested; one is a discontinuous method[5] and the other is continuous.[5,6]

DISCONTINUOUS AUTOMATIC MEASUREMENT

The discontinuous measurement involves a succession of partial plugging and unplugging operations.

The device shown in Fig. 5 was developed for this purpose.

The plugging-meter cap, which had twelve 1-mm-diameter holes, was placed within a section of finned tubing, and cooling air was directed over the fins. With this plugging meter the plugging temperature was defined as the temperature at the perforated cap when the measured flow began to cease. An adjustable contact on the NaK flow recorder shut off the cooling air when flow dropped below the preselected value (~ 0.28 gal/min, which is slightly less than the ~ 0.3 gal/min flow rate through the unplugged cap); 10 min after the flow rose above 0.28 gal/min again, time enough for the orifices to unplug completely, the ventilator resumed operation. Thus there was a succession of partial plugging and unplugging processes, and the plugging temperature could be read each time on the recorder.
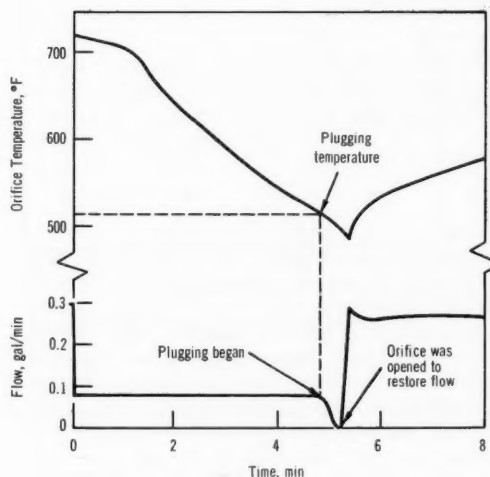

Fig. 4 Typical recorder display of sodium temperature and flow in plugging-meter orifice region shows temperature at which plugging began. Chart illustrates speedy plugging and unplugging.[4]
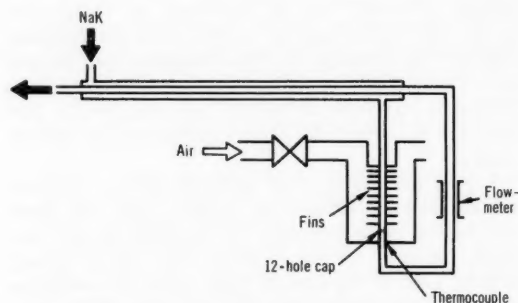

Fig. 5 Discontinuous automatic plugging indicator that was tested in a 1-Mw NaK circuit.[5]

This discontinuous plugging meter, which was tested in a 1-Mw NaK circuit, was accurate to within 9°F, and operation was satisfactory. A plugging cycle required about 30 min to complete; unplugging by simple reheating presented no difficulties. However, this meter was found impractical for two reasons:

1. When plugging begins, the cooling must not be faster than 9°F/min if the plugging temperature is to be determined precisely. Slower cooling would mean plugging cycles even longer than 30 min. Therefore the flow of cooling air must be modified whenever the circuit or plugging temperature varies considerably.

2. The preselected NaK flow rate must be readjusted whenever the feed pressure varies more than a few percent.

Improvements to remedy the first shortcoming of this system have been studied but have not been made. Rather, development effort has been concentrated on the continuous automatic measuring instrument because it appeared to be much more promising than this discontinuous indicator.

CONTINUOUS AUTOMATIC MEASUREMENT

Two continuous automatic measurement devices have been developed to measure the oxide in liquid-metal coolants—one in France[5] and the other in Great Britain.[6] Both devices operate with the plugging meter in a partially plugged condition and use a flowmeter on the sodium line to control cooling-air flow. One of the devices operates on the liquid-metal coolant-loop pressure[5] (low-pressure system); the other device has a pump to supply the liquid metal to a measuring loop.[6]

Low-Pressure System. With this plugging meter,[5] shown in Fig. 6, the sodium flowmeter signals the regulator to vary the air flow so that a continuous
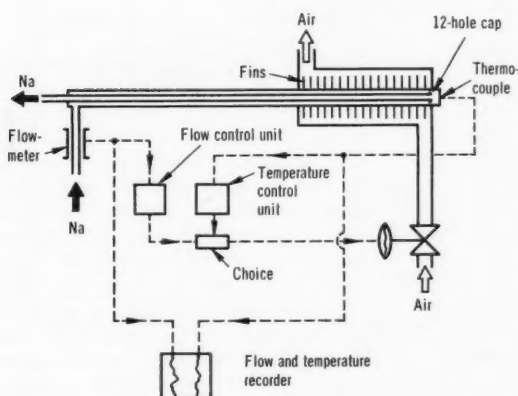

Fig. 6 Continuous automatic plugging indicator tested in 10-Mw NaK (secondary) and sodium (primary) prototype loops for Rapsodie.[5],[7]

solution equilibrium exists between the oxide deposit on the perforated cap (the cap has twelve 1- by 1-mm notches) and the oxide-saturated sodium. Then the temperature at the cap is the saturation or plugging temperature and provides a continuous measure of the impurity concentration in the liquid metal.

The liquid-metal flow rate through the unplugged cap was 0.66 gal/min. When the regulator was set to maintain flow at 0.484 gal/min, the air-flow valve opened to cool the instrument until enough oxide deposited on the cap that the sodium flow reduced to that value. If the oxide content of the sodium decreases, the temperature at the cap is above the saturation temperature, and the oxide on the cap begins to dissolve. Thus the flow of sodium increases and causes the regulator to open to the air valve until the sodium cools and oxide deposits on the cap and brings the flow back to the assigned value. If, on the other hand, the oxide content of the sodium increases, oxide tends to deposit on the cap and decrease the flow; the regulator then reduces the cooling until sodium flow returns to the stable assigned value, at which time the new saturation temperature is indicated. Experiments showed that the selected flow rate can be 30 to 95% less than the maximum (unplugged) flow.

In general, this plugging meter was reported to operate satisfactorily. When the upstream field pressure and temperature of the liquid metal are stable or vary slowly, the plugging-temperature measurement accuracy is within ~ 2°F for NaK and ~ 5.5°F for sodium at a plugging temperature of 265°F; the accuracy improves with increasing temperature.[7]

Despite the good operating results, minor difficulties suggested that further improvements be made. Momentary difficulties occurred when the temperature in the main liquid-metal circuit changed more rapidly than the regulator could follow; a secondary action could be built into the regulator so that temperature changes upstream from the economizer could be compensated for, but this was not tried because loop temperature variations were slow and hardly disturbing. If the plugging temperature decreases to near 230°F, fluctuations could bring the cap temperature below the sodium freezing point; this problem was avoided by having an auxiliary temperature regulator automatically replace the regulation of flow rate if the temperature dropped too low temporarily.

The solution of three other difficulties led to modifications to the instrument circuit and controllers; the revised indicator is called the differential automatic plugging meter. The problems were: (1) a momentary error if sodium feed pressure changed abruptly when system pump or valve settings were varied; (2) frequent flow instabilities if upstream pressure was high enough ($\gtrsim 7$ psi) to make the oxide deposit mechanically unstable, and (3) long-term deposit of metallic particles or insoluble materials on the cap restricted

flow through the orifice. The modifications to solve all three problems involved adding an inlet filter that supplies the indicator and a parallel uncooled tube that is equipped with a diaphragm and a flowmeter. The cooling is then regulated on the basis of the ratio of flows through the indicator and the diaphragm (this cancels out the effects of pressure disturbances upstream because the flow rates in the parallel tubes will vary in the same proportion) rather than by flow rate itself. A flow diagram of the modified differential indicator is shown in Fig. 7. Occasional manual ad-
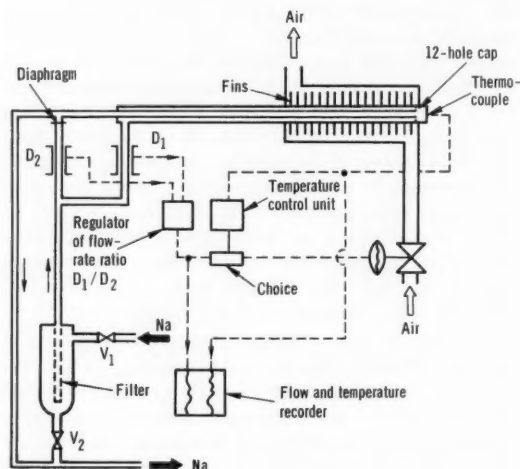

Fig. 7 Differential automatic plugging indicator tested in 10-Mw prototype loop for Rapsodie.[5]

justment of valve V_1 is required when a valve or the pump is manipulated in the purification circuit, and adjustment of valves V_1 and V_2 is required for periodic cleaning of the filter. The use of an independent pump to supply constant pressure to the indicator was also recognized as a means of alleviating some of the difficulties. This has been tested and has given good results. It is now used on new systems and has replaced the differential indicator.[7]

The regulation scheme which has given the best results and which is the simplest[7] is the arrangement shown in Fig. 6.

It is important to note that, if the temperature of the sodium in the circuit exceeds 660 to 750°F, a secondary plugging temperature is obtained (whose nature is not yet known).[8] Thus a continuous automatic indicator gives this secondary temperature and not the plugging temperature of the oxide. Therefore, for practical reasons, two indicators should be used on a reactor system: a continuous automatic indicator and a discontinuous indicator. These two complement each other. The first is more rapid but has limitations because of indicating the secondary plugging tempera-

tures; the latter will show primary plugging temperatures (more directly indicative of oxide level), even though it will show a minor reduction in flow as it passes through the secondary plugging temperature.[7]

Pumped System. Figure 8 illustrates a pumped system[6] in which an integral pump and valve V_1 maintain constant flow and prevent the plugging meter from being affected by flow variations in the main system being sampled. This arrangement also enables the sampling of static systems. The oxide collection site is a cap with twelve 1- by 1-mm notches.

Part of the total liquid-metal flow to the plugging meter bypasses the oxide collection site, as shown in Fig. 8. The bypass flow and the flow through the orifice are brought together again downstream of the valve on the bypass line. By allowing plugging to proceed without changing the liquid-metal flow through the cooler, this bypass arrangement virtually eliminates the unstable feedback that occurs when partial plugging upsets the balance between heat input and cooling and thus makes the system more amenable to automatic control. When the system is automatically controlled, the orifice is kept in a partially plugged state so that the liquid flow is restricted to some preselected reference value. Any departure from the preselected flow value is sensed by the control unit, which adjusts the cooling-air flow and thus changes
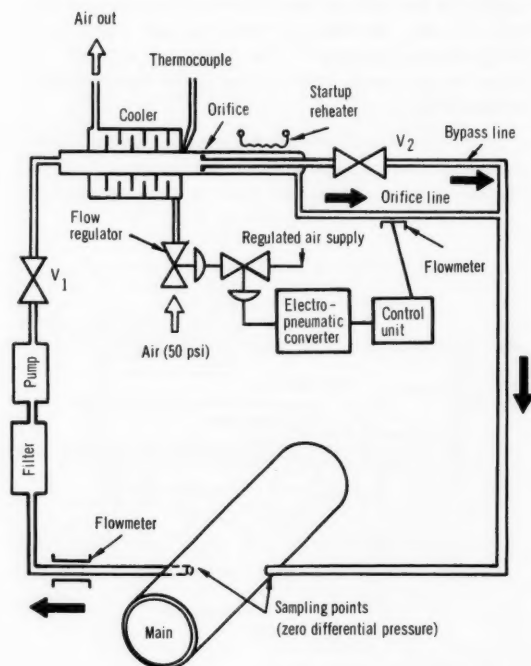

Fig. 8   Automatic plugging meter and separate circulating pump eliminate feedback effect and allow automatic control.[6]

the temperature at the orifice. This temperature change causes either further blocking or unblocking to restore the flow at the orifice to the preselected value.

Both the takeoff line from the main stream to the plugging meter and the return line operate at a zero-pressure differential. Nearly constant liquid-metal flow through the plugging meter is obtained with the pump and valve V_1. During instrument startup, bypass valve V_2 equalizes flow through the unplugged orifice and the bypass; a reheater immediately downstream of the orifice keeps precipitate from blocking the valve.

Flow through the plugging meter is maintained at 0.3 gal/min; of this, about 0.15 gal/min goes through the unplugged orifice. During automatic control operation, orifice flow is reduced by the formation of a partial plug; this reduction is expressed as a percentage of the unplugged flow. Experiments show that the plugging meter operates with 10, 50, and 75% plugged orifice flow without marked variation in performance.[6]

Steady drifts ($< 9°F/hr$) in the temperature of the liquid-metal supply to the indicator have no detectable effect on the saturation-temperature trace. However, faster changes will show up—particularly at low-saturation temperatures, where instrument response is slowest.

The largest cyclic variation in the saturation-temperature trace was $\pm 9°F$ at $257°F$. At this saturation temperature, where the oxygen concentration in sodium is <7 ppm, the $\pm 9°F$ variation allows estimating the impurity content within 1 ppm. At $482°F$ the oxygen concentration at saturation is ~50 ppm, and the actual value can be estimated within 2 ppm.

OTHER RELATED WORK

Recent work at Los Alamos Scientific Laboratory[9,10] indicates great potential for the partially plugged operational mode. By applying the results of their nucleation dynamics study[11] to the operation of an oscillating plugging indicator, the Los Alamos investigators are able to obtain two estimates of the saturation temperature. One is obtained during the cooling, and the other, during the heating part of a cycle. Under carefully controlled operating conditions, these temperatures are, in most cases, identical with the saturation temperature. The operating mode gives more precise end points, and the "seeded" orifice permits readings at very low oxide concentrations.

The General Electric Company has conducted interesting work on the isolation, recovery, and identification of the impurities in sodium responsible for

causing flow stoppage in plug indicators.[12] Special equipment for taking samples and procedures for their analysis were developed.

Conclusions

These new designs place plugging meters in the category of automatic, continuous purity-monitoring devices for dynamic systems.

Automatic operation and continuous readout should make the new plugging meters more convenient than earlier models for detecting gross changes in impurity concentration.

Like earlier plugging meters, these new models also provide only indirect measurements of oxide concentration. The accuracy of the measurement is restricted by the accuracy of the particular solubility–temperature relation employed and by the presence of other impurities.

References

1. *Alkali Metal Coolants*, Symposium Proceedings, Vienna, 1966, International Atomic Energy Agency, Vienna, 1967 (STI/PUB/143).
2. E. F. Batutis, Operating Experience with Oxide Monitors for Sodium Systems in Analytical Chemistry in Nuclear Reactor Technology, USAEC Report TID-7568 (Pt. 2), pp. 24-32, April 1958.
3. W. H. Bruggeman, Purity Control in Sodium-Cooled Reactor Systems, *A.I.Ch.E. (Amer. Inst. Chem. Eng.) J.*, 2(2): 153 (June 1956).
4. K. Davis, Development of a Rapid Operating Plugging Meter, USAEC Report NAA-SR-4537, Atomics International, May 1, 1961.
5. J. P. Delisle, Automatic Measurement of the Plugging Temperature of Sodium and NaK, USAEC Report AEC-tr-6353 (translated from paper presented at Liquid Metals Colloquium of the European Society of Atomic Energy, Aix-en-Provence—Cadarache, September 30—October 2, 1963), Apr. 16, 1964.
6. D. F. Davidson and P. F. Roach, An Experimental Continuous-Indication Plugging Meter for Impurity Monitoring in Liquid Alkali Metals, British Report TRG-Report-1640, 1968.
7. J. P. Delisle, Centre d'Études Nucléaires de Cadarache, France, personal communication, Apr. 24, 1968.
8. J. P. Delisle, Experience d'Exploitation des Indicateurs de Bouchage Automatiques, pp. 505-519 in Ref. 1.
9. C. C. McPheeters and J. C. Biery, The Dynamic Characteristics of a Sodium Oxide Plugging Indicator, *Tran. Amer. Nucl. Soc.*, 11(1): 115-116 (June 1968).
10. C. C. McPheeters, Mass Transfer of Oxygen in Sodium Cold Traps, *Trans. Amer. Nucl. Soc.*, 11(1): 116-117 (June 1968).
11. C. C. McPheeters, Mass Transfer of Oxygen in Sodium Cold Traps, USAEC Report LA-3936, Los Alamos Scientific Laboratory, May 1968.
12. D. Dutina and J. L. Simpson, Sodium Mass Transfer: XXIV. Methods of Separation and Identification of Sodium Impurities, USAEC Report GEAP-5020, General Electric Company, March 1967.

Research and Development
on Aqueous Processing

By C. E. Stevenson and D. M. Paige

A method for recovering both actinides and beryllium from an oxide-type high-temperature gas-cooled reactor (HTGCR) fuel is described; the method is based on successive leaching of the fuel with HNO_3 and H_2SO_4, followed by solvent extraction steps. A recent symposium described advances in fuel-reprocessing techniques and summarized the worldwide status of commercial processing facilities. At the Idaho Chemical Processing Plant, pilot-plant equipment is installed in easily removable modules having a novel design. Equations have been developed for the design of air-pulsing devices for solvent extraction columns, and their applicability has been confirmed by plant tests.

Process Methods

PROCESSING BeO-BASED FUEL

A reactor concept under development by the Australian Atomic Energy Commission utilizes a fuel consisting of compacts of $UO_2 - ThO_2$ (solid solution) dispersed in a BeO matrix. The pebble-like compacts would be sintered to produce fuel units for use in the HTGCR system. The nuclear material content of the proposed fuel units is rather low (atomic ratios of U : Th : Be = 1 : 20 : 450 to 2000), which would require that a considerable quantity of feed material be handled in the reprocessing and that consideration be given to recovery and reuse of the beryllium because of its high cost.

A considerable amount of development work aimed at providing an economic method of fuel recovery has been accomplished. The proposed reprocessing scheme[1] involves grinding of the fuel units, leaching of the fuel with HNO_3 to recover actinides, and decontamination of the actinides by extraction into TBP. The BeO residue would then be dissolved in H_2SO_4 and recovered either by conversion to the oxyacetate or by crystallizing $BeSO_4$ from the sulfate solution

after extracting residual actinides from it with an aliphatic primary amine.

A recent report by Shying, Lee, and Farrell[2] summarizes the laboratory development of the HNO_3 leaching process and of the process for dissolving the beryllia residue in H_2SO_4. In these studies the simulated fuel (U : Th : Be = 1 : 20 : 2000) was in the form of 0.25- by 1.0- by 6-in. bars that were sintered 2 to 4 hr at 1500°C and then ground in a stainless-steel ball mill to produce a material of which about 70% was in the size range −52 +150 British Standard Sieve (BSS) size and about 15% was finer than 300 BSS. In typical leaching tests in stainless-steel vessels with $13M$ HNO_3 containing $0.05M$ F^- and $0.01M$ Al^{3+} at 115°C, a recovery of about 99% of the uranium and thorium could be achieved from unirradiated fuel, but about 20% of the BeO was also dissolved in the HNO_3, as shown in Fig. 1.

Prolonged leaching times did not greatly change the relative degree of removal of the actinides as compared to BeO. For example, when the fuel was leached with $15.5M$ HNO_3, about 10% of the BeO and 88% of the $(U, Th)O_2$ was removed in 15 min compared to 32% of the BeO and ~100% of the $(U, Th)O_2$ in 360 min. The presence of silica (in the form of glass) did not significantly affect the leaching of the actinides, as indicated by the finding that similar degrees of leaching were obtained in glass and in stainless-steel vessels.

It was found that BeO could be readily and preferentially dissolved from fuel that had not been HNO_3 leached, by treatment with boiling, moderately concentrated H_2SO_4. For example, using 8 ml of $10M$ H_2SO_4 per gram of BeO, 81 to 100% of the BeO was dissolved in ‘6 hr, whereas only 0.4 to 1.2% of the ThO_2 and 4 to 11% of the UO_2 were dissolved in the same time; the degree of dissolution increased as the average particle size of the fuel decreased from

253 to <53 μ. When residues from HNO_3 leaching were treated with H_2SO_4 under similar conditions, 60 to 80% of the BeO was dissolved whereas only 0.8 to 1.0% of the remaining ThO_2 and 6 to 17% of the remaining UO_2 were dissolved.
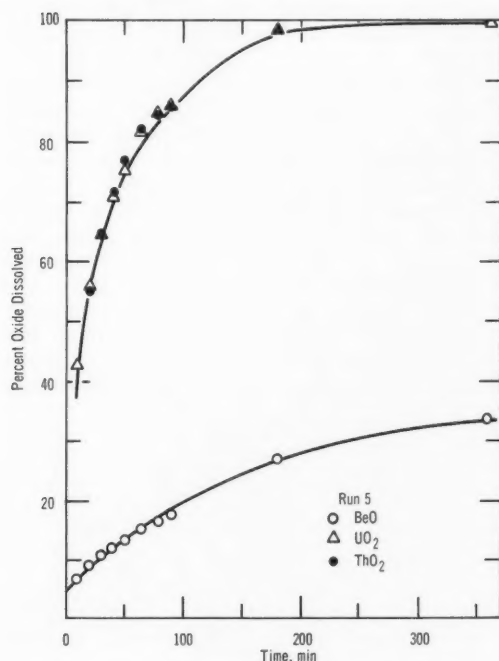

Fig. 1 Dissolution of $(U,Th)O_2$ and BeO in a single-batch leach.[2] Dissolution conditions: acid, 13M HNO_3, 3.22 ml/g; fluoride, 0.05M; aluminum, 0.01M; temperature, 115°C; agitation, mechanical; dissolver, stainless steel; sieve size, less than 152 μ.

On the basis of these results, a two-step cyclic process was devised in which the fuel is first leached with HNO_3 to get the maximum practical actinide recovery with minimum BeO removal, and the residue from this step is dissolved in H_2SO_4 for BeO recovery. The actinide heel remaining from the H_2SO_4 treatment is recycled with the charge to the next HNO_3 leaching operation. Sulfate must be washed thoroughly from this heel to prevent its inhibiting the fluoride-catalyzed dissolution of ThO_2. Periodically, to prevent actinide buildup, a dissolution of this heel with HNO_3 is conducted on the residue from H_2SO_4 treatment. The sulfate solution can then be cooled to 10°C to crystallize $BeSO_4 \cdot 4H_2O$; this operation leaves a mother liquor, which is recycled, and provides partially decontaminated $BeSO_4$, which is dissolved in water and processed by amine extraction for actinide recovery. The flow sheet for this process is shown in Fig. 2.

A three-cycle trial of this process was conducted with unirradiated material under the following conditions: (1) leaching with 15.5M HNO_3 for 47 to 60 min, (2) five contacts with 10M H_2SO_4 for 5 to 35 min, and (3) heel dissolution for 3 hr. The composite nitrate product contained 94% of the uranium, 89% of the thorium, and 17% of the beryllium, whereas the sulfate stream contained 6% of the uranium, 9% of the thorium, and 81% of the beryllium. Inadequate sulfate removal was alleged to be the cause of poor actinide recovery in the second cycle. A second trial was made with irradiated material to determine the path of the fission products. Problems in working in a lead-walled cave led to difficulties in grinding and washing operations, and the resulting separations of the actinides from beryllia were somewhat inferior to those obtained with the unirradiated material. From samples withdrawn during HNO_3 leaching, it was noted that percentages of the [144]Ce, [106]Ru, ^{137}Cs, and [95]Zr which were leached were very similar to the percentages of UO_2 leached. However, the ratio of gamma activity to uranium in the sulfate stream was 8 to 18 times that in the nitrate stream, indicating some tendency for fission-product activity to be separated from the primary actinide stream.
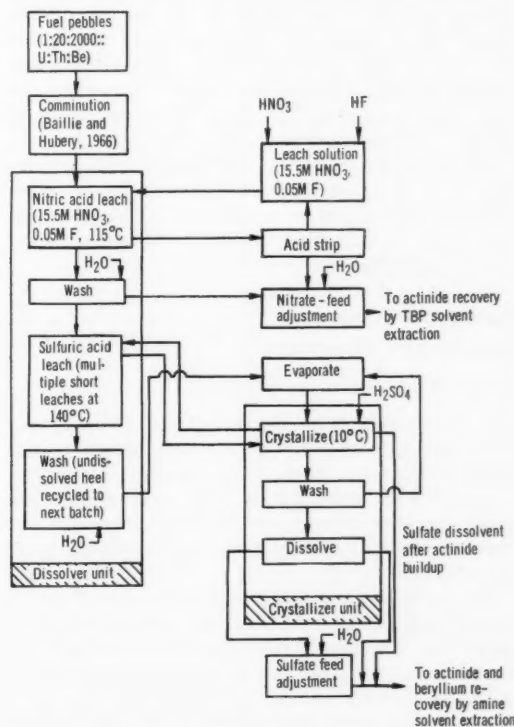

Fig. 2 Conceptual flow sheet for multibatch process for actinide and beryllium recovery.[2]

SYMPOSIUM ON RECENT ADVANCES IN REPROCESSING
OF IRRADIATED FUEL

In December 1967 the worldwide status of facilities
for the reprocessing of irradiated fuels from the
operation of commercial power and test reactors was
well summarized at a symposium sponsored by the
Nuclear Engineering Division of the American Insti-
tute of Chemical Engineers in New York City.[3]
Recent experiences in the operation of a number of
both U. S. and foreign plants were described, and
national plans for some new facilities were indicated.
Lacking were reports on plants projected by General
Electric Company, Allied Chemical Corporation, and
National Lead Company in the United States and any
discussion of Russian facilities.

Operating experiences in aqueous processing plants
that were described included those of the Nuclear
Fuel Services plant at West Valley, N. Y., the Savan-
nah River Plant, the French plant at La Hague, the
Eurochemic plant at Mol, and the Indian plant at
Trombay. No marked process variations were dis-
cussed except for the successful use of the chop–
leach head-end process[4] by Nuclear Fuel Services
for the Zircaloy-clad UO_2 fuel from the Dresden
reactor, and the plant-scale application of a short-
contact-time centrifugal mixer–settler for Purex
solvent extraction processing at the Savannah River
Plant.[5] The design and construction of the Italian
Eurex plant were also described, and brief informal
reports on the construction status of the German
reprocessing plant and on plans for construction of
a fuel-reprocessing plant in Japan were also given.

The proceedings of this symposium will be pub-
lished as a volume of the Chemical Engineering
Progress Symposium Series, Nuclear Engineering;
this series is published by the American Institute of
Chemical Engineers.

Plant and Equipment
Design and Operation

DESIGN OF MODULAR PILOT PLANT

S. J. Horn[6] of Idaho Nuclear Corporation recently
described a pilot plant of modular design that is
under construction at the Idaho Chemical Processing
Plant (ICPP). Providing a clean environment and
using the laboratory space efficiently were the two
basic criteria that were emphasized in the design of
the laboratories.

The basic feature of the modular design is that an
experiment can be contained and operated within a
structural framework having standardized external
dimensions. The apparatus for the experiment can be
built, assembled, tested, and calibrated in a cen-
tralized shop area. The modular unit is then trans-
ported to the laboratory area, installed, and service
connections are made. This procedure results in a
minimum of interference with experiments already in

operation. In addition, an experiment that is discon-
tinued temporarily can be disconnected and the entire
module removed and stored, essentially intact, for
future use.

Two laboratory buildings were designed using this
module concept. One of these, a high-bay area, will
be used for experiments that utilize equipment such
as pulse columns and dissolvers; the second, a low-
bay area, will be used for experiments requiring
less overhead clearance. Construction of the former
facility is complete, and construction of the latter is
in progress. The two laboratories have a number of
common design features, such as ventilation systems,
drainage facilities, and off-gas systems.

The high-bay laboratory (36 ft high) is equipped
with eight experimental modules. A block of offices
occupies the central portion of the building and divides
it into two parallel bays; the roof of the office block
serves as a control mezzanine from which all experi-
ments are operated. Experimental modules are low-
ered into the building through one of five roof hatches.
Figures 3 and 4 show several steps of the installa-

Fig. 3 Experimental module over open roof hatch of high-
bay laboratory.[6]

Fig. 4 Experimental module being lowered into high-bay laboratory.[6]

tion procedure. The average time required for installation of a module is about 1 hr.

The low-bay laboratory (14 ft high) has space for 20 modules. Installation in this laboratory is accomplished by rolling the modules into the laboratory on wheeled bases.

The advantages that are postulated for this type of pilot plant are as follows:

1. Lower fabrication costs resulting from more efficient use of construction equipment and craftsmen.

2. Standardized design criteria for the modules.

3. More efficient utilization of laboratory space, elimination of most shop activity in the laboratory, and minimum interference with operating experiments.

4. Extreme flexibility; the modules can be removed and stored, rebuilt and replaced, or salvaged.

CHARACTERISTICS OF AIR-PULSED SYSTEMS

Pulse columns are commonly used contactors for solvent extraction in the processing of irradiated

fuel. The use of air pulsers, rather than mechanical pulsers, has been described previously.[7,8] In a recent report, Weech and Knight[9] present a mathematical solution to the design of these air pulsers. Equations are derived for the air inlet system, the air exhaust system, and the liquid system. Solutions for these three systems are presented in detail. The authors state that a digital computer was required to obtain numerical solutions for a given in-plant column.

They present an example based on the performance of the extraction column for the second uranium cycle at the irradiated-fuel reprocessing plant of Nuclear Fuel Services at West Valley, N. Y.[10] This particular column was not operating at the desired performance level, and it was suspected that the pressure drop in the air system was excessive. The coefficients for the piping system of this column were set up for a machine solution using the proposed equations. The results of the calculations are plotted in Fig. 5 as a dashed line. As a check on the computed values, measurements of the pressure above the liquid in the pulse leg were made using a pressure transducer. The results of these measurements are also plotted in Fig. 5; good agreement is obvious.
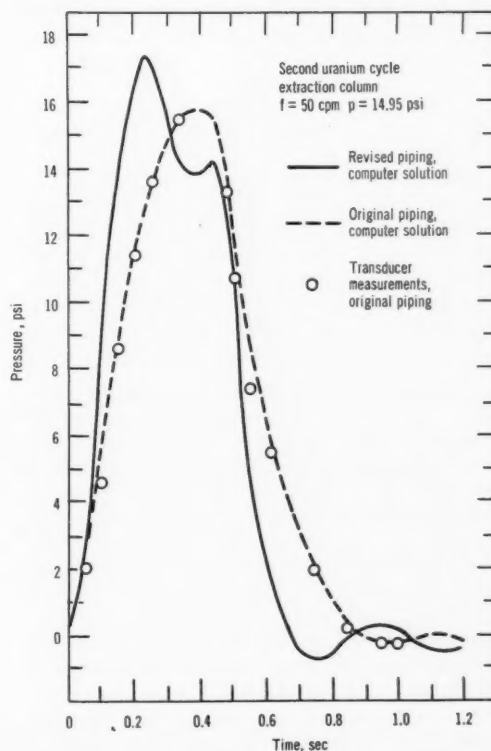

Fig. 5 Pulser air-pressure calculations and measurements.[9]

Further computer calculations were made to explore the results of minimizing friction by piping changes. These data are also plotted in Fig. 5 as a solid line showing much better pressure characteristics. The authors indicate that a rapid rise and decay of the pressure is desirable. Also, for efficient use of the available air pressure, it is necessary to have the pressure decay to zero at one-half the cycle time (0.6 sec in Fig. 5). It can be seen from the figure that, with the original piping, a pressure of 6.3 psi remains at 0.6 sec and that, with the revised piping, the residual pressure at 0.6 sec is greatly decreased.

The authors present some further curves for the specific system and state that column performance using air pulsers has been just as satisfactory as with reciprocating pulsers. The major advantages of air pulsers are lower cost, greater accessibility for repair and replacement, and inherent reliability.

References

1. *Power Reactor Technol. Reactor-Fuel Process.*, 10(1): 65 (Winter 1966–1967).
2. M. E. Shying, E. J. Lee, and M. S. Farrell, Laboratory Development of the Grind–Leach Process for the HTGCR Fuel Cycle. Part 4. Leaching and Dissolution of Beryllia Based Fuels, Australian Report AAEC/E-180, July 1967.
3. "Recent Advances in Reprocessing of Irradiated Fuels," W. A. Rodger, Chairman, presented at American Institute of Chemical Engineers meeting, New York, Nov. 30, 1967.
   a. Eurex Plant: Problems Encountered During the First Construction Phase, G. Calleri and M. Fiorelli, Nuclear Center of Saluggia, Italy.
   b. Recent Developments in the Industrial Treatment of Irradiated Fuels in France, J. Couture, CEN Chatillin-sous-Bagneux (Seine), France.
   c. Construction and Operation of the West Valley Reprocessing Plant, T. C. Runion and W. H. Lewis, Nuclear Fuel Services Inc.
   d. Performance of Centrifugal Mixer–Settlers in the Reprocessing of Nuclear Fuel, D. S. Webster, A. S. Jennings, and A. A. Kishbaugh, Savannah River Laboratory.
   e. Operating Experience with the Fuel Reprocessing Plant at Trombay, H. N. Sethna, Bhabha Atomic Research Center.
   f. Aqueous Reprocessing in a Multipurpose Plant, T. J. Barendregt, E. Detilleux, and R. Rometsch, Eurochemic, Mol, Belgium.
4. *Power Reactor Technol. Reactor-Fuel Process.*, 10(1): 61 (Winter 1966–1967).
5. *Reactor Fuel Process.*, 8(3): 148 (Summer 1965).
6. J. R. Bower (Ed.), Chemical Technology Branch Annual Report Fiscal Year 1967, USAEC Report IN-1087, pp. 119-122, Idaho Nuclear Corporation, October 1967.
7. *Reactor Fuel Process.*, 5(3): 14-15 (July 1962).
8. *Reactor Fuel Process.*, 5(2): 13 (April 1962).
9. M. E. Weech and B. E. Knight, Design of Air Pulsers for Pulse Column Applications, *Ind. Eng. Chem.*, *Process Design Develop.*, 6: 480-485 (October 1967).
10. *Reactor Fuel Process.*, 6(4): 9 (Fall 1963).

Volatility Processes

By G. J. Vogel

Fluid-Bed Fluoride-Volatility Process for Ceramic Oxide Fuels

A fluid-bed fluoride-volatility process has been under development to recover uranium and plutonium values from low-enriched, irradiated UO_2 fuel. Most of the recent development work on the process has been a joint effort of Argonne National Laboratory (ANL), Oak Ridge National Laboratory (ORNL), and Oak Ridge Gaseous Diffusion Plant (ORGDP). The sequential steps of the process are (1) the removal of Zircaloy cladding by reaction with HCl, (2) the oxidation of the ceramic oxide to a fine powder (stainless-steel-clad elements are simultaneously declad and oxidized by reaction with a mixture of HF and O_2), (3) the fluorination of uranium oxide with BrF_5 to form UF_6, which is volatile, and (4) fluorination of the plutonium with fluorine to form volatile PuF_6. Purification of the uranium and plutonium completes the processing steps. Work on this process has been reviewed[1,2] and a flow sheet presented[1] in previous issues of *Reactor and Fuel-Processing Technology*. Recent studies are discussed below.

DECLADDING BY HYDROCHLORINATION

Decladding by hydrochlorination was studied[3] at ORGDP to determine conditions for conducting the decladding step on a semiworks scale. The decladding operation was simulated using 45.5 kg of alumina as the fluidizing medium and approximately 23 kg of Zircaloy tubing and zirconium strip, the amount of metal that will be present in a simulated fuel element that is being fabricated for future decladding tests. Prior to the HCl treatment, about 65 kg of UO_2 pellets were added to the reactor for subsequent oxidation studies. The UO_2 pellets were EGCR (Experimental Gas Cooled Reactor) annular pellets, about $\frac{3}{4}$ in. in outside diameter, $\frac{5}{16}$ in. in inside diameter, and $\frac{3}{4}$ in. long. Pertinent conclusions of the hydrochlorination studies were as follows:

1. At 400°C the hydrochlorination reaction could be controlled successfully on this scale by gradually increasing the HCl concentration of the entering gas from 20 to about 60%.

2. A coating of powder on the sintered nickel filters, through which the reactor off-gas was passed, resulted in loss of permeability. Some of the flow capacity was regained by mechanical removal of the powder, and most of the original permeability was restored by a water backflush. However, after the water flush the filter tubes seemed more susceptible to plugging.

OXIDATION

The UO_2 EGCR pellets from the hydrochlorination experiment described above were used to study conditions for their oxidation to U_3O_8 fines on a semiworks scale.[3] Other studies[4,5] had previously been conducted with EGCR pellets and also with solid, cylindrical pellets, $\frac{1}{2}$ in. in diameter by $\frac{1}{2}$ in. long. The results of tests with both types of pellets may be summarized as follows:

1. Exposure of the UO_2 pellets to HCl had no effect on the subsequent oxidation of the pellets.

2. A stepwise increase in oxygen concentration from 5 to 21% was effective in controlling the oxidation rate at a bed temperature of about 480°C.

3. The EGCR annular pellets could be processed at lower superficial fluidization gas velocities (1.0 to 1.5 ft/sec) than the cylindrical pellets (3.0 ft/sec) because the pellet bed did not plug as readily.

4. High elutriation rates of Al_2O_3 and U_3O_8 fines (up to 94% of the uranium charge) from the reactor were experienced in the oxidation runs with cylindrical pellets and gas velocities of 3.0 ft/sec. This suggests that elutriation may be a suitable method for leaving behind the bulk of the Al_2O_3 and transporting the uranium and plutonium between reactors if one reactor is used for decladding–oxidation and the other for the fluorinations.

FLUORINATION WITH BrF₅

The process step that follows the oxidation step is the fluorination of the oxide fines with BrF_5 to convert the U_3O_8 to volatile UF_6. Because BrF_5 off-gas handling equipment was not available at the ORGDP plant, the BrF_5 step was simulated in two runs by using fluorine to fluorinate[4] the U_3O_8 to UF_6. Although the heat of reaction was higher with fluorine than with BrF_5, the runs were completed without difficulty.

The fluorination of UO_2 pellets with BrF_5 was studied at ANL[6] in a $1\frac{1}{2}$-in.-diameter fluid-bed reactor using $\frac{1}{2}$-in.-diameter cylindrical pellets previously oxidized to U_3O_8. Data on the rate of fluorination were obtained for U_3O_8, and the following conclusions were drawn from the results:

1. The lowest fluorination temperature for practical operation was 200°C.

2. At about 200°C the fluorination rate increased with BrF_5 concentration in the range of 10 to 50% BrF_5 in nitrogen.

3. Simultaneous oxidation and fluorination of the pellets with 10 to 20% BrF_5, 30% oxygen, and the remainder nitrogen at temperatures of 300 to 400°C were unsuccessful.

4. All BrF_5 fluorinations proceeded smoothly without any evidence of caking in the fluid bed.

FLUORINATION WITH FLUORINE

In the final process step, the plutonium, which is present in the reactor as PuF_4, is fluorinated with fluorine to produce volatile PuF_6, which is collected in cold traps. A series of campaign-type experiments was conducted[7,8] at ANL to demonstrate the production, transport, and recovery of PuF_6. A campaign consisted of three separate fluorinations (260 g of −325 mesh PuF_4 powder each) and a single fluorination-cleanup step after the fluorinations to recover the plutonium deposited in the lines and equipment. A single bed of alumina, about 6.5 kg of nominal 48 to 100 mesh, was used in each campaign. A 90% F_2−10% N_2 gas mixture served as the fluidizing gas and reactant.

In two campaigns completed thus far, the temperature of the fluidized bed was increased incrementally (about 25°C every 15 min) from the initial temperature of 300 to 375°C to 550°C. Previous work had shown that starting at lower temperatures (300 to 375°C) decreased plutonium retention in the alumina bed. The total fluorination time in each run was 5 hr.

The fluorinator off-gas was passed through cold traps to collect the PuF_6. Except for a bleed stream, the remaining gas was recycled to the fluorinator. Makeup fluorine was added to counter the dilution effect of nitrogen added as instrument purges and as blowback gas for the fluorinator filters.

The significant results from the two campaigns are as follows:

1. Production rates of PuF_6 averaged 2.4 lb of PuF_6/(hr) (sq ft).

2. Plutonium material balances were 97 and 101%; both values are within the range expected for these experiments.

3. Less than 0.5% of the plutonium charge was discarded in the final alumina bed, which is a process-waste stream.

4. About 2% of the PuF_6 decomposed by radiation decomposition to PuF_4, which was refluorinated and recovered.

BEHAVIOR OF FISSION PRODUCTS

Behavior of inert-gas and volatile fission products during the decladding, oxidation, and fluorination steps must be known if satisfactory decontamination and containment procedures are to be developed for process gases containing these fission products.

A small-scale study[9] was conducted at ANL with irradiated fuel to obtain data on fission-product distribution. A $1\frac{1}{2}$-in.-diameter fluid-bed reactor within a shielded cave facility was used to process about 100 g of UO_2 fuel. The fuel had been irradiated to 33,000 Mwd/metric ton and cooled about 1 year. The following results were obtained:

1. During the oxidation step, at 400°C, only small amounts of ruthenium and krypton were released.

2. In the BrF_5 fluorination step, at 300°C, from one-half to three-fourths of the molybdenum and ruthenium and almost all the tellurium were volatilized. Less than 1% of the niobium and antimony were found in the UF_6 product. The UF_6 also contained small amounts of nonvolatile fission products—Ce, Cs, Sr, and Zr—apparently because of inadequate filtration of the gas leaving the reactor. Most of the krypton was released in this step.

3. The PuF_6 product from the fluorination with fluorine contained less than 10% of the ruthenium and 1% or less of the antimony and niobium.

Another study[10] of fission-product behavior was made in a 2-in.-diameter fluid-bed reactor using UO_2−PuO_2−synthetic fission-product pellets to which ^{106}Ru tracer had been added. During fluorination with BrF_5 at 250 to 300°C, about 70 to 78% of the ruthenium and greater than 95% of the molybdenum were volatilized. These results generally confirm the data obtained with irradiated fuel.

The decontamination of the uranium and plutonium hexafluorides from accompanying fission products and the collection of inert fission-product gases are necessary parts of the volatility process. Because the alkaline-earth fluorides form complexes with RuF_5, the sorption of ruthenium on alkaline-earth fluorides was studied[11] as a means of decontamination. A mixture of UF_4 and ruthenium metal containing radioactive ^{106}Ru was reacted with fluorine at 350°C (uranium was used as a stand-in for plutonium). The gaseous products were then passed

through traps containing the solid fluorides. Decontamination factors of 374, 55, and 9 were obtained with BaF_2, CaF_2, and MgF_2, respectively. These values are somewhat higher than were expected from data on the partial pressure of RuF_5 over the complexes.

The sorption of gaseous TeF_6 on solids is being studied as a means of removing TeF_6 from process off-gas streams. In a survey study[12] the following materials showed promise as sorbents for TeF_6: activated alumina, Linde Molecular Sieve 13X, magnesium fluoride, and activated charcoal. In recent experiments[11] the sorption characteristics of activated alumina were studied more extensively using radioactive TeF_6. The radioactive TeF_6 was prepared by reacting powdered tellurium metal containing ^{125m}Te with liquid fluorine. Results of a factorially designed experiment with alumina indicated that temperature (25 and 100°C) had no effect on sorption capacity; flow velocity (20 and 40 ft/min) and TeF_6 concentration (250 and 500 ppm) had a moderate effect; and bed height (1 and 2 in.) exhibited a strong effect on capacity. The sorption appears to be a diffusion-controlled, physical process since the efficiency is dependent on gas velocity, and the rate of sorption appears to be temperature-independent and varies logarithmically with loading.

A flow sheet and design data have been presented for a process for preferentially sorbing the noble gases, xenon and krypton, in a high-capacity fluorocarbon solvent.[13] When refrigerant-12 solvent is used, pressure and temperature conditions for sorption are 14 atm and 94°F; for fractionation, 3 atm and 32°F; and for stripping, 2 atm and 10°F.

Decomposition of PuF₆

Volatile PuF_6 is reduced to nonvolatile PuF_4 by both radiation and thermal-decomposition mechanisms. The amount of PuF_4 produced is important in designing volatility-plant equipment since the decomposition occurs generally in the lower temperature regions (less than 150°C). To recover the plutonium requires that the equipment be heated to about 300°C and the PuF_4 refluorinated to PuF_6.

Data on the radiation decomposition of PuF_6 have been reported. For solid PuF_6 the observed rate of decomposition was 1.5% per day;[14] for gaseous PuF_6 the observed rates, 0.06 to 1.8% per day, depending on conditions, were found to decrease with time, slightly with PuF_6 pressure, and slightly with helium or krypton present.[15]

In the thermal composition of PuF_6, the amount of PuF_4 formed will depend on the amounts of the components present, and on time and temperature, since an equilibrium reaction ($PuF_6 \rightleftharpoons PuF_4 + F_2$) is involved. A review of the results of several types of experiments[16] in which PuF_6 was thermally decomposed, yielded the following decomposition-rate equation:

$$\ln \frac{R_t - K_{eq}}{R_0 - K_{eq}} = k't \, (s/v)$$

where

$$\log k' = \frac{-3169}{T} + 5.367$$

where R_0, R_t, and K_{eq} are mole ratios of PuF_6 to F_2, initially, after a reaction period of t min, and at equilibrium, respectively; s/v is the surface-to-volume ratio of the equipment, cm^{-1}; T is the temperature, degrees Kelvin. This equation is applicable when appreciable back reaction can occur (i.e., when fluorine is present). The authors have calculated the percent of PuF_6 decomposed, for different PuF_6/F_2 ratios, when a gas containing PuF_6, fluorine, and nitrogen is cooled from 500°C to 100°C. This is a typical process application since the gas leaving the fluorinator reaction zone is at 500°C and must be cooled to about 100°C before it reaches the porous metal filters. For the case in which the PuF_6/F_2 ratio in the fluorinator reaction zone is about $\frac{1}{10}$ of equilibrium, the calculated amount of PuF_6 decomposed is 0.02%.

In the absence of appreciable back reaction, the rate of thermal decomposition of PuF_6 is represented by the equation

$$-d_p/d_t = k_0 + k_1 p$$

where k_0, k_1 are constants, p is PuF_6 partial pressure, and t is time.

Purification of Plutonium by Volatility Methods

Many of the techniques developed for purifying and recovering plutonium from irradiated nuclear fuels can be applied to the recovery of plutonium from scrap materials. At Rocky Flats Division of Dow Chemical Co., plutonium from machining-operation scrap and from impure PuO_2 generated in the production of plutonium metal is being purified by reacting these materials with fluorine to form volatile PuF_6.

Equipment for the batchwise production of PuF_6 in a boat reactor includes a fluorine supply system, gas-rotameter manifold, gas-sampling manifold, cold traps, and halogen disposal units.[17] The operating experience in over 600 hr has been good, and corrosion problems have been minimal. Detailed operating procedures for fluorination and gas-sampling steps and for changing a fluorine cylinder are presented.

The fluorination reactor, which is positioned in a furnace, was constructed from 2-in.-diameter pipe. The boat that fits into the reactor is 2 in. long, $1\frac{1}{2}$ in. wide, and $\frac{1}{2}$ in. deep. Plutonium hexafluoride is collected from the reactor off-gas in two in-series

cold traps consisting of $3/4$-in.-diameter, 8-in.-long cylinders each containing a dip leg.

Fluorine—Production Costs, Properties, Storage, and Disposal

Because large quantities of fluorine are required for the fluorination of plutonium and uranium, the production, costs, properties, storage and disposal of fluorine are of interest. Data from a recent report[18] indicated that a two-cell, on-site plant could produce fluorine at $1.78/lb of which $0.78 and $1.00 were for operating and capital costs, respectively. The fluorine would be generated at 17 lb/hr, compressed to 75 psig, and passed through a cold trap and NaF sorbent to eliminate the HF contaminant. Complete sets of drawings of a 6000-amp cell[19] and of a fluorine plant[20] can be purchased.

A handbook[21] on the use of fluorine contains data on its physical and thermodynamic properties and on compatibility of materials with both liquid and gaseous fluorine. Design criteria are presented for mobile and fixed storage tanks and for pumps that will handle liquid fluorine. The methods of handling fluorine in controlled and uncontrolled releases, and the use of charcoal, propane, and alkaline solutions in these applications are described. Production and purification of fluorine, its transport in 6-lb cylinders, and the applicable shipping regulations are reported.

Tests have been made on the controlled disposal of fluorine by reacting it with activated alumina in a fluidized bed.[22] The bed was 99.9% effective in removing fluorine and near-theoretical conversion of the alumina to aluminum fluoride was achieved. A capability for high disposal rate and production of a free-flowing product for waste disposal was demonstrated. Results of a factorially designed experiment showed that increased bed temperature (300 to 400°C), increased ratio of bed depth to reactor diameter (3 to 6), and decreased alumina particle size (399 to 183 μ) significantly increased the capacity of the alumina. Changing the fluorine concentration (5 to 75%) or velocity (1.25 to 1.65 times the minimum fluidizing velocity) had no significant effect. A gas velocity of 3 times the minimum decreased the capacity. Soda ash, which was one of the other reagents tested, also appeared promising for use in disposing of waste fluorine.

Corrosion of Metals by Bromine

Bromine is formed when U_3O_8 is reacted with BrF_5. The corrosion of various materials of construction by gaseous bromine is therefore of interest. Exposure of Monel to bromine at 300°C produced a penetration rate of 5 mils per month, whereas with other nickel-base alloys, namely, Nickel 201, Duranickel 301, and

Huyck Felt metal, the rate of penetration was negligible.[23] At 500°C the rate was of the order of 0.5 mil per month for Nickel 201 and Duranickel 301, and some intergranular attack was detected; welded specimens behaved similarly. The presence of oxygen, a product of the BrF_5 reaction with oxide fuels, did not significantly affect corrosion behavior.

Properties of Fluorides

Data on the density of liquid NpF_6 have become available.[24] Neptunium hexafluoride was prepared by reacting NpF_4 with fluorine at 300 mm pressure and collecting the NpF_6 in a cold trap at −78°C. The pycnometer used for the density measurements was a sapphire tube, $1/8$ in. in diameter. For the temperature range 56 to 77°C, the data may be represented by the following equation:

$$d = 3.938 - 4.25 \times 10^{-3}\ T$$

where T is in degrees centigrade. The density was found to decrease from 3.698 to 3.613 as the temperature increased from 56.41 to 76.49°C.

A pycnometer for measuring density of corrosive liquids has been described and used to determine the density[25] of liquid UF_6. The pycnometer, a nickel container 6 in. long and 1.5 in. in diameter, was weighed on a 2-kg laboratory balance. The following equation[26] was derived for the density of liquid UF_6:

$$\rho = 2.0843 - 0.0031t + 0.3710\ (230.2 - t)^{0.3045}$$

where ρ is in grams per cubic centimeter and t is in degrees centigrade.

A literature survey[27] on the syntheses and on the physical and thermodynamic properties of molybdenum fluorides and oxyfluorides has been published. The volatile molybdenum compounds are of interest because they appear with the actinide hexafluoride products of the fluoride-volatility process and must be separated from them. Most of the data appearing in the survey article are for MoF_6.

For the hexafluorides[28] of uranium, neptunium, and plutonium, the long-wavelength, infrared-active fundamentals, v_4, have been observed at 186.2, 198.6, and 206.0 cm^{-1}. From the P−R branch separations, Coriolis zeta constants have been calculated for these bands.

Miscellaneous

A 78-reference bibliography on the conversion of UF_6 to UO_2 has been compiled by Nystrom.[29] Analytical methods, instrumentation, handling procedures, purification, fluorine recovery properties, and safety are considered.

Proceedings of a conference on the reprocessing of nuclear power fuel, held at Augusta, Ga., in

May 1967, have become available.[30] The conference was attended by representatives of the AEC, power utilities, fuel-processing companies, and companies who contemplate processing fuel. The discussion, mostly nontechnical, covered various aspects of processing: a history of spent-fuel reprocessing, descriptions of the AEC and Nuclear Fuel Services reprocessing facilities and the planned facilities of General Electric Company and Allied Chemical Corporation, nuclear fuel-reprocessing experience and costs, the current AEC research program, and the importance of nuclear fuel reprocessing to utilities. Although volatility processing was discussed, most of the material was on aqueous processing because all commercial processing plants that have been built are of this type.

A recent Japanese report, "Present Status and Problems on Nonaqueous Reprocessing,"[31] summarizes the present status of nonaqueous processing and presents a statement of the technical problems involved in each.

References

1. *Reactor Fuel-Process. Technol.*, 10(4): 310-312 (Fall 1967).
2. *Reactor Fuel-Process. Technol.*, 11(2): 101-102 (Spring 1968).
3. J. H. Pashley, ORGDP Fuel Reprocessing Studies, Progress Report for Period Ending June 30, 1967, USAEC Report K-L-1780, Part 21, Oak Ridge Gaseous Diffusion Plant, Sept. 22, 1967.
4. S. H. Smiley, ORGDP Fuel Reprocessing Studies, Progress Report for Period Ending April 30, 1967, USAEC Report K-L-1780, Part 20, Oak Ridge Gaseous Diffusion Plant, July 21, 1967.
5. S. H. Smiley, ORGDP Fuel Reprocessing Studies, Progress Report for Period Ending Feb. 28, 1967, USAEC Report K-L-1780, Part 19, Oak Ridge Gaseous Diffusion Plant, Apr. 3, 1967.
6. J. D. Gabor and D. Ramaswami, Engineering Development of Fluid-Bed Fluoride-Volatility Processes. Part 12. Exploratory Tests on Fluorination of Uranium Oxide with BrF_5 in a Bench-Scale Fluid-Bed Reactor System, USAEC Report ANL-7362, Argonne National Laboratory, August 1967.
7. C. L. Chernick and A. Glassner (Comps.), Reactor Development Program, Progress Report, November 1967, USAEC Report ANL-7399, pp. 132-133, Argonne National Laboratory, Dec. 28, 1967.
8. C. L. Chernick and A. Glassner (Comps.), Reactor Development Program, Progress Report, December 1967, USAEC Report ANL-7403, pp. 119-120, Argonne National Laboratory, Jan. 31, 1968.
9. A. A. Chilenskas, Fission-Product and Actinide Distribution During Reprocessing of Irradiated UO_2 by Fluid-Bed Fluoride Volatility Methods, *Trans. Amer. Nucl. Soc.*, 10(1): 157 (June 1967).
10. C. L. Chernick and M. Weber (Comps.), Reactor Development Program, Progress Report, October 1967, USAEC Report ANL-7391, pp. 145-146, Argonne National Laboratory, Nov. 30, 1967.
11. R. C. Vogel, E. R. Proud, and J. Royal, Chemical Engineering Division Semiannual Report, January—June 1967, USAEC Report ANL-7375, Argonne National Laboratory, October 1967.
12. R. C. Vogel, E. R. Proud, and J. Royal, Chemical Engineering Division Semiannual Report, July—December 1966, USAEC Report ANL-7325, Argonne National Laboratory, April 1967.
13. J. R. Merriman, J. H. Pashley, and S. H. Smiley, Engineering Development of an Absorption Process for the Concentration and Collection of Krypton and Xenon, Summary of Progress Through July 1, 1967, USAEC Report K-1725, Oak Ridge Gaseous Diffusion Plant, Dec. 19, 1967.
14. B. Weinstock and J. G. Malm, The Properties of Plutonium Hexafluoride, *J. Inorg. Nucl. Chem.*, 2: 380-394 (1956).
15. R. P. Wagner, W. A. Shinn, J. Fisher, and M. J. Steindler, Laboratory Investigations in Support of Fluid-Bed Fluoride-Volatility Processes. Part VII. The Decomposition of Gaseous Plutonium Hexafluoride by Alpha Radiation, USAEC Report ANL-7013, Argonne National Laboratory, May 1965.
16. L. E. Trevorrow and M. J. Steindler, Laboratory Investigations in Support of Fluid-Bed Fluoride-Volatility Processes. Part XV. Estimation of Rates of Thermal Decomposition of Plutonium Hexafluoride in Process Streams, USAEC Report ANL-7347, Argonne National Laboratory, July 1967.
17. J. D. Moseley and H. N. Robinson, Static Bed Reactor for Studies of a Plutonium Hexafluoride Volatility Process, USAEC Report RFP-1048, The Dow Chemical Co., Rocky Flats Division, Dec. 5, 1967.
18. S. H. Smiley and J. H. Pashley, Economic Analysis of Fluorination Processes for the Recovery of Valuable CVD Materials, USAEC Report K-L-6151, Oak Ridge Gaseous Diffusion Plant, May 1967.
19. 6,000 Ampere, ORGDP Fluorine Cell, CAPE-486, 33 drawings, Clearinghouse for Federal Scientific and Technical Information, U. S. Department of Commerce, 5285 Port Royal Road, Springfield, Va., 22151.
20. Paducah Fluorine Plant, CAPE-55, 34 drawings, Clearinghouse for Federal Scientific and Technical Information, U. S. Department of Commerce, 5285 Port Royal Road, Springfield, Va., 22151.
21. H. W. Schmidt, Handling and Use of Fluorine and Fluorine—Oxygen Mixtures in Rocket Systems, Report NASA-SP-3037, Lewis Research Center, 1967.
22. J. T. Holmes, L. B. Koppel, and A. A. Jonke, Fluidized-Bed Disposal of Fluorine, *Ind. Eng. Chem., Process Design Develop.*, 6(4): 408-413 (October 1967).
23. P. D. Miller, E. F. Stephan, W. E. Berry, and W. K. Boyd, Corrosion Resistance of Nickel and Two Nickel Alloys to Gaseous Bromine, USAEC Report BMI-X-489, Battelle Memorial Institute, Jan. 4, 1968.
24. B. Frlec, The Density of Liquid Neptunium Hexafluoride, *J. Inorg. Nucl. Chem.*, 29: 1804-1805 (July 1967).
25. W. D. Hedge, Density of Volatile Corrosive Liquids: Method and Equipment, USAEC Report K-L-6163, Oak Ridge Gaseous Diffusion Plant, October 1967.
26. R. J. Wertz and W. D. Hedge, Density of Liquid Uranium Hexafluoride, USAEC Report K-1466, Oak Ridge Gaseous Diffusion Plant, Feb. 1, 1965.
27. C. F. Weaver and H. A. Friedman, A Literature Survey of the Fluorides and Oxyfluorides of Molybdenum, USAEC Report ORNL-TM-1976, Oak Ridge National Laboratory, October 1967.
28. B. Frlec and H. H. Claassen, Long Wavelength, Infrared-Active Fundamentals for Uranium, Neptunium, and Plutonium Hexafluorides, *J. Chem. Phys.*, 46(12): 4603-4604 (1967).
29. A. Nystrom, Conversion of Uranium Hexafluoride to Uranium Dioxide, FTB-4, Aktiebolaget Atomenergie, Studovik, Sweden, July 1967.
30. Conference on Nuclear Power Fuel Reprocessing: Technology and Economics, Augusta, Georgia, May 11-12, 1967, USAEC Report CONF-670542, Savannah River Operations Office.
31. Present Status and Problems on Nonaqueous Reprocessing (in Japanese), *Nippon Genshiryoku Gakkaishi*, 9: 530-542 (September 1967).

NONAQUEOUS PROCESSING

Compact Pyrochemical Processes

By W. E. Miller and R. K. Steunenberg

Pyrochemical processes consist of high-temperature, nonaqueous procedures for the decontamination and recovery of fissile and fertile constituents in irradiated reactor fuels. Most of the processes currently under development employ liquid metals and molten salts as process solvents at temperatures in the range 500 to 800°C. Process separations are usually accomplished by volatilization, precipitation, liquid–liquid extraction, or electrolysis. Although these processes are being developed primarily for fuel reprocessing, they also have potential application in the production or refining of other nuclear materials. Much of the current development work is directed toward processing fuels for the types of reactors whose operating economy would benefit from on-site processing, e.g., fast breeder reactors and homogeneous reactors.

Salt-Transport Process for Fast Breeder Reactor Fuels

A number of pyrochemical steps are being investigated at Argonne National Laboratory in connection with the development of the salt-transport process for fast breeder reactor fuels. Investigations of the process steps may include work on process chemistry, corrosion, process kinetics, and equipment design. The individual steps have been combined into conceptual processes for oxide fuel from fast breeder reactors. A process flow sheet was presented earlier in *Power Reactor Technology and Reactor Fuel Processing.*[1] In this earlier flow sheet, batch processing steps were employed exclusively.

Recent work with countercurrent extraction columns has shown that they are suitable continuous contactors for liquid metals and molten salts[2,3] and make feasible continuous or semicontinuous processes with potentially higher capacities and more efficient separations than those obtained in batch processes. A

conceptual flow sheet incorporating some continuous contacting steps was developed and is shown in Fig. 1 (Ref. 4). The stream quantities listed in the flow sheet are illustrative only and have not yet been optimized for maximum performance.

The following is a summary of the steps in the new flow sheet. The stainless-steel cladding is removed from the spent fuel by dissolution in molten zinc in the decladding step (1). The fuel is reduced by a Cu–33 wt.% Mg/salt system at 800°C in the reduction step (2). In this step, the volatile fission products are released, the alkali and alkaline-earth fission products distribute to the salt phase, and the reduced uranium metal precipitates from the Cu–Mg alloy. The uranium is subsequently charged to a salt-transport separation step (3) to remove residual fission products. A Zn–14 wt.% Mg acceptor alloy is specified, but if the plutonium content of the uranium is high, a magnesium-rich acceptor alloy with low uranium solubility and high plutonium solubility would be used for further plutonium recovery. The purified uranium is subsequently recovered by vacuum retorting (4). The decanted Cu–Mg–Pu metal phase from the reduction step is processed at 600°C in a multistage, rare-earth-extraction column (5) where the rare-earth fission products are extracted into a salt containing approximately 15 mole % $MgCl_2$. The salt is reused after the rare earths are removed through contact with a Bi–Mg alloy in a mixer–settler (6). The Cu–Mg–Pu alloy leaves the rare-earth-extraction column and enters a noble-metal separation column (7) where the plutonium is extracted into a salt phase containing 50 or 60 mole % $MgCl_2$ at 600°C. A single-stage mixer–settler (8) is used to remove any copper that may be entrained in the plutonium-bearing salt. The plutonium is then extracted into a Cd–Mg metal phase at 600°C in a small extraction column (9). The Cd–Mg solvent alloy is then separated from the plutonium product by vacuum distillation (10).
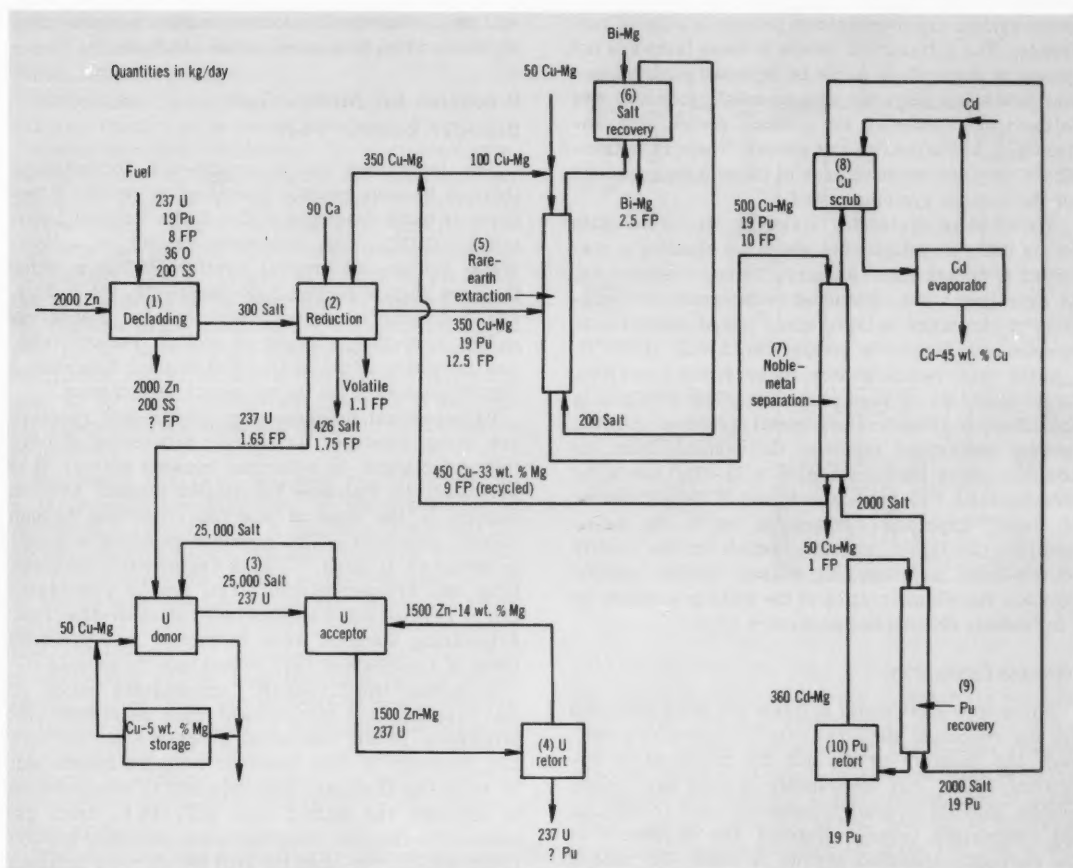
Fig. 1 ANL conceptual pyrochemical flow sheet incorporating continuous contacting steps.[4]

PROCESS DEVELOPMENT

An initial series of experiments in a program for determining phase-disengagement properties of various metal–salt systems was completed.[5] In these experiments, a metal alloy and a salt mixture were stirred together to attain a steady-state dispersion of metal droplets in the salt phase. The melt was then allowed to settle for a fixed period of time (~1 min), and the bulk of the salt phase (~70%) was quickly poured into a receiver. The amount of metal remaining in the salt phase was then determined and compared with the amounts left in the salts in other tests with different salt compositions and alloys. The vessel geometry, mixing conditions, and salt-to-metal volume ratio (2 to 1) were the same in all tests. The salt and alloy compositions and the temperature were the variables.

A few typical results are presented in Table 1. The observed entrainment levels varied over a range of approximately 10^4. The data on the Wood's metal–

Table 1   PARTIAL RESULTS
OF PHASE-DISENGAGEMENT EXPERIMENTS[5]

System	Application	Entrainment level, wt.%
Wood's metal–water, 85°C	For reference only	0.0003
Cu–33 wt.% Mg/ternary salt* + 5 wt.% MgF_2, 600°C	Candidate plutonium-transport donor system	0.01
Cd–18 wt.% Mg/ternary salt,* 600°C	Candidate plutonium-transport acceptor system	0.032
Zn–4 wt.% Mg/ternary salt,* 600°C	Candidate plutonium-transport acceptor system	0.11
Cu–33 wt.% Mg/$CaCl_2$–15 mole % CaF_2 (CaO level of 12 wt.% after a UO_2 reduction), 800°C	Current reference-flow-sheet reduction system	0.37
Cu–33 wt.% Mg/ternary salt,* 600°C	Candidate plutonium-transport donor system without 5 wt.% MgF_2 (see second system above)	0.87

*Ternary salt = 50 mole % $MgCl_2$–30 mole % NaCl–20 mole % KCl.

water system are presented to provide a point of reference. The entrainment levels in these tests are not typical of those which would be expected in pyrochemical processes since the experimental procedure was deliberately designed to produce measurable entrainment in the poured salt phases. These results indicate only the relative ease of phase disengagement for the various systems tested.

A method of decladding stainless-steel-clad oxide fuel is being investigated in which the cladding is dissolved in molten zinc.[3] As part of these investigations, an experiment was conducted to determine the solubility of chromium in liquid zinc.[5] Initial results indicate the solubility to be greater than 1 wt.% at 650°C.

In the oxide reduction step, as presently conceived, large quantities of precipitated uranium accumulate and adhere to the refractory-metal reduction crucible. Several methods of removing the uranium from the crucible (other than dissolution in Zn−Mg) are being investigated.[4] One method is based on the production of finely dispersed suspensions of U−Hg intermetallics in liquid mercury, which can be readily poured from a processing vessel. Another method involves the disintegration of the solid precipitate by a hydriding−dehydriding procedure.

PROCESS CHEMISTRY

Alternative salt−metal systems are being evaluated for the reduction step. The rate and extent of reduction, the capacity of the salt for taking up the by-product oxide, and adaptability of each salt−metal system into the overall process are used as criteria for comparison between systems. One alternative to the currently specified system is $CaCl_2$−20 mole % CaF_2/Cu−33 wt.% Mg−5 wt.% Ca. In a recent experiment,[4] PuO_2 was added to the salt, which was then premelted and contacted with the liquid metal at 800°C. Analyses of metal samples taken during the experiment indicated that at least 97% of the PuO_2 charged was reduced within 1 hr.

CORROSION OF MATERIALS

Investigations have continued on the corrosion of candidate materials of construction for pyrochemical equipment.[5,6] A niobium crucible was exposed to a Cu−33 wt.% Mg−0.1 wt.% U/$MgCl_2$−30 mole % NaCl−20 mole % KCl system at 700°C for 962 hr to investigate the suitability of the crucible with this particular system. Metallographic examination of the crucible revealed a 0.2-mm-thick reaction layer on the portion of the crucible exposed to the metal phase. Although its composition has not been identified, the film, which has the appearance of an intermetallic compound, may be the result of copper penetration into the niobium-based material. The portions of the crucible that were exposed to the salt and vapor phases showed no evidence of corrosion, but physical tests indicated that some embrittlement had occurred. Further tests

will be conducted with niobium to determine its compatibility with plutonium-bearing solutions.

Processes for Molten-Salt Breeder Reactor Fuel

The technology for a molten-salt homogeneous thermal breeder reactor operating on the Th−U fuel cycle is being developed at Oak Ridge National Laboratory (ORNL). The reference reactor is a 1000-Mw(e) molten-salt breeder reactor (MSBR) in which the core fuel is molten $LiF-BeF_2-UF_4$ (65.5, 31.2, and 3.3 mole %, respectively) and the blanket is molten $LiF-ThF_4$ (71 and 29 mole %, respectively). The operation of the Molten Salt Reactor Experiment (MSRE) is part of the technological development.

Pyrochemical processes for molten-salt reactors are being developed for on-site processing of core fuel and blanket. In a thermal breeder reactor, it is necessary to maintain the fission-product neutron poisons in the core at low concentrations through regular processing. The greatest operating economy is achieved if bred ^{233}Pa is continuously removed from the breeder blanket. This type of processing can be carried out most efficiently at an on-site plant. Processing methods were discussed in a previous issue of *Reactor and Fuel Processing Technology*.[7]

A recent ORNL report[8] summarizes much of the research and development work on molten-salt processes. In the conceptual processes for the core fuel, uranium is first removed from the molten salt by volatility methods. The core salt is then distilled to separate the matrix salt, LiF_4-BeF_2, from the rare-earth-fluoride neutron poisons. Requisite vapor−liquid equilibrium data for still design were obtained in 45 experiments.

Thirty vapor−liquid equilibrium experiments were performed with binary systems consisting of LiF and various individual fluorides of process interest, and 15 experiments were conducted with ternary systems that were prepared by adding the fluorides of interest to an 88 mole % LiF−12 mole % BeF_2 mixture. The operating temperature of the still was 1000°C in all instances. The operating pressure was 0.5 mm Hg with the binary system and 1.5 mm Hg with the ternary system. The data obtained from these experiments are presented in Table 2. The relative volatility

Table 2   RELATIVE VOLATILITIES OF SEVERAL COMPONENTS IN LiF AND $LiF-BeF_2$ MIXTURES[8]

Compound	Liquid-phase mole fraction	Relative volatility with respect to LiF	
		In LiF	In $LiF-BeF_2$
LaF_3	0.02−0.05	3×10^{-4}	1.4×10^{-4}
CeF_3	0.01−0.02	3×10^{-3}	3.3×10^{-4}
PrF_3	0.055	6.3×10^{-4}	1.9×10^{-3}
NdF_3	0.05−0.06	6×10^{-4}	$<3 \times 10^{-4}$
SmF_3	0.05	2×10^{-4}	$<3 \times 10^{-4}$
ZrF_4	0.0003−0.01		1.1
BeF_2	0.10		4.73

data obtained indicate that required rare-earth removal efficiencies can be obtained in stills of simple design without rectification.

Information concerning the rate of distillation of LiF as a function of pressure was obtained in a 1-in.-diameter-tube still−condenser. For distillations conducted at 1000°C, the distillation rate increased by a factor of about 30 as the condenser pressure was lowered from 1.0 to 0.1 mm Hg. At 1.0 mm Hg pressure, the rate is believed to be controlled by diffusion through the argon cover gas. At 0.1 mm Hg pressure, the rate appears to be controlled by viscous drag in the passage to the condenser. It was concluded that a still for the MSBR, which would produce the required distillation rate of 15 cu ft of salt fuel per day, would need 43 sq ft of distillation surface area, if the highest experimentally observed distillation rate were to be achieved.

Equipment has been designed and fabricated for a large-scale demonstration of the distillation of molten-salt reactor fuel. A diagram of the still appeared in a recent issue of *Reactor and Fuel Processing Technology.*[7] The system will be operated for 500 to 700 hr with nonradioactive salt having the MSRE fuel-carrier composition (65 mole % LiF−30 mole % BeF_2−5 mole % ZrF_4) and containing small quantities of rare-earth and/or other fluorides. During the operating period, data will be obtained on the variation of throughput with operating conditions and on the effective relative volatilities of components of the salt mixture. In addition, corrosion data will be obtained on candidate construction materials for future distillation systems.

The still and the c o n d e n s e r will be examined thoroughly after the nonradioactive operation by means of dimensional, radiographic, and ultrasonic methods. The system will then be installed in a cell adjacent to the fuel-processing cell at the MSRE site and will be used to distill approximately 48 liters of radioactive MSRE fuel salt from which the uranium has been removed by fluorination.

Operation of the MSRE with ^{233}U fuel would provide valuable nuclear and chemical data for future molten-salt-reactor research programs. Therefore refueling and operating the MSRE with this type of fuel were planned for early 1968. Approximately 71 kg of $^{233}UF_4 - {}^7LiF$ eutectic salt, containing 40 kg of ^{233}U, was to be prepared for this refueling. Work with this material would require shielding because of the ^{232}U content (240 ppm) of the ^{233}U.

A simplified chemical flow sheet (Fig. 2) was developed at ORNL for the preparation of the $^{233}UF_4 - {}^7LiF$ eutectic salt. The flow sheet involves simultaneous reduction and hydrofluorination of uranium oxide and lithium fluoride.[8]

The methods proposed for preparing the fuel concentrate are similar to those used for the routine preparation of UF_4 from oxides. The modifications of
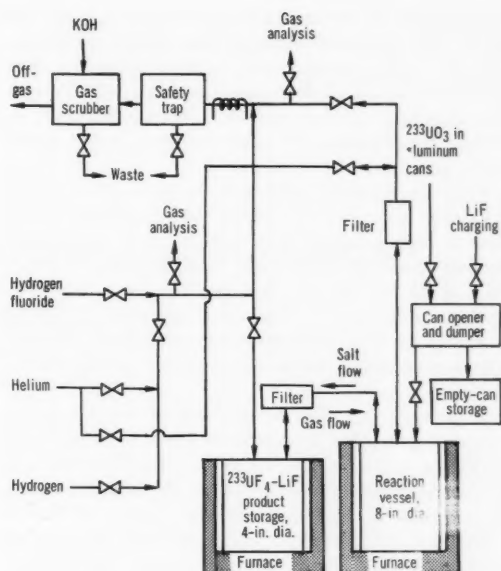

Fig. 2   MSRE ^{233}U fuel-salt preparation system.[8]

the established processing methods that are required include the following: (1) use of a vertical cylindrical reaction vessel for handling the molten fluoride product instead of trays or fluidized-bed reactors, (2) incorporation of LiF in the initial charge of materials, and (3) operation of the process at temperatures sufficient to maintain all of the LiF in a molten state. The mixture of starting materials will be heated to 900°C in a helium atmosphere to melt the LiF and to achieve some thermal decomposition of the uranium oxides (to an overall composition of about $UO_{2.6}$). Subsequent treatment with hydrogen will reduce this oxide mixture to near-stoichiometric UO_2. The conversion of UO_2 to UF_4 will be accomplished by hydrofluorination. In the hydrofluorination a mole ratio of hydrogen to HF of about 10 will be used to maintain a highly reducing atmosphere to minimize corrosion during the conversion.

Development of the chemical flow sheet and the detailed design of processing equipment had progressed to the final stages in the fall of 1967. Construction and installation of the processing equipment were scheduled so that the salt production could start in January 1968.

MISCELLANEOUS DEVELOPMENTS

The extraction of ^{65}Zn from falling liquid-metal drops of pure zinc and Zn−Pb alloys by $PbCl_2$ or $ZnCl_2$ in solution in a KCL−LiCl eutectic was investigated under a Euratom research program.[9] Both chemical and isotopic exchange processes were found

to be controlled by external mass transfer in the salt phase. The measured external resistances were comparable to those predicted by models based on a rigid drop. Extraction in the pure zinc metal−$PbCl_2$ system appeared to proceed by a mechanism that involves subchlorides as intermediates in the interfacial reaction.

A number of developments at Ames Laboratory are discussed in a recent report.[10] Wetting characteristics of Pb−Bi eutectic on 316 stainless steel were studied in sessile drop tests. Corrosion of 430 stainless steel by Pb−Bi was studied in a thermal-convection-loop test. Vaporization rates of binary mixtures of lead and indium were obtained. The distribution of solute within metal drops is being determined.

A process for the purification of uranium oxide fuel was developed in which the oxide is halogenated and suspended in molten alkali-metal salts.[11] The oxide is precipitated from this melt by reduction of the halogenation product in two or more steps.

A recent British patent was granted for the electrorefining of plutonium.[12] In this process, impure plutonium is mixed with equimolar $MgCl_2$, KCl, and NaCl at 700 to 830°C and stirred for 30 to 120 min to acquire a supply of plutonium ions in the electrolyte. Electrolysis is then initiated using the impure plutonium as the anode.

A method of decanning nuclear fuel elements was patented in France.[13] Magnesium cans are removed from uranium fuel elements by dissolution in mercury at room temperature. The dissolution can be accelerated by application of ultrasonics. The mercury is recovered for reuse.

A recent article[14] discusses a Los Alamos procedure for the preparation of americium metal from the oxide by a three-step process. In the first step, AmO_2 is reduced by lanthanum metal at 1500°C in a tantalum reaction vessel. In the next step, the tantalum reaction vessel is heated to 1500°C under 1μ absolute pressure; the americium metal distills and is condensed on a tantalum condenser. In the last step the condenser is heated over a Y_2O_3 mold to melt the metal from the condenser and produce a molded ingot. The routine production of metal yielded a product of 99.9% purity. Physical properties of the product metal were determined.

The volatilization of polonium from bismuth oxide was measured[15] at Battelle Memorial Institute, Richland, Wash., by a transfer method between 580 and 780°C. The apparent vapor pressure, π, which is defined as the observed partial pressure of polonium divided by the mole fraction of polonium in bismuth oxide, was found to be represented by

$$\log \pi \text{ (atm)} = \frac{-15.51 \times 10^3}{T} + 11.83$$

over a polonium mole-fraction range of between 10^{-8} and 10^{-5}. A comparison is made of the measured apparent vapor pressure with both the partial pressure of polonium in the Po−Bi system and the vapor pressure of pure polonium metal.

A recent German article discusses pyrochemical processing of breeder reactor fuels.[16] The application of pyrochemical processing in the EBR-II fuel cycle is reviewed, and the basis for the salt-transport method of separations is presented along with applications of the method. A conceptual pyrochemical process is given for processing fuel from a 1000-Mw(e) breeder reactor. Problem areas in the development of pyrochemical processes are reviewed, and possible future applications of salt-transport separation methods are given.

References

1. *Power Reactor Technol. Reactor Fuel Process.*, 10(1): 80 (Winter 1966−1967).
2. C. L. Chernick and A. Glassner (Comps.), Reactor Development Program Progress Report, September 1967, USAEC Report ANL-7382, pp. 119-122, Argonne National Laboratory, Oct. 31, 1967.
3. *Reactor Fuel-Process. Technol.*, 11(2): 98-99 (Spring 1968).
4. C. L. Chernick and A. Glassner (Comps.), Reactor Development Program Progress Report, November 1967, USAEC Report ANL-7399, pp. 134-137, Argonne National Laboratory, Dec. 28, 1967.
5. C. L. Chernick and A. Glassner (Comps.), Reactor Development Program Progress Report, January 1968, USAEC Report ANL-7419, pp. 124-126, Argonne National Laboratory, Feb. 27, 1968.
6. C. L. Chernick and A. Glassner (Comps.), Reactor Development Program Progress Report, December 1967, USAEC Report ANL-7403, pp. 121-124, Argonne National Laboratory, Jan. 31, 1968.
7. *Reactor Fuel-Process. Technol.*, 11(1): 60-64 (Winter 1967−1968).
8. Oak Ridge National Laboratory, Chemical Technology Division Annual Progress Report for Period Ending May 31, 1967, USAEC Report ORNL-4145, pp. 95-103, October 1967.
9. Donald R. Olander, Drop Extraction Between Liquid Metals and Fused Salts, *Nucl. Sci. Eng.*, 31(1): 1-18 (1968).
10. F. H. Spedding, G. Burnet, L. E. Burkhart, P. Chiotti, F. O. Shuck, M. Smutz, and F. D. Stevenson, USAEC Report IS-1600, Paper 2, Ames Laboratory, July 1967.
11. A. Avogadro and S. Krawczynski, Process for the Purification of Nuclear Fuels, British Patent No. 1,084,340, to EURAEC, Sept. 20, 1967 (filed Dec. 19, 1963).
12. Electrorefining of Plutonium, British Patent No. 1,084,936, to USAEC, Sept. 27, 1967.
13. Method of Decanning Nuclear Fuel Elements, French Patent No. 1,438,507, to CEA, April 4, 1966.
14. W. Z. Wade and T. Wolf, Preparation and Some Properties of Americium Metal, *J. Inorg. Nucl. Chem.*, 29(10): 2577-2587 (October 1967).
15. R. A. Hasty, Volatilization of Polonium from Bismuth Oxide, *J. Inorg. Nucl. Chem.*, 29(11): 2679-2684 (November 1967).
16. W. Knoch, Pyrochemical Processing of Breeder Reactor Fuel, *Chem.-Ing.-Tech.*, 39(17): 1030 (1967).

Progress in Research and Development on Waste Disposal

By Phillip Fineman

Conversion of High-Level-Activity Wastes to Solids

FLUID-BED CALCINATION

Stored aqueous plant wastes that were generated at the Idaho Chemical Processing Plant (ICPP) as a result of reprocessing spent reactor fuels continued to be fluid-bed calcined in the Waste Calcining Facility (WCF) located at the ICPP.[1,2] The wastes are converted to free-flowing solids that are continuously removed from the calciner and transported pneumatically to underground storage bins. Presented below are further results of the second radioactive-waste-processing campaign, currently in progress,[2] and the results of a laboratory study of the volatilization of ruthenium.[3]

Second Waste-Processing Campaign. Calcination of aluminum nitrate-bearing waste solutions[2] in the WCF was terminated in November 1967. Since the start of this campaign in April 1966, about 850,000 gal of aluminum nitrate wastes were converted to 10,200 cu ft of solid waste. About 40,000 gal of aluminum nitrate wastes (most of which are short cooled) remain unprocessed. Overall decontamination factors (ratio of activity of feed to activity of stack off-gas) were approximately 2000 for ^{106}Ru and 3×10^7 for ^{90}Sr.

Operation of the WCF was then successfully shifted to the calcination of fluoride-bearing zirconium waste solutions; their calcination represented the culmination of several years of development work at ICPP.[2,4] Some 15,300 gal of the zirconium waste solution were converted to about 220 cu ft of solids. In general, WCF operation was satisfactory. Radioactive release rates for ruthenium and strontium were satisfactorily low; they were well below the established guide limits.

Laboratory Investigations. Ruthenium that is volatilized in the fluid-bed calcining of plant aqueous wastes is successfully removed from the off-gas stream in the WCF through the use of silica-gel absorbers. To better understand the mechanism of this removal and to assist in developing more efficient methods for removing ruthenium from off-gas streams, the volatilization of ruthenium tetroxide, formed by the reaction RuO_2 (solid) + O_2 = RuO_4 (gas), was studied[3] in the temperature range 453 to 723°C. On the basis of this work, a calculation was made of ruthenium volatilization as ruthenium tetroxide from the WCF calciner. Results of this calculation suggested that either nonequilibrium concentrations of RuO_4 (gas), very fine particulate matter, or another ruthenium vapor species plays an important role in ruthenium volatilization in the calciner, since the partial pressure of ruthenium tetroxide accounted for only a few percent of the observed volatility.

Final Disposal Methods

CALCINED STORAGE IN SALT MINES

Further results[5] have become available on the field experiment known as Project Salt Vault,[6] which Oak Ridge National Laboratory (ORNL) has been conducting since November 1965 to demonstrate the use of salt mines for the storage of packaged solids from the processing of high-level-activity wastes. Related studies include ORNL work concerned with scale-model tests[5] in support of this field experiment and an examination of the use of salt domes and other geologic formations as storage sites for packaged radioactive waste materials.[7]

Results of Field Experiment. The experiment is installed in an inactive mine of the Carey Salt Mine at Lyons, Kans., and utilizes irradiated fuel assemblies* from the Engineering Test Reactor at the Na-

---

*Supplemental electric heat was delivered to each hole to compensate for the decrease in fuel-assembly decay heat in an array hole.

tional Reactor Testing Station, Idaho, and electric heaters* in lieu of actual solidified wastes.[5] [A plan of the experimental area (Fig. 1), which was presented previously in *Power Reactor Technology and Reactor Fuel Processing*,[6] is repeated here for
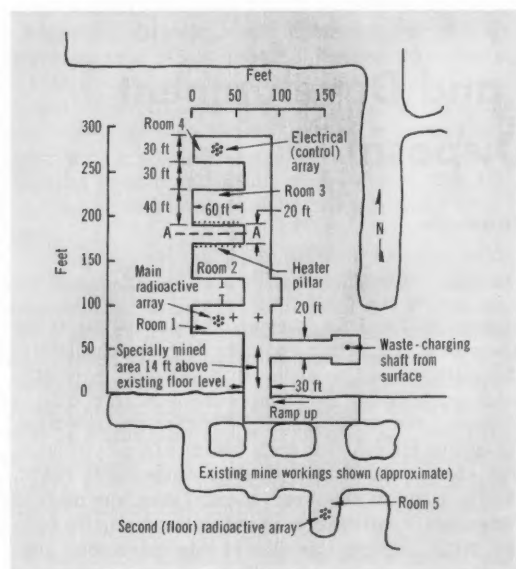

Fig. 1 Layout of experimental area.[6]

greater ease of understanding.] The major objectives of the experiment are as follows: (1) confirmation of the feasibility and safety of waste disposal in salt mines, (2) demonstration of required waste-handling equipment and techniques, (3) determination of stability of salt under the influence of heat and radiation, and (4) collection of information on the creep and plastic flow of salt to establish the basis for the design of a disposal facility.

ORNL believes that the first two objectives have been successfully achieved. In the handling of fuel subassemblies during changes of canisters and other operations, no accidental exposures† nor releases of

activity to the off-gas system occurred; moreover, equipment was operated with a minimum of difficulty.

The radioactive phase[5] of the experiment was terminated in June 1967, when the measured peak radiation dose in the main array had reached 5.3×10^8 rads.‡ A minimum radiation goal of 5×10^8 rads had been originally selected because data showed that at 10^8 rads there was no indication of any change in the physical properties of salt, whereas at 5×10^8 rads there was an indication of a small change in such properties as the compressive strength. However, since both field and laboratory studies now confirm that the radiation effects on salt do not appear to have any detrimental effects for waste disposal, ORNL decided not to use the fourth set of subassemblies which would have extended the accumulated peak dose (a calculated value) in the main array to about 6.8×10^8 rads§ by November 1967. It was thought that this 30% increase in total dose would be unlikely to produce any new data.

Effects of Radiation and Heat. The only distinguishable effect of radiation so far determined has been the intermittent production of extremely small quantities (less than 1 ppm in the off-gas) of an oxidizing gas.[5] The generation of this gas, which is not radiolytic chlorine or hydrogen peroxide, appears to be a function of dose rate and dependent upon a threshold salt temperature of 175°C. A chromatographic analysis of this material indicates that it is a molecule with a weight greater than 200. The material does not appear to attack stainless steel, and the quantities appear to be too low to constitute a health hazard in a waste-disposal operation. Further attempts to identify the material are planned.

The objectives of the experiment called for reaching a peak temperature in the centers of the arrays of about 200°C. Initially, a constant heat generation of 1.5 kw was maintained on each of the array holes by compensating for the decrease in fuel-assembly decay heat by gradually increasing the supplemental electric heat delivered to each hole; the peak temperature attained in the center of the arrays was ~150°C. Insulating each array resulted in higher temperatures in the salt above the centers of the arrays, but there was no appreciable increase in the peak temperature at the periphery of the array holes. However, the desired peak temperature was reached

---

*An array consisting of electric heaters only (no radioactivity present) was provided as a control for the main radioactive array. Thus any differences in the behavior of the salt can be ascribed to the effects of radiation. Electric heaters are also being used to obtain information on the thermomechanical properties of salt under transient-temperature conditions.[5] This study (see the subsection "*Heated-Pillar Test*" below) involves the heating of a 20-ft-thick rib pillar between the two central rooms of the experimental area by means of heaters buried in the floor along the base of the pillar.

†All handling operations at the mine were performed by remote control and without the aid of hot cells. Radiation exposures to personnel were low; the highest dose was 200 mrads to the head and hands only.

‡This radiation level was achieved with the use of three different sets of ~90-day-cooled subassemblies. (Originally, the use of four sets was planned.) A set consisted of seven sealed canisters; each canister contained two subassemblies and a total curie content of ~200,000 when received at the mine.

§For comparison, a hypothetical acid Purex waste of the future would deliver a peak dose of about 4×10^9 rads in 2 years and more than 10^{10} rads ultimately. ORNL believes that it would be impractical to attempt to reach these levels until actual waste solids become available.

by increasing the total power input (fission product plus electric) about 40% (to 2.1 kw/hole).

Some of the deformations of the salt around the main radioactive array are illustrated in Fig. 2. These data are also typical of the electrical (control) array. The dashed curve on Fig. 2 shows the temperature increase of the salt in the central region of the array. The disrupting influence of the two exchanges of canisters and the effect of the increase in heating rate to 2.1 kw/hole can also be seen. Curve 1 on Fig. 2 shows the uplift of the floor at the center point of the array due to thermal expansion of the salt. This thermal expansion of the floor under the edges of the pillar caused an immediate acceleration of the deformation of the pillar, the vertical component of which is shown by curve 2 on Fig. 2. Although an accelerated deformation of the pillars with heat was anticipated, heating for several weeks was required before there was any significant temperature increase in the pillar.
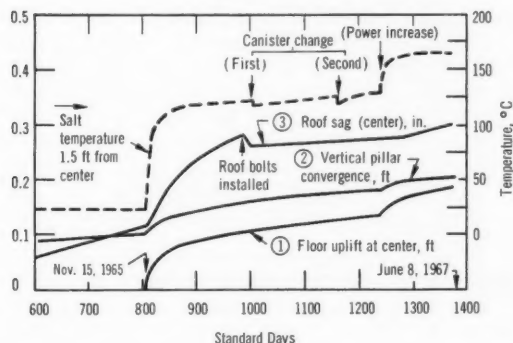
Fig. 2 Thermal effects on salt around experimental rooms.[5]

The immediate roof of the entire experimental area consists of a 2-ft-thick bed of salt that had separated from the overlying material along a thin shale parting. Instruments in the area indicated that this roof bed was sagging into the experimental rooms at the rate of about 0.1 in./year during the period immediately prior to startup on Nov. 15, 1965 (curve 3, roof sag in center of room). Roof sags of this type are well known in salt mines, and this sag rate was not considered to be excessive. As can be seen on curve 3, Fig. 2, the accelerated deformation of the pillar was transferred to the sagging roof bed in the form of an axial load, which caused a fivefold increase in the rate of sag immediately after startup.

Because of the nature of the experiment and the planned extensive heating of the pillar in the center of the experimental area, roof bolts were installed throughout the area to support the 2-ft-thick roof bed,[6] even though this accelerated sag by itself did

not create a hazardous condition. The effect of these roof bolts is shown on the continuation of curve 3, where it can be seen that the roof was lifted slightly at about standard day 1080, and the rate of sag was reduced to about one-fourth of its original (preheating) rate.[5] It may also be noticed from curve 3 that the rate of separation increased slightly after the power increase at 1240 days, but it is still lower than it was before the start of the test in November 1965. Although the curves for the control array (room 4) corresponding to the curves in Fig. 2 were essentially the same, the increase in curve 3 after the power boost was not observed. This apparently is not due to the absence of radiation but rather to slight variation in the salt from room to room.

The results for the second (floor) radioactive array (room 5) are similar, except that there has been no separation of salt in the roof; and none was expected, since there are no significant shale layers in the first 8 ft of roof. Temperature rises and floor uplift in room 5 are a few percent higher due to the poorer heat-transfer properties caused by the presence of layers of shale and anhydrite in the floor.

The experience with the roof bed illustrates several important points pertaining both to the Project Salt Vault demonstration and to the operation of any high-level-activity disposal facility in salt deposits. First, the structural properties of salt are not completely understood, especially the mechanical behavior at elevated temperatures and under thermal gradients. With the present state of knowledge, it is impossible to predict in detail all the responses of the salt to any given set of thermal conditions. Second, rock mechanics instrumentation should be fairly extensive so that (a) incipient structural problems can be detected at an early stage, (b) sufficient information will be available to enable the best solution to those problems to be found, and (c) the solutions can be checked. After routine operations have been established, a limited number of rock mechanics instruments should be maintained for proper control of the operation. Third, underground mine disposal, in salt or any other formation, is still a mining operation. The solutions to any problems should be sought first within the body of existing mining technology.

Water Release and Possible Effects. Small quantities of water trapped in negative crystal cavities in the salt have been found to migrate toward a heat source.[5] Measurements indicate that water is being released into the radioactive and electrical (control) arrays at the rate of about 0.3 to 3 ml/(day)(hole). This small quantity of water poses no problems for the demonstration since it is removed by the off-gas system. In an actual disposal facility, the waste-container holes will be backfilled with crushed salt. Thus the water coming into the hole would move as vapor upward through the void spaces in the crushed

salt, where it would condense as it reached the cooler regions.*

The salt that is normally mined is relatively pure and is free of significant quantities of interbedded shale, which contains several percent water; therefore, the water content is generally of the order of less than $\frac{1}{2}$ vol.%. Quantities such as this should pose no problem in a disposal operation, since inflow rate is very low. In the array in the original mine floor, however, owing to the presence of shale, the water inflow rate is about 40 to 90 ml/(day)(hole), a much more significant volume than in the other arrays. Tests are planned that would determine what happens to the integrity of waste containers and to the fairly large quantities of water; in these tests waste containers of mild steel and 304L stainless steel would be placed in holes in the original Lyons mine floor and the holes backfilled with crushed salt.

Heated-Pillar Test. Results of the heated-pillar test are presented in Fig. 3, which shows the vertical deformation of this pillar as measured at seven gauge points.[5] The initial portions of the curves represent the normal squeezing and plastic deformation of the pillar resulting from the overburden pressure. The middle part of the curves illustrates the effect of only one of the heaters (adjacent to gauge 125), which was started with a 3-kw input as a preliminary to the main experiment. The effect of this single heat source can also be seen at gauges 122 and 128, 20 ft away.

On Nov. 14, 1966, all 22 of the heaters were turned on with a power input of 1.5 kw each.† The resulting increase in the rate of convergence of the pillar was about an order of magnitude, from 0.2 to 2.0 in./year. This rate of convergence is approximately the same rate that would result from a doubling of the overburden pressure or depth. The strong temperature dependence of the pillar deformation is further illustrated by the distribution of the convergence around the pillar. The largest convergence and the greatest rate (gauges 125 and 138) occur at the center region of the pillar, which is the hottest. The least amount of convergence (gauges 128, 136, and 137) takes place around the end of the pillar, where the heat losses to the air result in the lowest temperatures.

*Should the water corrode through a container filled with calcined solids and should there be a gas buildup (not anticipated) in the container, the container might release such gases as oxides of nitrogen, hydrogen, volatile fission products and perhaps unknown compounds. However, most of these materials would be expected to remain in the 7 to 8 ft of crushed salt above the waste containers.

†The application of 33 kw of electric power to the pillar represents a heat input to the pillar of approximately three times that which would be expected if the rooms were filled with actual solidified wastes. In addition, the heat input is concentrated at the pillar; this tends to exaggerate further the rate of convergence.
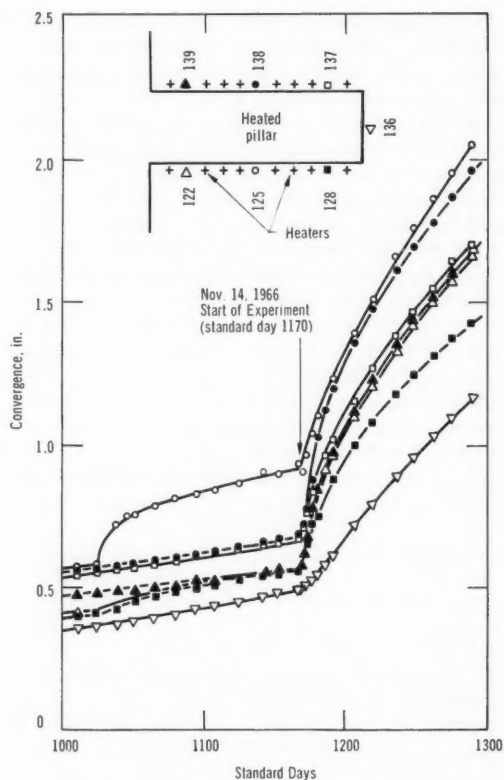
Fig. 3 Vertical deformation (convergence) of the heated pillar.[5]

In Fig. 4 are shown the floor-uplift profiles along the south−north center lines of rooms 2 and 3 (which border the heated pillar) as of June 1, 1967. At that time the temperature under the center of the pillar (9 ft down in the salt, at the center plane of the heaters) was 68°C, and at the ends of the pillar at 9-ft depth, it was about 50°C. Halfway up the pillar, in the center, the temperature was 43°C.
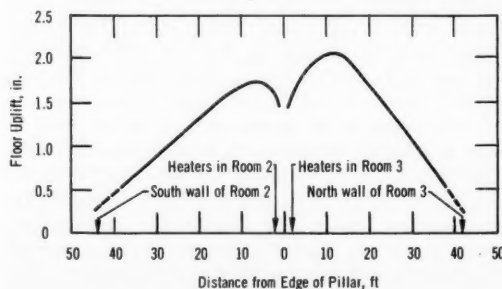

Fig. 4 Floor uplift along south−north center lines of rooms 2 and 3 as of June 1, 1967 (1369 standard days).[5]

Temperatures in excess of 100°C (at the 9-ft depth) extended to distances of more than $2\frac{1}{2}$ ft from the centers of the heaters. At the 9-ft depth in the center of the rooms, the temperature was 43°C; this same temperature was recorded at a depth of 17 ft.

The uplift in rooms 2 and 3 is not quite symmetrical, with somewhat more uplift being recorded in room 3 than in room 2. This was caused by a separation (floor heave) taking place at some plane of weakness more than 5 ft down into the salt in room 3. Again, this is considered to be a normal variation caused by slight differences in the salt from room to room.

Stratigraphy of Salt Section in the Vicinity of the Demonstration Site. A detailed stratigraphic study[5] has been completed of the salt section extending from 30 ft below the floor of the old mine workings to 10 ft above the ceiling in the demonstration site, a total thickness of 75 ft. X-ray diffraction was the principal means used to identify mineral species. Halite was by far the predominant mineral. In that section below the floor of the old mine workings, halite beds up to several feet in thickness are separated by shale layers that may be as much as 6 in. thick. In the demonstration area the salt section contains several prominent shale layers, of which the lowermost layer is several feet thick in some places. The salt in the roof of the experimental area is, in general, quite similar to the salt immediately below it.

Laboratory Tests on Deformation of Rocks. In the simulation of mine conditions in scale-model tests, the deformational characteristics of rocks are an extremely important consideration. This was illustrated in recent ORNL tests to determine the stability of model mine pillars of rock salt and dolomite.[5] The results showed the following: (1) For quasi-plastic rocks like rock salt, it is absolutely necessary to simulate in the models as nearly as possible not only the mine pillar but also the roof and floor conditions. (2) For brittle rocks like dolomite, the roof and floor conditions apparently do not affect greatly the deformation of the pillar.

Use of Dome Deposits and Other Geologic Formations for Waste-Storage Sites. Lomenick and Bradshaw,[7] ORNL, point out that the widespread occurrence of rock salt over the United States has been commonly accepted as one of the principal advantages for the use of these rocks as storage sites for radioactive waste materials, since salt deposits underlie a portion of 24 of the 50 states.[8] However, from recent laboratory and field studies on the flowage of rock salt at elevated temperatures and high overburden loads, it is apparent that many of these deposits are unsuitable for disposal sites.[9,10] At present there are perhaps three principal areas in the United States where disposal in salt would appear to be

highly desirable: (1) the Silurian salt deposits of the Northeast, which underlie parts of New York, Pennsylvania, West Virginia, Ohio, and Michigan; (2) the Permian basin salts, which underlie parts of Kansas, Oklahoma, Texas, and New Mexico; and (3) the Gulf Coast Embayment salts, which underlie parts of Louisiana, Texas, Arkansas, and Mississippi.[8] The first two areas are bedded deposits, whereas the third area contains only salt domes at reasonable depths. Most of the other deposits throughout the United States appear less suitable because of their great depths below the surface, their numerous inclusions of other rock types, or a general lack of knowledge concerning their extent, depth, and other factors.

The principal concern in the disposal of waste in bedded deposits is the stability of the structure at elevated temperatures and stresses. This has been found to be especially significant when shale beds occur interbedded with the salt.[11] These shale beds are usually absent in dome deposits; thus, in this respect, domes may be favored over bedded deposits for waste-disposal sites. Although recent laboratory and field tests indicate that an efficient and safe operation in bedded rock salt can now be designed, several problems unique to salt-dome deposits will require investigation before a similar operation can be designed for these structures.[7]

A principal technical concern in the disposal of waste in salt domes is ensuring that migrating waters do not reach stored waste.[7] Flooding of dome mines has been reported in the United States (Winnfield, La.) and in Germany (occurring in at least 20 dome mines). At present, little appears to be known about the movement of groundwater in the vicinity of salt domes.[12] Thus investigations should be initiated to ascertain the geohydrological factors or other parameters that were, or appeared to be, instrumental in the flooding of these salt domes.[7]

The effect of decay heat on the stability of the dome should also be investigated.[7] For waste concentrations that produce temperature rises compatible with safe operation, the average heat generation in a disposal mine would be about two orders of magnitude greater than the normal geothermal flux. (This estimate is based on the assumption that wastes are interim-stored for at least 10 years, until only the 30-year half-life cesium and strontium remain.) So it is conceivable that there might be some effect on dome movement.

There is also a need for the installation of a plastic-flow gauge in at least one dome mine in an effort to determine whether the creep behavior is the same as that in bedded deposits.[7] One would suspect that there might be residual tectonic stresses in the salt, as well as differences in the way the overburden loads are transmitted into the interior of the dome; both of these would exert considerable influence on flow behavior.

Investigation of Other Geologic Formations. Excavations in rocks other than salt may be suitable for the ultimate disposal of high-level-activity radioactive wastes.[7] Impervious or dry excavations have been reported in limestone, shale, granite, and chalk deposits. However, their possible uses as disposal sites have not been investigated. With model specimens of mine pillars, it has been demonstrated that hard rocks like dolomite do not exhibit such accelerated flow characteristics at elevated temperatures and pressures as does rock salt.[11] Consequently it appears that the structural integrity of the excavated openings in these rocks would not be of primary concern in the event that these rocks are used as disposal media.[7] However, it is likely that such things as ensuring the isolation of these excavations from migrating groundwaters and the geographic location of suitable deposits and their vertical and lateral extents would be critical.

Selected Current Literature

Reports on the management of radioactive wastes at ORNL[13] and CRNL[14] (Chalk River Nuclear Laboratories) have become available. Manneschmidt and Witkowski,[13] ORNL, in their report, which is a revision of a similarly titled report issued in 1962, describe the systems employed at ORNL for the disposal of radioactive liquid and gaseous wastes. Steps in the treatment and monitoring of the wastes are outlined below:

1. The low-level-activity liquid waste is chemically treated, and the greater part of the radioactivity is removed prior to discharge into the stream and river system. Dilution in the river then reduces the concentration of radioactivity to levels well below the maximum concentrations established by the National Committee on Radiation Protection and the International Commission on Radiological Protection.

2. The intermediate-level-activity liquid waste is concentrated by evaporation, and then the concentrate is finally disposed of by injection, as a concrete grout, into shale beds lying approximately 900 ft below the surface.[6,15]

3. All gaseous wastes are filtered and/or chemically treated before discharge to the atmosphere. Final discharge to the atmosphere is made through stacks of sufficient height to ensure the dilution of the released radioactivity to levels below the maximum permissible concentration (at ground level).

4. All waste streams are monitored before and after discharge to verify safe operation.

Mawson,[14] CRNL, outlines the history of waste-management practices at CRNL and describes the waste facilities used for handling of radioactive solid and liquid wastes. He also discusses specific waste-disposal experiments designed to test the behavior of fission products moving through the groundwater and

other experiments conducted to determine the dispersion of radionuclides through the environment. Finally, he outlines the bases for establishing the disposal policies for solid and liquid wastes.

Slater,[16] Brookhaven National Laboratory, describes laboratory work carried out on the extraction of cesium polyiodides into $0.2M$ I_2 in nitrobenzene from various simulated reprocessing-plant wastes (Purex acid wastes, TBP-25 acid waste, and concentrated TBP-25 acid waste) containing added tracer-level radionuclides. The extraction procedure consisted in the following steps: (1) addition of sodium citrate to complex the cations of aluminum and heavier metals in order to keep them in solution at the relatively high pH values needed; (2) pH adjustment of the solution from step 1 to between 6.3 and 6.7 with sodium hydroxide; (3) addition of sodium iodide to form iodine-extractable polyiodide ions; and (4) contacting of the aqueous phase with equal volumes of $0.2M$ I_2 in nitrobenzene. In experiments conducted at ~25°C, extraction coefficients for cesium from the various synthetic wastes were found to range approximately from 10 to 20, and cesium separation factors from fission products and process chemicals were observed to be very large. Cesium extraction data were also obtained at other temperatures, which were varied from 10 to 70°C; these data showed that the cesium extraction was increased at the lower temperatures (particularly at 10°C). The cesium can be essentially completely extracted from waste solutions at concentrations in the order of magnitude found in actual wastes. This was demonstrated in a run using a 16-stage miniature mixer–settler extraction unit to remove cesium (present at ~5 × 10^{-4} M) from a concentrated TBP-25 waste; a separation factor of $1 × 10^6$ was achieved. However, the author acknowledges that there are problems in using a polyiodide extraction system to recover cesium from reprocessing wastes. Some of the difficulties are as follows: (1) corrosiveness of the solutions to metallic components used in processing vessels, (2) volatile character of iodine, and (3) poisonous nature of nitrobenzene. Nevertheless, he believes that the extraction procedure described above should be suitable for the analysis of cesium in reprocessing-plant streams where large separation factors for cesium from other fission products, process chemicals, and corrosion products are required.

References

1. *Reactor Fuel-Process. Technol.*, 11(1): 65 (Winter 1967–1968).

2. J. A. Buckham, Idaho Nuclear Corporation, unpublished, Dec. 4, 1967.

3. B. D. Penman and R. R. Hammer, The Ruthenium Dioxide–Oxygen–Ruthenium Tetroxide Equilibrium, USAEC Report IN-1013, Idaho Nuclear Corporation, January 1968.

4. *Reactor Fuel-Process. Technol.*, 11(2): 112-113(Spring 1968).

5. Oak Ridge National Laboratory, Health Physics Division Annual Progress Report for Period Ending July 31, 1967, USAEC Report ORNL-4168, pp. 18-29, October 1967.

6. *Power Reactor Technol. Reactor Fuel Process.*, 10(2): 177 (Spring 1967).

7. R. E. Blanco and F. L. Parker, Waste Treatment and Disposal Semiannual Progress Report July—December 1966, USAEC Report ORNL-TM-1887, pp. 76-80, Oak Ridge National Laboratory, November 1967.

8. W. G. Pierce and E. I. Rich, Summary of Rock Salt Deposits in the United States as Possible Storage Sites for Radioactive Waste Materials, U. S. Geological Survey Bulletin 1148, 1962.

9. R. L. Bradshaw, T. F. Lomenick, W. C. McClain, and F. M. Empson, Model and Underground Studies of the Influence of Stress, Temperature, and Radiation of Flow and Stability in Rock Salt Mines, in *Proceedings of the First Congress of the International Society of Rock Mechanics, Lisbon, September 25 to October 1, 1966*, pp. 429-433, 1966.

10. T. F. Lomenick and R. L. Bradshaw, Accelerated Deformation of Rock Salt at Elevated Temperatures, *Nature*, 207(4993): 158-159 (1965).

11. Oak Ridge National Laboratory, Health Physics Division Annual Progress Report for Period Ending July 31, 1966, USAEC Report ORNL-4007, p. 26, October 1966.

12. An Analysis of Contour Maps of 1955 Water Levels with a Discussion of Saltwater Problems in Southwestern Louisiana, in *Water Resources Pamphlet No. 4*, p. 23, Department of Conservation, Louisiana Geological Survey and Louisiana Department of Public Works, Baton Rouge, La., July 1957.

13. J. F. Manneschmidt and E. J. Witkowski, The Disposal of Radioactive Liquid and Gaseous Waste at Oak Ridge National Laboratory, December 1966, USAEC Report ORNL-TM-1832, Oak Ridge National Laboratory, August 1967.

14. C. A. Mawson, Philosophy and Practice of Waste Management at CRNL, Canadian Report AECL-2710, February 1967.

15. *Reactor Fuel-Process. Technol.*, 11(2): 113 (Spring 1968).

16. L. M. Slater, Extraction of Cesium Polyiodides from Synthetic Waste Solutions into Nitrobenzene, USAEC Report BNL-50085 (T-478), Brookhaven National Laboratory, November 1967.

AEC SYMPOSIUM SERIES

NUCLEAR SCIENCE ABSTRACTS

The U. S. Atomic Energy Commission, Division of Technical Information, publishes *Nuclear Science Abstracts (NSA)*, a semimonthly journal containing abstracts of the literature of nuclear science and engineering.

NSA covers (1) research reports of the U. S. Atomic Energy Commission and its contractors; (2) research reports of government agencies, universities, and industrial research organizations on a worldwide basis; and (3) translations, patents, books, and articles appearing in technical and scientific journals.

Complete indexes covering subject, author, source, and report number are included in each issue. These are cumulated quarterly, semiannually, and annually providing a detailed and convenient key to the literature.

Availability of NSA

SALE *NSA* is available on subscription from the Superintendent of Documents, U. S. Government Printing Office, Washington, D. C., 20402, at $30.00 per year for the semimonthly abstract issues and $22.00 per year for the four cumulated-index issues. Subscriptions are postpaid within the United States, Canada, Mexico, and all Central and South American countries, except Argentina, Brazil, Guyana, French Guiana, Surinam, and British Honduras. Subscribers in these Central and South American countries, and in all other countries throughout the world, should remit $37.00 per year for subscriptions to semimonthly abstract issues and $25.00 per year for the four cumulated-index issues.

EXCHANGE *NSA* is also available on an exchange basis to universities, research institutions, industrial firms, and publishers of scientific information. Inquiries should be directed to the Division of Technical Information Extension, U. S. Atomic Energy Commission, P. O. Box 62, Oak Ridge, Tennessee, 37830.

order form

SUPERINTENDENT OF DOCUMENTS
U. S. GOVERNMENT PRINTING OFFICE
WASHINGTON, D. C. 20402

Please send — 1, 2, or 3 years

☐ Isotopes and Radiation Technology _____
☐ Nuclear Safety _____
☐ Reactor and Fuel-Processing Technology _____
☐ Reactor Materials _____

Enclosed: document coupons ☐ check ☐ money order ☐

Charge: Superintendent of Documents No._____

SUPERINTENDENT OF DOCUMENTS
U. S. GOVERNMENT PRINTING OFFICE
WASHINGTON, D. C. 20402

(Print clearly)

_____
Name

_____
Street

_____
City, State, ZIP Code